Supplemental Material for Secondary Organic Aerosol Production from Local Emissions Dominates the Organic Aerosol Budget over Seoul, South Korea, during KORUS-AQ

B. A. Nault[1,2], P. Campuzano-Jost[1,2], D. A. Day[1,2], J. C. Schroder[1,2], B. Anderson[3], A. J. Beyersdorf[3,*], D. R. Blake[4], W. H. Brune[5], , Y. Choi[3,6], C. A. Corr[3,**], J. A. de Gouw[1,2], J. Dibb[7], J. P. DiGangi[3], G. S. Diskin[3], A. Fried[8], L. G. Huey[9], M. J. Kim[10], C. J. Knote[11], K. D. Lamb[2,12], T. Lee[13], T. Park[13], S. E. Pusede[14], E. Scheuer[7], K. L. Thornhill[3,6], J.-H. Woo[15], and J. L. Jimenez[1,2]

Affiliations
1. Department of Chemistry, University of Colorado, Boulder, CO, USA
2. Cooperative Institute for Research in Environmental Sciences, University of Colorado, Boulder, CO, USA
3. NASA Langley Research Center, Hampton, Virginia, USA
4. Department of Chemistry, University of California, Irvine, Irvine, CA, USA
5. Department of Meteorology and Atmospheric Science, Pennsylvania State University, University Park, Pennsylvania, USA
6.6. Science Systems and Applications, Inc., Hampton, Virginia, USA
7. Earth Systems Research Center, Institute for the Study of Earth, Oceans, and Space, University of New Hampshire, Durham, New Hampshire, USA
8. Institute of Arctic and Alpine Research, University of Colorado, Boulder, CO, USA
9. School of Earth and Atmospheric Sciences, Georgia Institute of Technology, Atlanta, Georgia, USA
10. Division of Geological and Planetary Sciences, California Institute of Technology, Pasadena, CA, USA
11. Meteorologisches Institut, Ludwig-Maximilians-Universität München, München, Germany
12. Chemical Sciences Division, Earth System Research Laboratory, National Oceanic and Atmospheric Administration, Boulder, CO, USA
13. Department of Environmental Science, Hankuk University of Foreign Studies, Republic of Korea
14. Department of Environmental Sciences, University of Virginia, Charlottesville, VA, USA
15. Department of Advanced Technology Fusion, Konkuk University, Seoul, Republic of Korea
* Now at: Department of Chemistry and Biochemistry, California State University, San Bernardino, San BernardinoBernardino, California
** Now at: USDA UV-B Monitoring and Research Program, Natural Resource Ecology Laboratory, Colorado State University, Fort Collins, CO, USA

Correspondence to: J. L. Jimenez (jose.jimenez@colorado.edu)

SI 1. KORUS-AQ Overview

SI Table 1. List of NASA DC-8 research flights and date of take-off. Unless noted, the take-off dates are different than the local dates since the data was recorded in UTC. We document the research flights with the UTC dates to correspond with the data repository (Aknan and Chen, 2018).

Research Flight Number	*Date of Take-off*	*Regions Sampled*	*Number of Seoul Missed Approaches*
01	01/May/2016	Jeju jetway (×2)	3
02	03/May/2016	West Sea, Jeju jetway	3
03	04/May/2016	Jeju jetway	2
04	06/May/2016	Busan jetway (×2)	3
05	10/May/2016	Jeju jetway, other[b]	2
06	11/May/2016	West Sea, other[c]	3
07	12/May/2016	West Sea, other[d]	0
08	16/May/2016	Jeju jetway, Busan jetway	3
09	17/May/2016	West Sea, Busan jetway	3
10	19/May/2016	Busan jetway (×2)	3
11	21/May/2016	West Sea	3
12	24/May/2016	West Sea	2
13	26/May/2016[a]	Jeju Jetway	2
14	29/May/2016	West Sea, Busan jetway	4
15	30/May/2016	West Sea, Jeju jetway	3
16	01/June/2016	Busan jetway, Jeju jetway	3
17	02/June/2016	Busan jetway, Jeju jetway	3
18	04/June/2016	West Sea, other[e]	5
19	08/June/2016	Busan jetway (×2)	3
20	09/June/2016	Jeju jetway, other[b]	2

[a]For RF13, the DC-8 took-off after 00:00 UTC, corresponding to the date in local time and UTC time being the same.
[b]The DC-8 sampled south of the Korean peninsula.
[c]The DC-8 sampled east of Seoul to the Sea of Japan.
[d]The DC-8 sampled the Sea of Japan.
[e]The DC-8 remained in the greater Seoul area to sample point sources.

SI Table 2. Description of the geographical locations used in Figure 1 and throughout the text, and shown in SI Figure 1..

Location	*Lat Min (°N)*	*Lat Max (°N)*	*Lon Min (°E)*	*Lon Max (°E)*
Seoul	36.8	37.6	124.6[a]	128.0
West Sea			124.0	126.0
Jeju jetway	34.2	36.8	126	127
Busan jetway	35.2	36.8	128.6	129.9

[a]This value was chosen to include the Seoul outflow observed during RF11 and RF18.

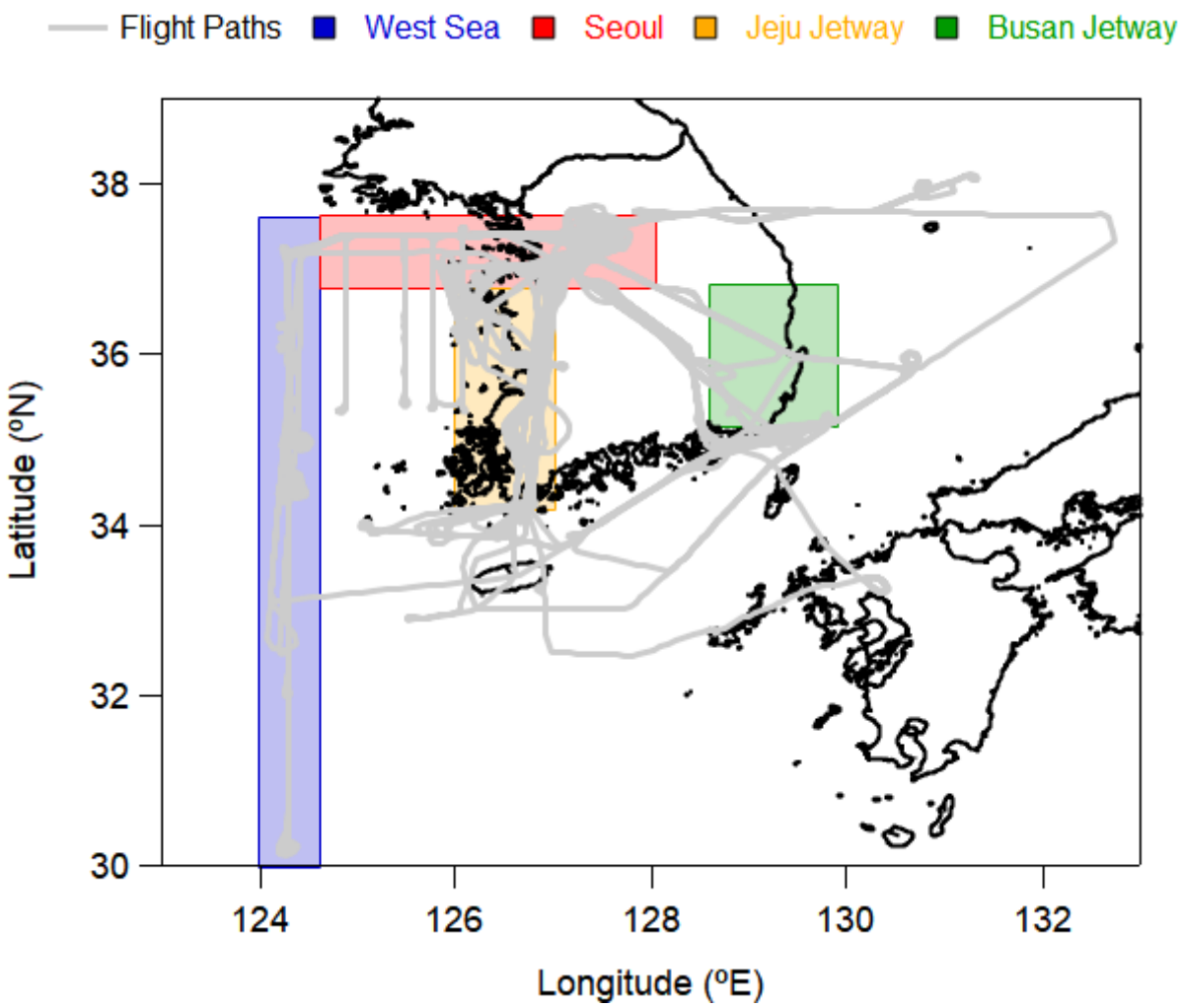

SI Figure 1. Geographical regions shown in SI Table 1. Note, the Seoul box is extended into the West Sea to capture the outflow of Seoul emissions for two flights (RF11 and RF18).

SI 2. CU-AMS Sampling and Calibration

After almost every flight, the ionization efficiency (IE) was calibrated (SI Figure 3) using the single particle technique. Briefly, air containing 150 – 250 particles/cm^3 of NH_4NO_3, of 400 nm (mobility diameter, sized with a built-in differential mobility analyzer, DMA, TSI model 3080) was sampled by the AMS. Thresholds of 4 (*m/z* 30) or 3 (*m/z* 46) ions per event were selected to produce a low, but detectable background (typically ~7 events/cm^3 background). An event would be recorded, after evaporation and ionization of NH_4NO_3 particle, if at least 4 (*m/z* 30) or 3 (*m/z* 46) ions were observed. These values were analyzed using the ToF AMS Ionization Efficiency Calibration Panel for ET, v1.0.5F (http://cires1.colorado.edu/jimenez-group/ToFAMSResources/ToFSoftware/index.html#ToF_IE_Cal), to process the data and calculate IE and IE/AB (AB is air beam). Typical values during KORUS-AQ, for 400 nm (geometric diameter) NH_4NO_3 calibrations were the following: 10 baseline segments and minimum and maximum ions per particle values of 1 and 200. During KORUS-AQ, the average IE/AB was 8.10(±0.64)×10^{-13} ions/molecule of nitrate, which leads to an overall 10% variability for this value during the whole campaign. Further details about using single particle technique for IE/AB calibrations can be found in Nault et al. (2016).

These IE calibrations also provided relative ionization efficiency (RIE) calibrations of NH_4 after nearly every flight, as well (SI Figure 3), along with the NO^+ and NO_2^+ ratios of ammonium nitrate, which are useful to estimate particle organic nitrate concentrations, as detailed in Fry et al. (2013). The SO_4 and Chl RIEs were measured about once every week, and the interpolated values were used for the SO_4 and Chl concentrations. For the organic aerosol, we used an RIE of 1.4 (Jimenez et al., 2016; Xu et al., 2018). Finally, to test the effects of solution mixtures on RIE for SO_4 and NH_4, we made calibration solutions ranging from 0 – 100% NH_4NO_3, with the balance

coming from $(NH_4)_2SO_4$. We find no effects, both on the calculated NH_4 balance (SI Figure 6), when using the NH_4 and SO_4 RIE's from the pure calibration, and on the recalculated NH_4 (SO_4) RIE when keeping a constant SO_4 (NH_4) RIE from the pure calibrations (SI Figure 6). The consistency in the NH_4 balance, as observed in prior studies (Docherty et al., 2011; Jimenez et al., 2016), and the high precision (3% precision in all calculations) provides further confidence in the stability of the RIEs for the species in calculating their mass in mixed particles, and indicates that there are no effects on the RIE with changing composition, and, thus, CE (Jimenez et al., 2016).

Also, the IE calibrations performed after each flight provided an opportunity to calculate the effect of pNO_3 on producing a small artifact CO_2^+ signal, as detailed in Pieber et al. (2016), and of pNO_3 on producing small artifact HCl^+ and Cl^+ signal, as detailed in Hu et al. (2017a) (SI Figure 3). The CU-AMS data has been corrected for these small effects. The corrections were typically 1% of CO_2^+ and 0.8% Chl.

Three different lens transmission calibrations to characterize the high end of the AMS transmission curve were performed: (1) comparing the NH_4NO_3 mass measured with the CPC and the CU-AMS between 200 – 450 nm (mobility diameter, d_m); (2) comparing the number of particles measured with the CPC and the CU-AMS between 300 – 450 nm (d_m) using the single particle vaporization technique detailed above; and (3) comparing the $(NH_4)_2SO_4$ mass measured with the CPC and the CU-AMS between 250 – 450 nm (d_m), normalizing to the value at 250 nm. The NH_4NO_3 diameters were converted to vacuum aerodynamic diameters (d_{va}), as discussed in DeCarlo et al. (2004). As seen in SI Figure 4, both techniques show good agreement for the particle transmission, and this transmission is similar to the recommended transmission curve in the literature (Knote et al., 2011; Hu et al., 2017b). For this curve, it is assumed that the transmission linearly increases from 0 – 100% between 40 – 100 nm (d_{va}) (Q. Zhang et al., 2004), remains 100%

between 100 – 550 nm (aerodynamic diameter), and decreases linearly from 100 – 0% between 550 nm – 1500 nm (d_{va}). This leads to a 50% cut-off of ~900 nm (d_{va}) during KORUS-AQ.

The particle sizing in the AMS Particle Time-of-Flight (PToF) mode was calibrated with PSLs, ranging from 70 – 700 nm (geometric diameter) (SI Figure 5). This calibration was compared against the velocities calculated from data collected during the NH_4NO_3 lens transmission measurements. As seen in SI Figure 5, these two different methods to calibrate the PToF velocity show comparable results, falling within the 95% confidence interval of the PSL calibration. The fact that both PToF calibrations agree, and that the SMPS used for the AN calibrations showed less than 2 nm deviation from the nominal PSLs diameters at all sizes increases our confidence in accuracy of the IE calibration described above, and in particular on lack of evaporation of NH_4NO_3 after its size selection in the DMA.

Finally, the vaporizer power, and thus, temperature, was calibrated by using monodisperse $NaNO_3$ particles of d_m = 350 nm (SI Figure 8), as recommended by Williams (2010) and Hu et al. (2017b). This method is more accurate than relying on the temperature reported by the thermocouple on the AMS vaporizer, which can often be unreliable (Williams, 2010; Hu et al., 2017b). The general idea is to increase the vaporizer power between ~1 – 7 W and locate where the $NaNO_3$ full-width half maximum nearly remains constant, indicating that the vaporizer temperature is ~600°C and allowing for maximum peaks in OA, pNO_3, and SO_4 while minimizing the influence of refractory species (Williams, 2010; Hu et al., 2017b).

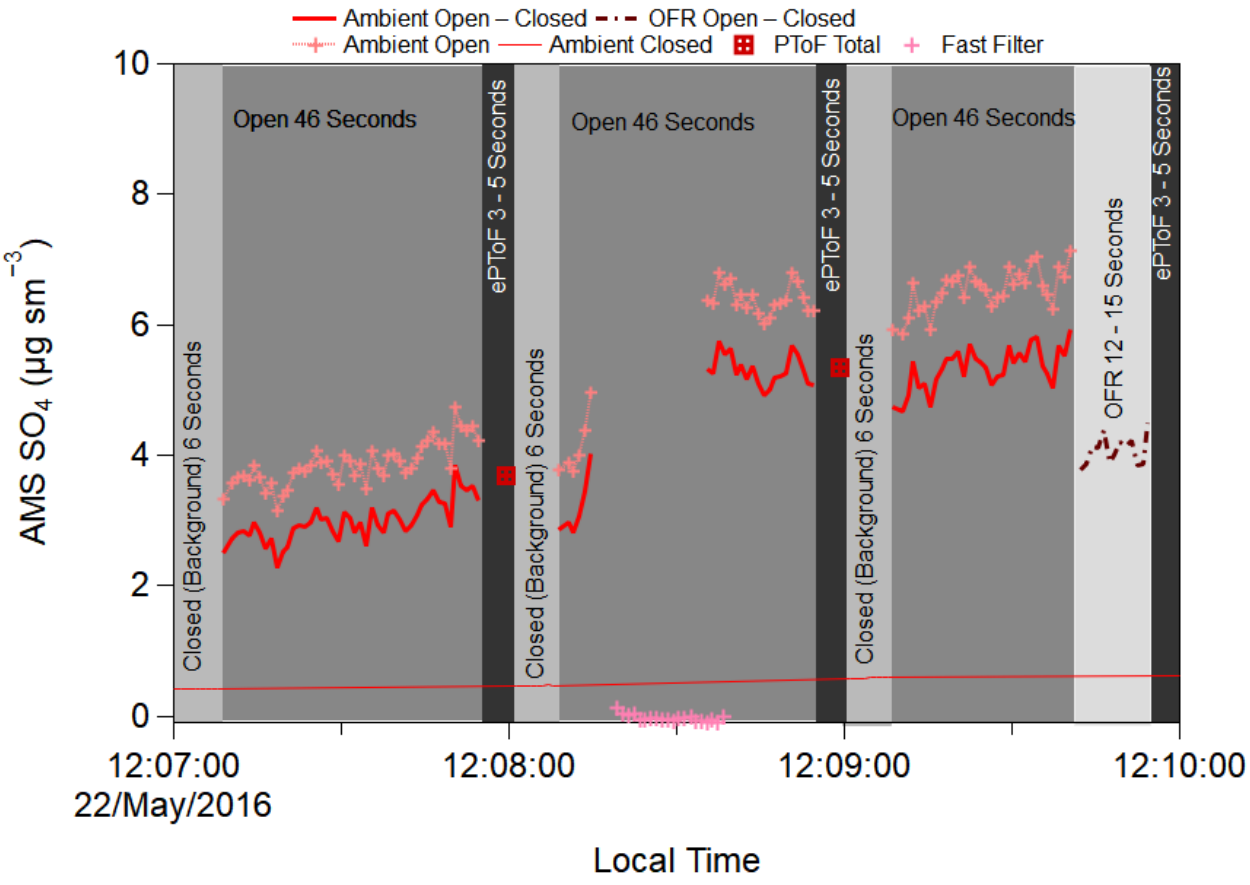

119

120 **SI Figure 2.** Example time series of the CU-AMS sampling scheme during KORUS-AQ.

121

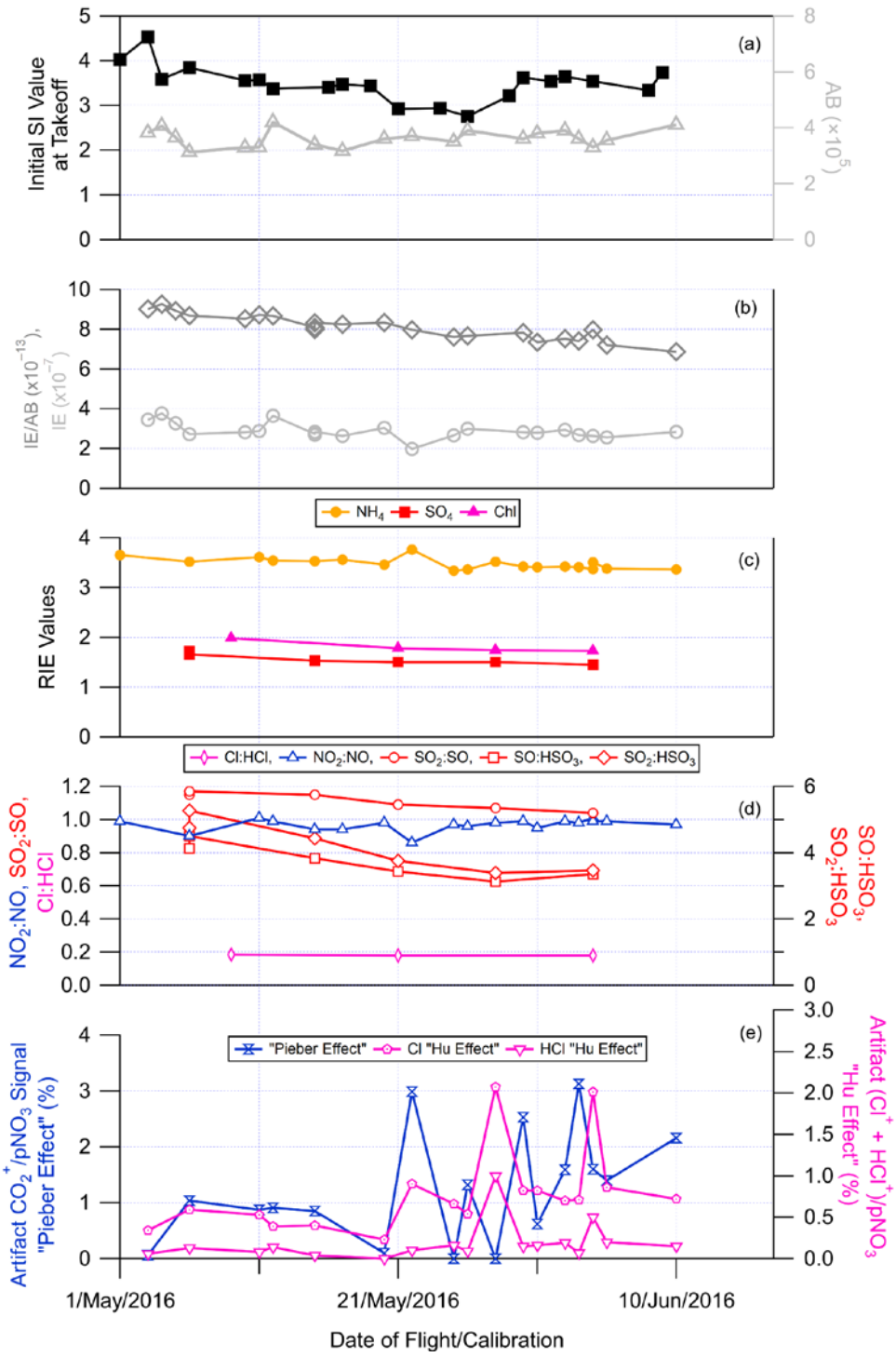

SI Figure 3. Time series of the (a) the Single Ion (SI) at take-off for each flight; (b) the air beam (AB, dark grey), ionization energy (IE, light grey), and IE/AB (middle grey) for each calibration; (c) the relative ionization energies (RIE) for ammonium (NH_4), sulfate (SO_4), and chloride (Chl) for each calibration; (d) the ratios of different ions for each calibration; and, (e) measured artifact signal ratios for CO_2^+/pNO_3 "Pieber effect" (Pieber et al., 2016) and $(Cl^+ + HCl^+)/pNO_3$ "Hu efffect" (Hu et al., 2017a) effects from each calibration.

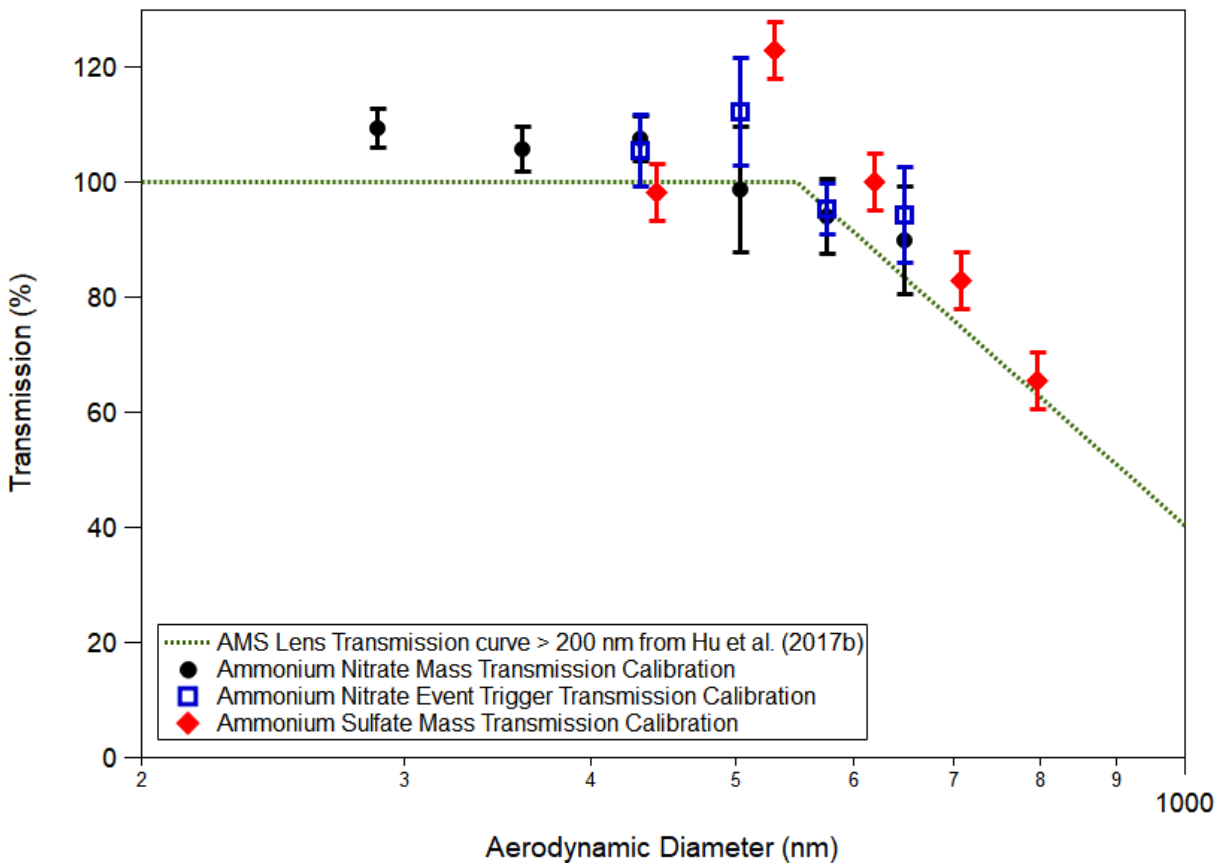

129

130 **SI Figure 4.** Measured transmission percentage of ammonium nitrate and ammonium sulfate
131 versus vacuum aerodynamic diameters (nm) during KORUS-AQ. The green dashed-line is the
132 expected transmission curve for the CU-AMS from the literature (Knote et al., 2011; Hu et al.,
133 2017b). The black data represents the ammonium nitrate transmission curve using mass closure,
134 from an experiment conducted on 09/May/2016. The blue data represents the ammonium nitrate
135 transmission curve using single particle ("event trigger") number closure, from an experiment
136 conducted on 17May/2016. The red data represents the ammonium sulfate transmission curve
137 using mass, from an experiment conducted on 06/May/2016. Finally, the error bars represent 1σ
138 variability for the transmission at each size.

139

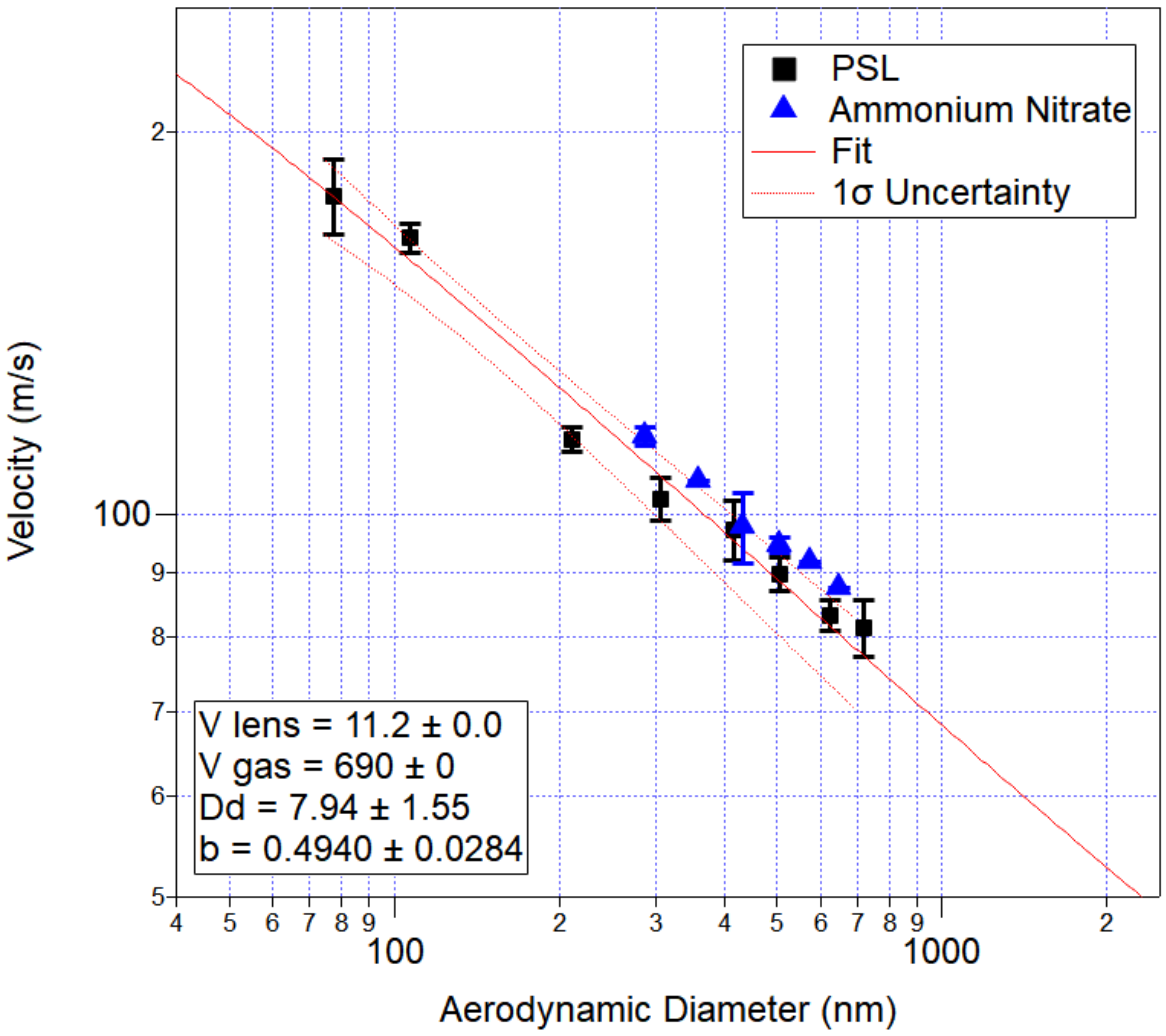

SI Figure 5. Particle velocity (m/s) inside the AMS vacuum chamber (after exiting the aerodynamic lens) versus vacuum aerodynamic diameter (nm) calibrations for the ePToF mode, using PSLs (black). Solid red line is the fit to the PSLs. The ammonium nitrate measured for the mass closure transmission curves (SI Figure 4) for comparison to the PSL values.

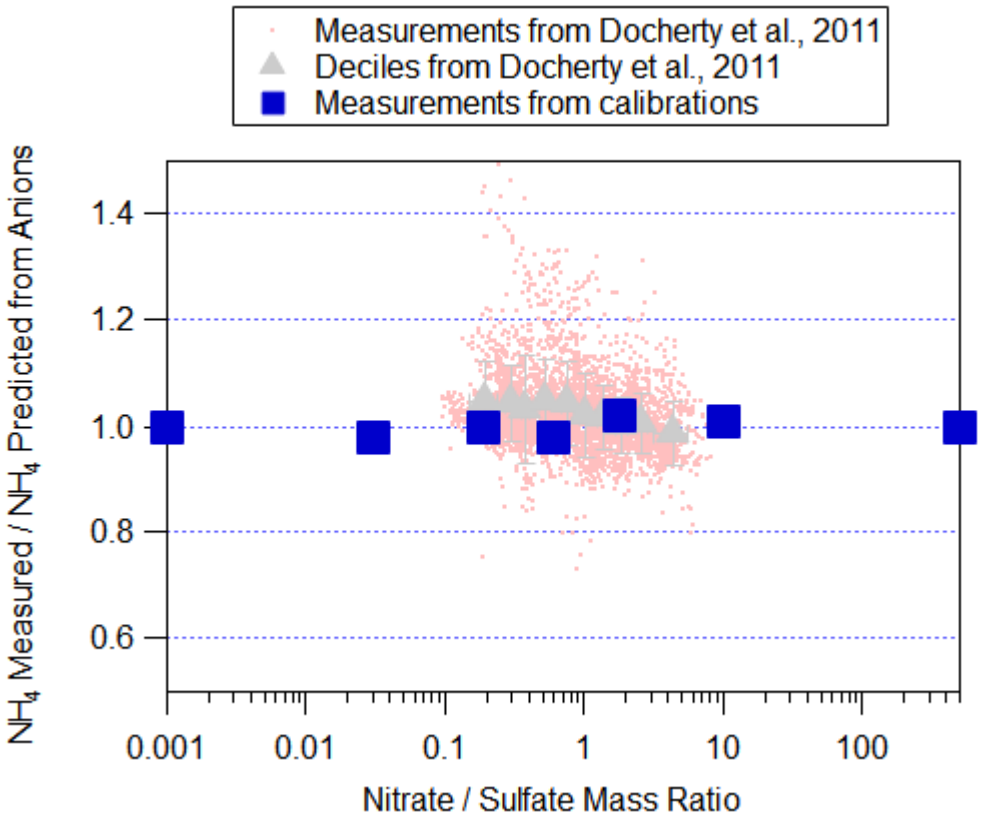

145

146 **SI Figure 6**. Ratio of measured and predicted NH_4 from anions versus ratio of nitrate to sulfate
147 mass. Red points are from Docherty et al. (2011), grey triangles are deciles of the data from
148 Docherty et al., and blue points are measurements from calibration solutions of varying mixtures
149 of NH_4NO_3 and $(NH_4)_2SO_4$. Such consistency would be unexpected if a major fraction of the
150 particle NH_4^+ evaporated as intact salts, as suggested by Murphy (2016) (Hu et al., 2017b) .

151

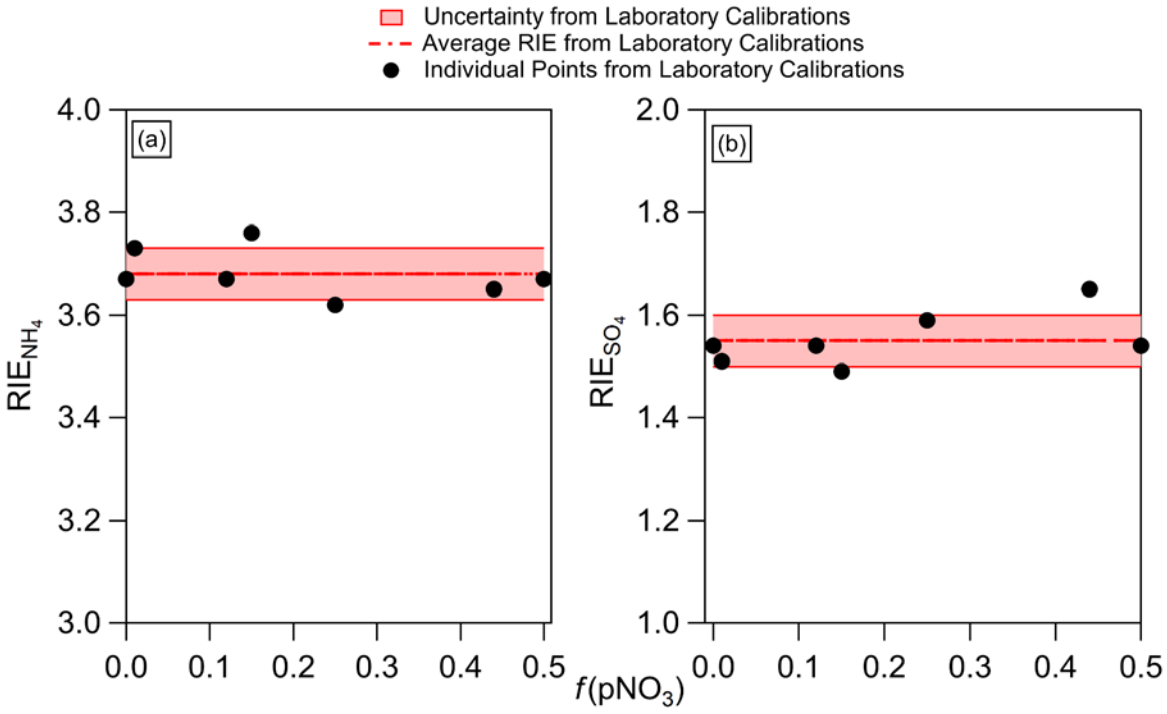

SI Figure 7. (a) Plot of NH_4 RIE, keeping SO_4 RIE constant, versus the molar fraction of pNO_3 measured in the solution, for calibration solutions of varying mixtures of NH_4NO_3 and $(NH_4)_2SO_4$. (b) Same as (a), but for SO_4 RIE and keeping NH_4 RIE constant. For both figures, the black dots are the values from the calibrations, the thick red line is the average of all the values, and the shaded red area is ±1σ.

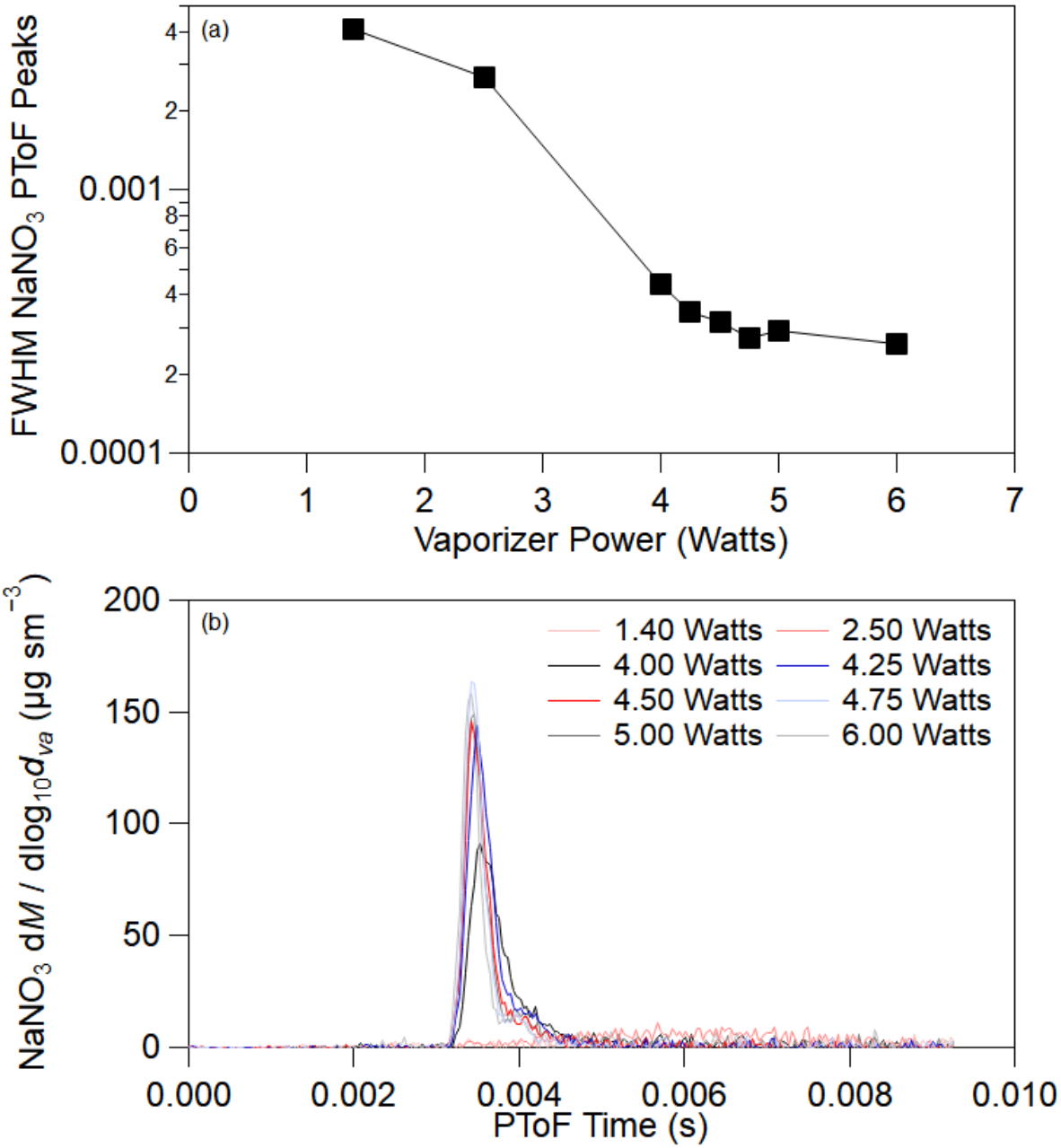

158

159 **SI Figure 8.** (a) Full-width half-maximum (FWHM) of $NaNO_3$ size distributions in PToF mode
160 (b) vs. different vaporizer power inputs. See text for further details.

161

SI 3. Application of Positive Matrix Factorization (PMF)

Positive matrix factorization analysis (PMF, performed using the CU-Boulder PMF Evaluation Tool PET-Panel v3.00A, http://cires1.colorado.edu/jimenez-group/wiki/index.php/PMF-AMS_Analysis_Guide#PMF_Evaluation_Tool_Software) (Ulbrich et al., 2009) was used to apportion the total OA aerosol into several components. PMF was run on the combined CU-AMS 1 min organic ion matrix for all RFs together during KORUS-AQ. A 6-factor solution was derived with an FPEAK value of 0. Based on comparisons with reference mass spectra from the AMS high-resolution spectral database (http://cires1.colorado.edu/jimenez-group/HRAMSsd/#Ambient), comparisons of time series (SI Figure 9), and correlations with other trace species (SI Figure 11), the factors were recombined into more-oxidized, oxidized organic aerosol (MO-OOA), less-oxidized, oxidized aerosol (LO-OOA), and hydrocarbon-like organic aerosol (HOA) (SI Figure 10). HOA correlated with primary emissions (e.g., NO_x, various hydrocarbons) whereas LO-OOA and MO-OOA correlated with secondary photochemical products (e.g., CH_2O, PAN, pNO_3, SO_4). Here, primary OA is defined as the HOA factor and total oxidized OA (OOA) as the LO-OOA plus MO-OOA factors. OOA is assumed to be dominantly composed of secondary organic aerosol, which is supported by its strong correlation with other secondary photochemical products as documented in the paper, as well as by many prior studies (e.g., Jimenez et al., 2009; and references therein).

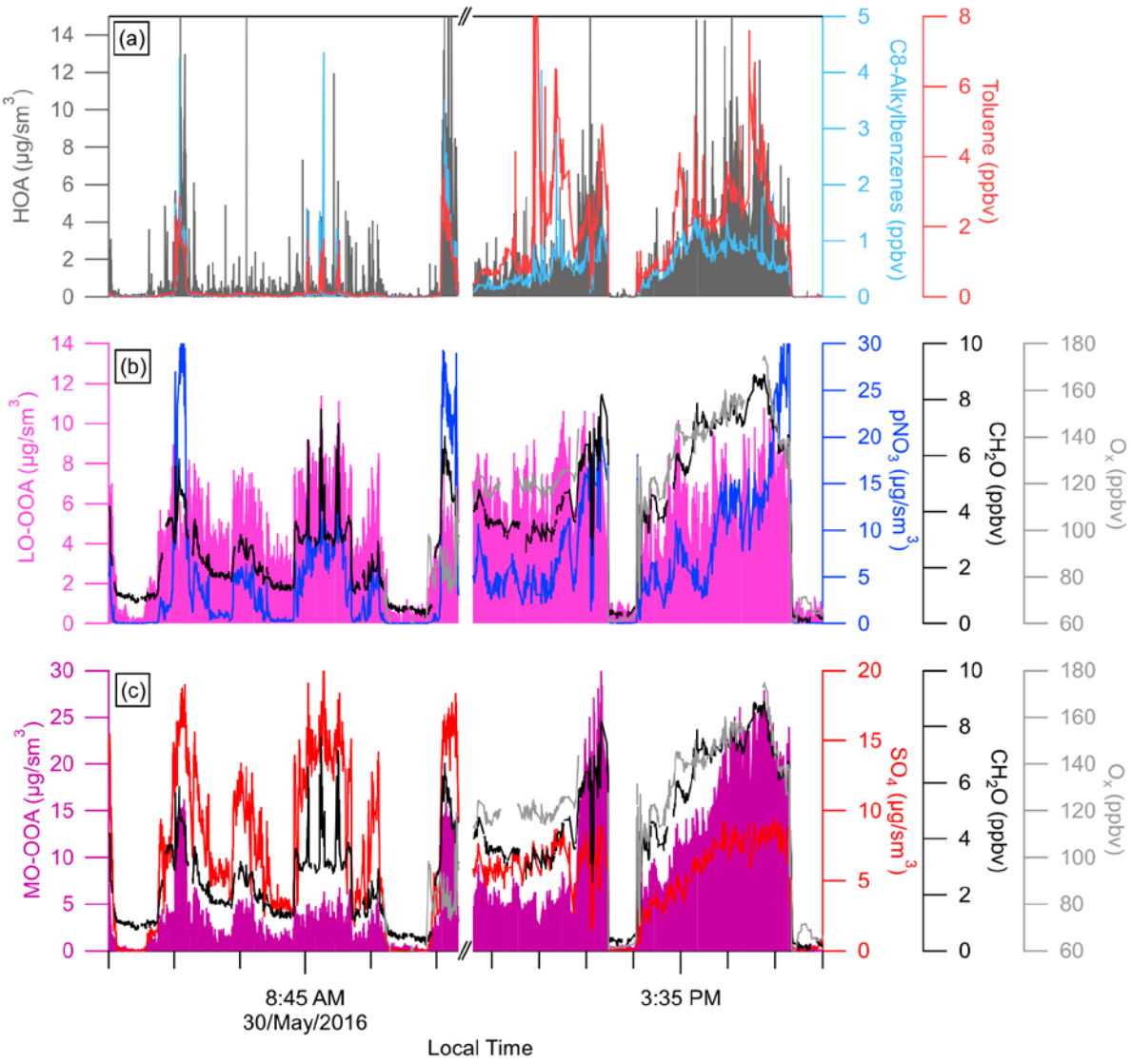

181

182 **SI Figure 9.** Example time series of the 3 PMF ((a) HOA, (b) LO-OOA, and (c) MO-OOA) results
183 (left axes) and some species that correlate with the corresponding PMF results (right axes) from
184 RF14. The morning and afternoon overpasses over Seoul, South Korea, are shown.

185

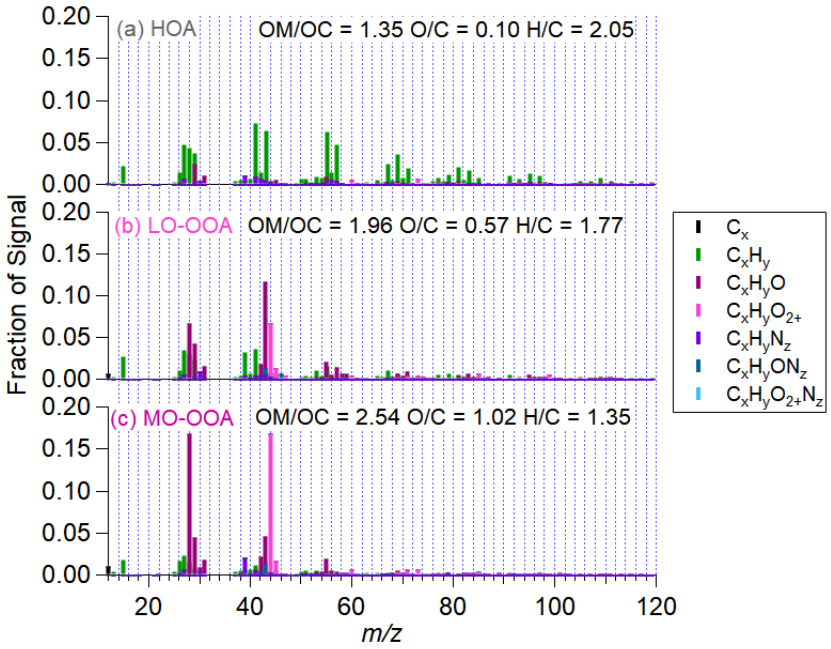

186

187 **SI Figure 10.** Mass spectra for PMF solution (a) HOA, (b) LO-OOA, and (c) MO-OOA for all of
188 KORUS-AQ.

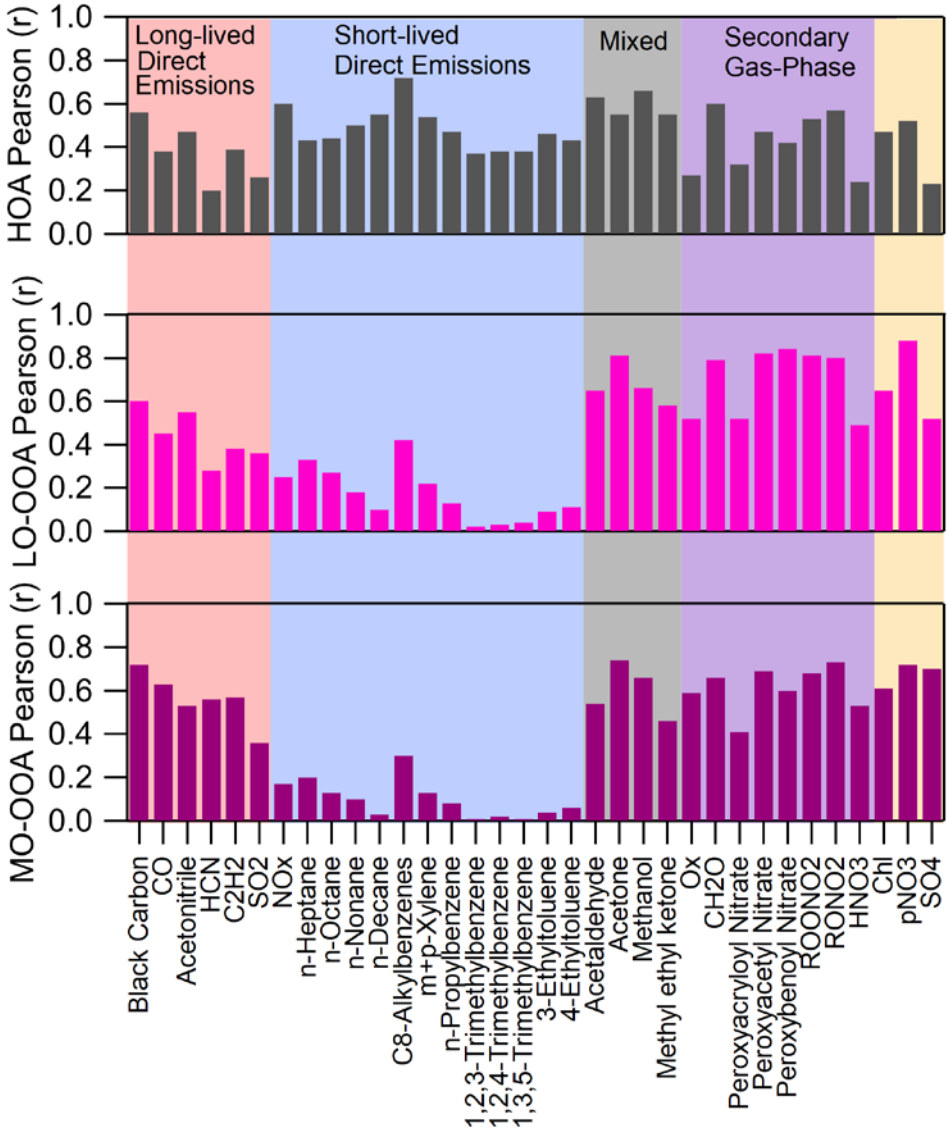

189

190 **SI Figure 11.** Pearson correlation coefficients for HOA (grey, top), LO-OOA (light pink, middle),
191 and MO-OOA (dark pink, bottom) factors versus species listed in x-axis. The background colors
192 represent the dominant group of sources of the correlating species. The yellow in the far right
193 indicates other PM_1 components measured by the CU-AMS.

194

SI 4. Oxidation Flow Reactor (OFR) Sampling

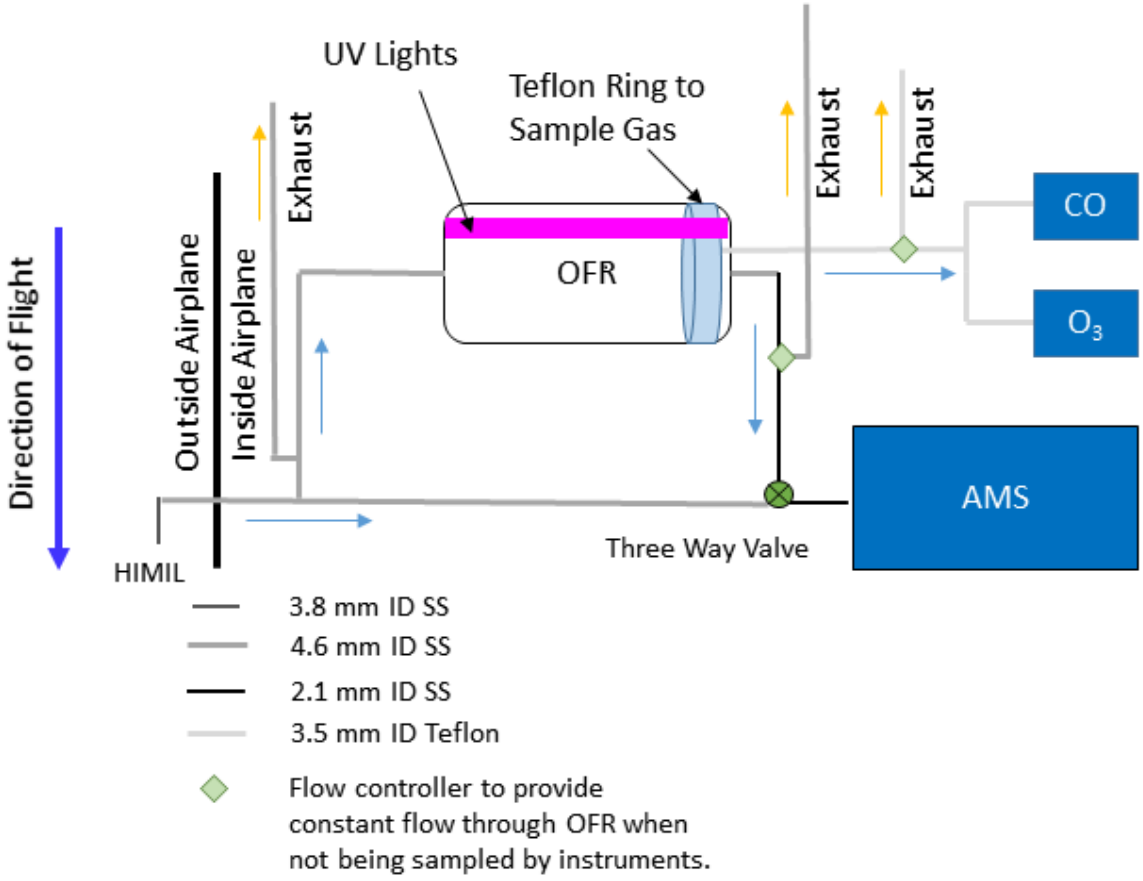

SI Figure 12. Schematic of the OFR sampling during KORUS-AQ. UV lamp is represented by the purple light in the OFR. Size and type of tubing is represented in figure, where ID is internal diameter and SS is stainless steel. Tubing distances were always as short as feasible and often shorter than represented, but they are stretched in this drawing for clarity

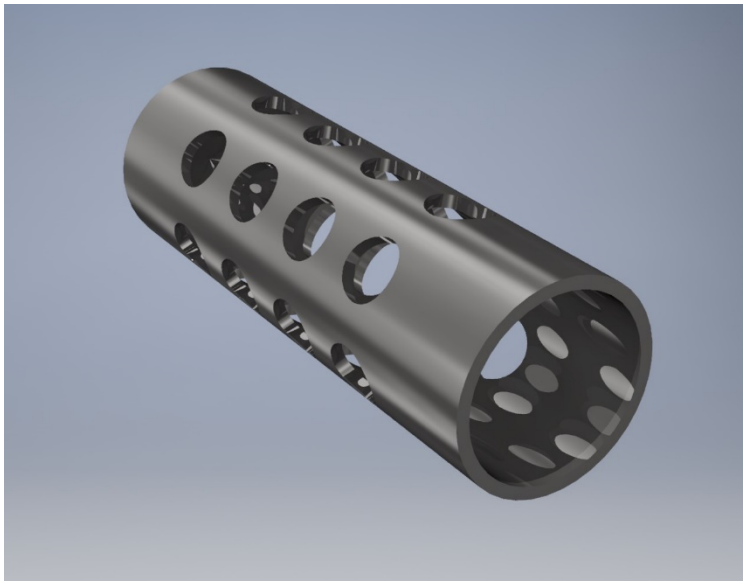

SI Figure 13. 3D rendition of the computer model of the ½" press fitted stainless steel inlet, coated in SilcoNert (SilcoTek Co, Bellefonte, PA), used in the inlet of the OFR during KORUS-AQ, to avoid "short-circuiting" between the inlet and outlet of the OFR.

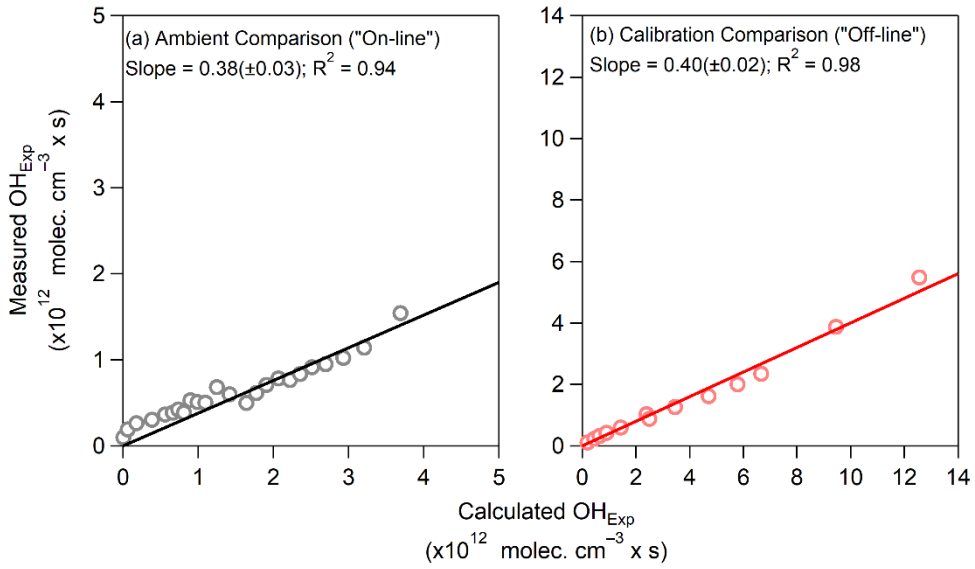

SI Figure 14. (left) Measured OH_{exp} from the decay of CO in ambient air (measured by the DACOM instrument, see text) and OFR output air (measured by the Picarro instrument) and (right) measured OH_{exp} from the decay of CO from a calibration cylinder versus calculated OH_{exp} using the predictive expression in Peng et al. (2015). The calibration factor determined by this analysis was similar to past studies (Palm et al., 2016) and was applied to all data shown in this paper.

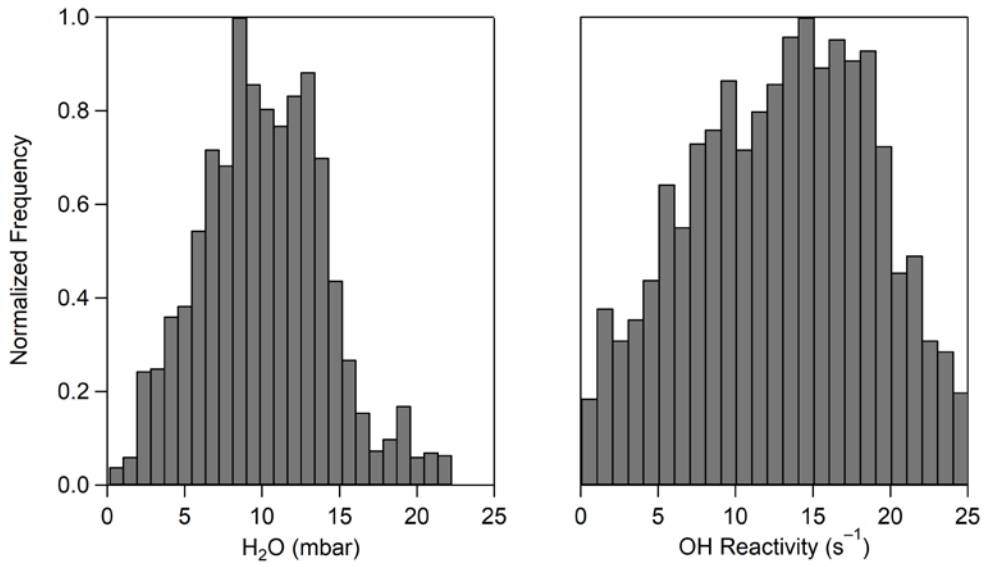

212

213 **SI Figure 15.** (left) Frequency distribution of water vapor below 2 km during KORUS-AQ. (right)
214 Normalized histogram of measured OH reactivity (OHR) below 2 km during KORUS-AQ.

215

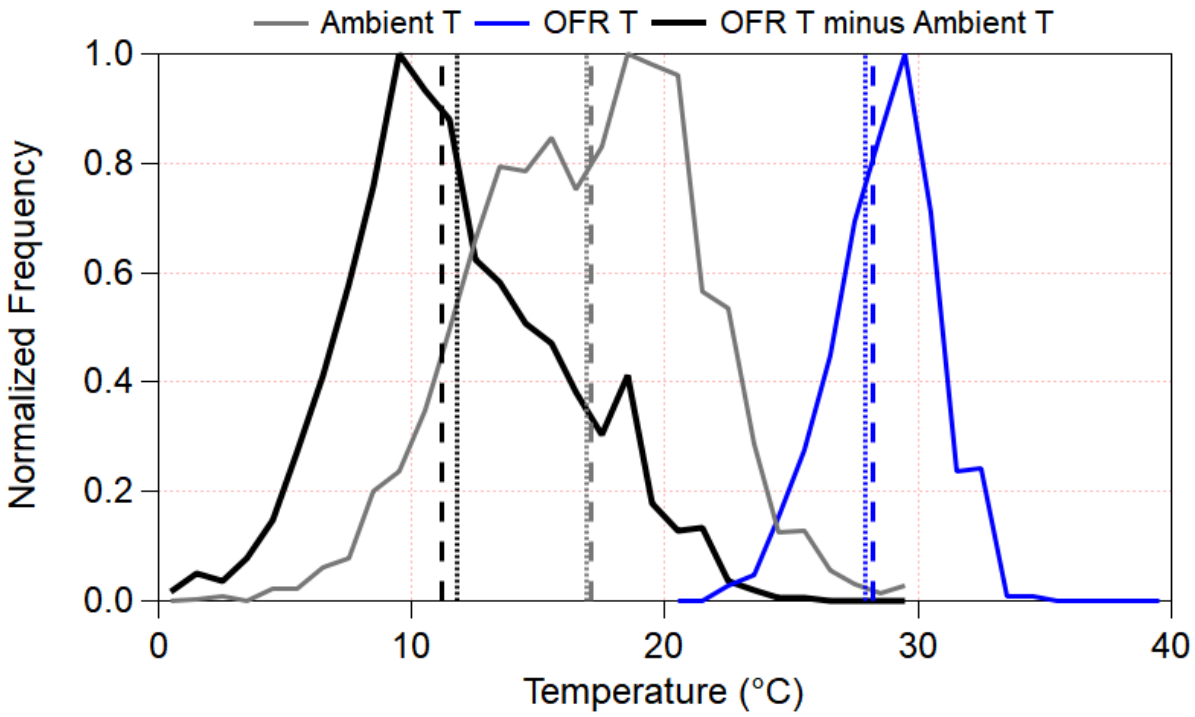

216

217 **SI Figure 16.** Frequency distribution of the ambient (black), OFR (blue), and difference between
218 OFR and ambient temperature (grey) (°C). Vertical lines show the mean (long-dashed) and median
219 (short-dashed) temperatures for the ambient, OFR, and difference between the two.

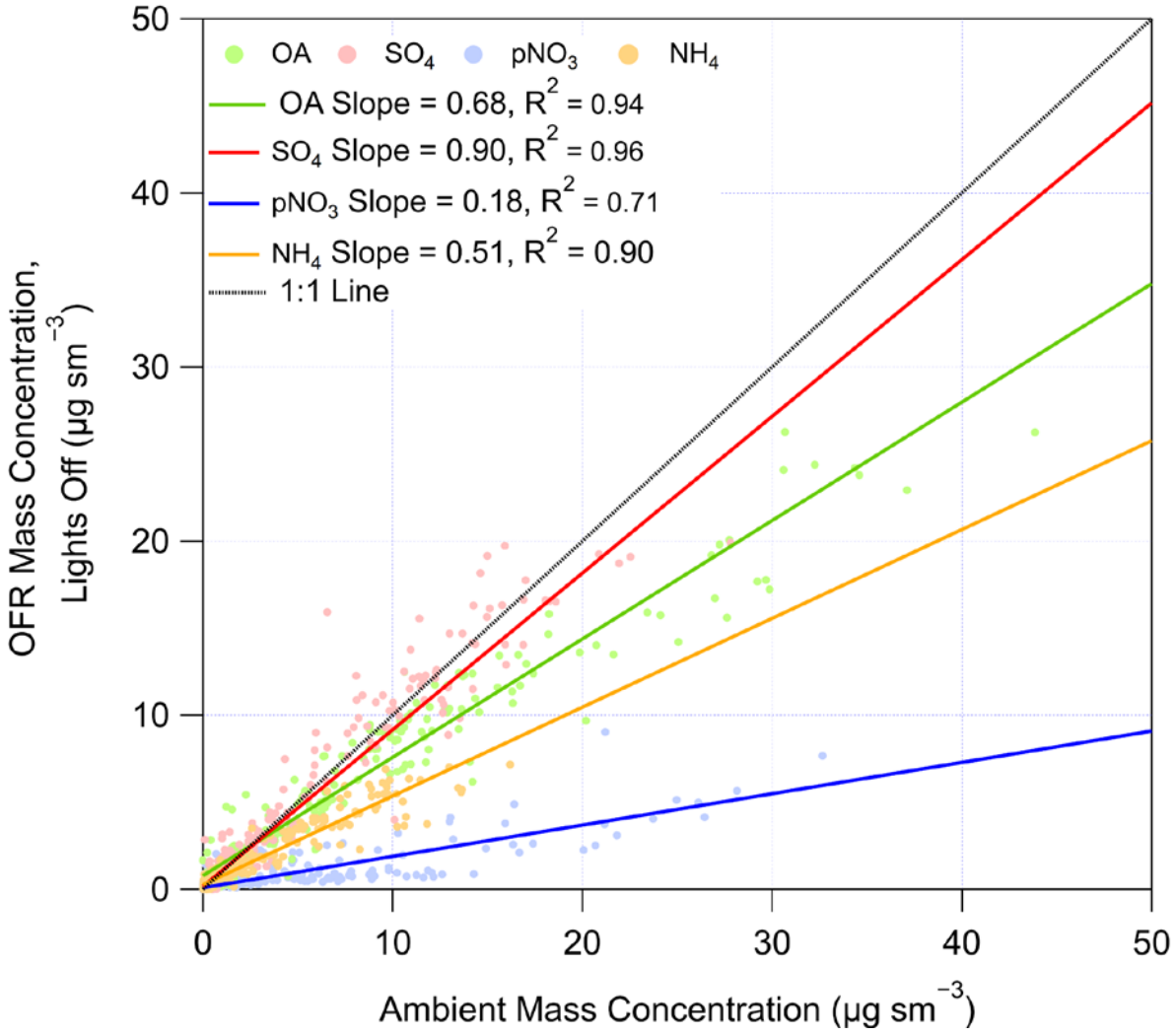

220

221 **SI Figure 17.** Comparison of organic (green), sulfate (red), nitrate (blue), and ammonium (orange)
222 aerosol sampled through the OFR, with lights off, versus ambient aerosol. Under these conditions
223 the OFR is just acting as a thermal denuder (e.g. Huffman et al., 2009), leading to evaporation of
224 some aerosols due to increased temperature in the aircraft cabin vs. outside. In addition, small
225 particle losses in lines and the OFR are observed for sulfate, which is generally non-volatile. Figure
226 is adapted from Heim et al. (2018). See text for further details and discussion.

227

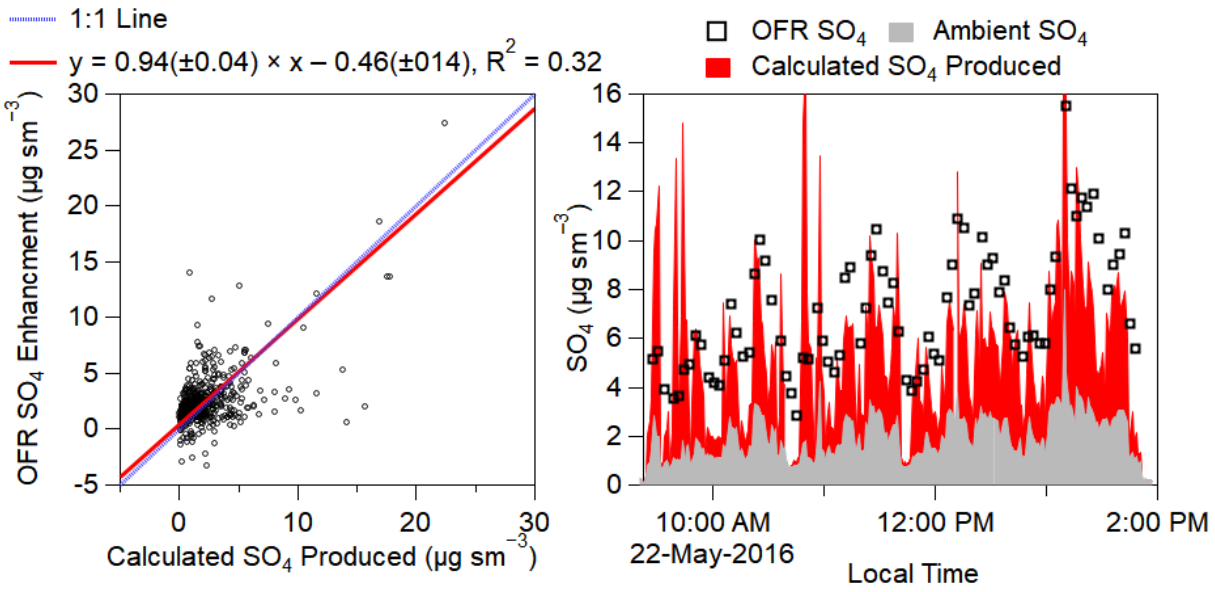

228

229 **SI Figure 18.** (a) Scatter plot of OFR SO_4 Enhancement (OFR – Ambient) versus calculated SO_4
230 produced, using SO_2 observations, estimated OH_{exp}, and condensation fate correction. (b) Time
231 series of OFR SO_4 (black squares), ambient SO_4 (light grey), and calculated SO_4 (dark red) for the
232 RF11 flight.

233 *Analysis of CS Values for KORUS-AQ*

234 If we used the condensational sink from just the ambient data, which neglects the added particle
235 surface area formed in the OFR as described in Section 2.4 and Eq. 1 (Ortega et al., 2016; Palm et
236 al., 2016, 2017, 2018), the agreement between calculated and measured SO_4 enhancement
237 decreases to a slope of 0.74 (R^2 = 0.28), indicating that the condensational sink is likely too low.
238 This suggests that, to first order, the aerosol surface area, estimated from observations and Eq. 1
239 (in the main paper), provides a reasonable estimate of the condensational sink within the OFR
240 during KORUS-AQ. Thus, similar to other studies (Ortega et al., 2016; Palm et al., 2016, 2017,
241 2018), we find, at the typical OH_{exp} in the OFR, that 50 – 60% of the oxidized condensable organic
242 gases are condensing onto aerosol, with 20 – 25% undergoing further reactions with OH leading
243 to highly volatile compounds, 8 – 13% exiting the OFR prior to condensing on aerosol, and 12%

condensing to the wall (SI Figure 19). Note that the further reactions with OH are not relevant for H_2SO_4, and thus they have not been included in the analysis shown in in Fig. SI-18.

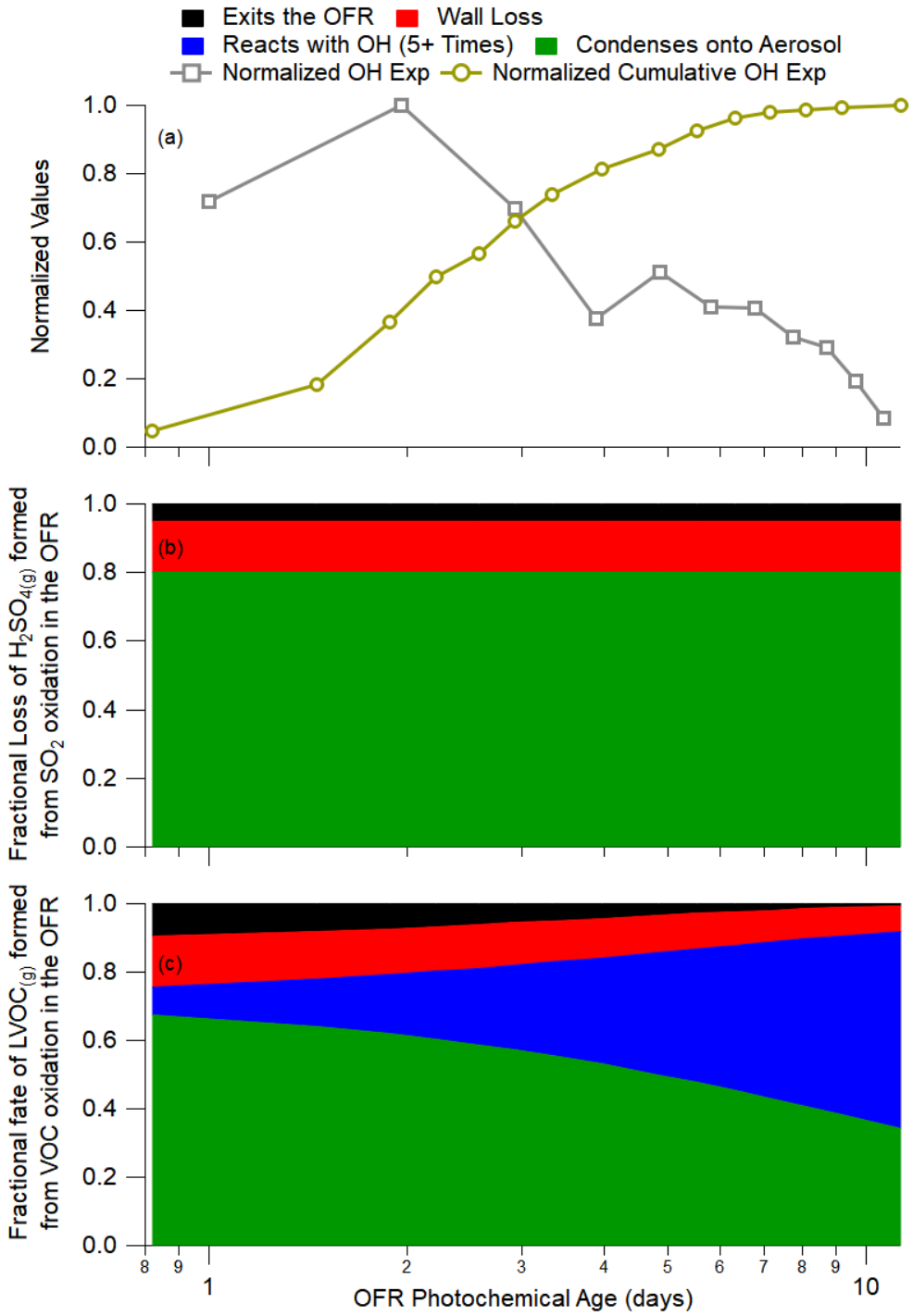

SI Figure 19. (a) Observed normalized frequency and cumulative frequency of OH Exposure observed during KORUS-AQ in the OFR. (b) Calculated fate of the SO_2 oxidized in the OFR

versus OFR OH Exposure. (c) Calculated fate of low-volatility condensable vapors (formed from VOC oxidation) versus OFR OH Exposure. For (b) and (c), the losses include flowing through the OFR without condensing onto aerosol (black), condensing onto the wall (red), condensing onto the aerosol (assuming a median value of 85.8 s, green), and reacting with OH enough to make it too volatile to condense onto aerosol (blue).

SI 5. Calculation of Photochemical Age over Seoul, South Korea

The photochemical clock calculations used throughout this work are described here. The rate constants used for these clocks are located in SI Table 3. For the NO_x/NO_y photochemical clock (e.g., Kleinman et al., 2007) (herein referred to as the NO_x photochemical clock), Eq. S1 is used, with the updated rate constant from Mollner et al. (2010).

$$t = \frac{ln\left(\frac{NO_x}{NO_y}\right)}{k_{OH+NO_2}[OH]} \quad \text{(S1)}$$

where *t* is the time, in days, [OH] is assumed to be 1.5×10^6 molecules/cm^3 (for standarization), and NO_x and NO_y are the chemiluminescence measurements. The NO_x clock is used for photochemical ages less than 1 day to (1) reduce the effect of loss of HNO_3 and other oxidized reservoirs due to deposition (lifetime ~6 hours) (Neuman et al., 2004; Nguyen et al., 2015; Romer et al., 2016) and (2) to ensure that t was still sensitive (and precise) to the NO_x and NO_y concentrations (~20% of NO_x still remaining at *t* = 1 day).

For the aromatic photochemical clock over Seoul, the more reactive aromatics (ethylbenzene in the denominator) are utilized, which should be more sensitive to the short photochemical aging observed over Seoul (Parrish et al., 2007), along with Eq. SS2.

$$t = -\frac{1}{[OH]\times\left(k_{aromatic_i}-k_{ethylbenzene}\right)} \times \left(ln\left(\frac{aromatic_i(t)}{ethylbenzene(t)}\right) - ln\left(\frac{aromatic_i(0)}{ethylbenzene(0)}\right)\right) \quad \text{(S2)}$$

where *t* is the time, in hours, the *k*'s are the corresponding OH rate constants for each aromatic compound (SI Table 3), and the third term ($\ln\left(\frac{\text{aromatic}_i(0)}{\text{ethylbenzene}(0)}\right)$) corresponds to the emission ratios for those two aromatic compounds. Similar to the NO_x clock, we assume [OH] = 1.5×10^6 molecules/cm^3 for standardization. The aromatics measurements used in this calculation are from WAS.

To evaluate which aromatic compounds to use in the clock, the behavior of the ratios of each aromatic compound with ethylbenzene versus the three missed approaches (morning, noon, and afternoon) over Seoul during KORUS-AQ (SI Figure 20) are compared. The idea is that if the 2 aromatic compounds are co-emitted, the ratios should be removed proportionally to their OH rate constants. E.g. for faster reacting compounds (e.g., o-xylene), the ratio to ethylbenzene should decrease with time as more o-xylene was consumed, compared to ethylbenzene, by OH (de Gouw et al., 2017). On the other hand, for slower reacting compounds (e.g., toluene), the ratio to ethylbenzene should increase with time as more ethylbenzene was consumed by OH. Also, this analysis provides an indication of which ratios would provide meaningful results throughout the entire day (de Gouw et al., 2017). Ideally, there should be a decrease with each later missed approach, and not a leveling off after two missed approaches (e.g., the trimethylbenzenes and ethyltoluenes). Only the m+p-xylene/ethylbenzene and o-xylene/ethylbenzene ratios meet this criterion. Finally, to determine the emission ratios, we calculated what the m+p-xylene/ethylbenzene and o-xylene/ethylbenzene ratio was for observations where the NO_x photochemical was less than 0.07 days (corresponding to less than 10% of either species being consumed). Comparing these two aromatic clocks to the NO_x photochemical clock (SI Figure 21), a similar agreement between the two aromatic clocks with the NO_x photochemical clock was observed, providing confidence in using all three clocks to calculate photochemical age to evaluate OA production over Seoul. For the remainder of the paper, we mainly use the NO_x photochemical clock to eliminate the uncertainty of the emission ratios, unless otherwise noted.

Finally, for observations over the West Sea, the aromatic clock (Eq. SS2) was used, but benzene and toluene were used since these air masses are more photochemically processed (Parrish et al., 2007). For the emission ratios, values reported by Yuan et al (2013) were used.

299

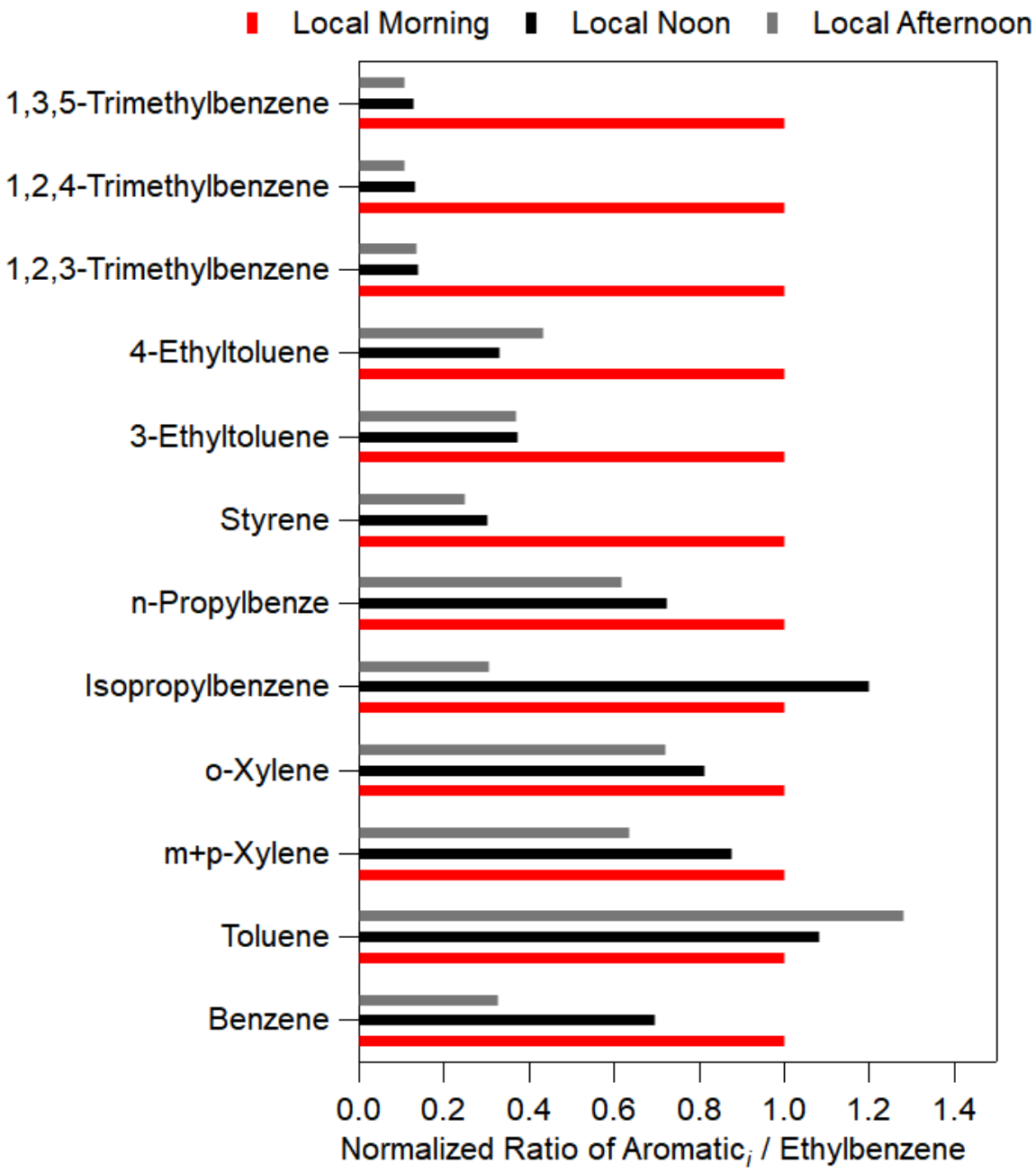

300

301 **SI Figure 20.** Comparison of various aromatic compounds/ethylbenzene ratios sampled over
302 Seoul, South Korea, during KORUS-AQ. The ratios are normalized by the morning ratios.

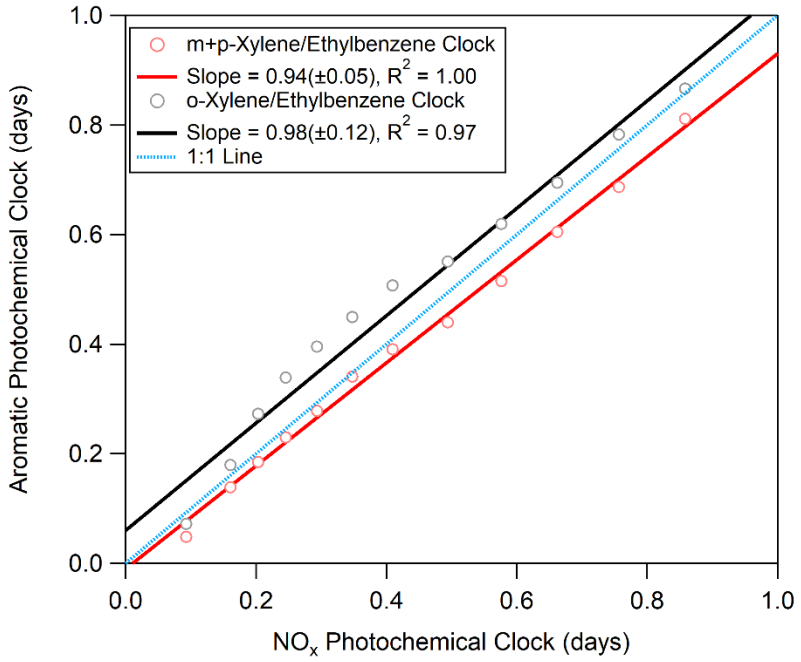

303

304 **SI Figure 21.** Binned scatter plot of the aromatic photochemical clock ages versus NO_x
305 photochemical clock ages for all observations over Seoul. All ages are normalized to OH = 1.5×10^6
306 molecules/cm^3.

SI Table 3. Rate constants used throughout this study. Unless noted otherwise, rate constants without temperature dependence only have a value measured at 298 K.

Reaction	Rate Constant (cm^3/molecules/s)	Reference
Inorganic		
CO	$2.28\times10^{-13,a}$	Sander et al. (2011)
NO_2	$1.23\times10^{-11,a}$	Mollner et al. (2010)
SO_2	$8.94\times10^{-13,a}$	Atkinson et al. (2004)
Alkanes		
Ethane	$6.9\times10^{-12}\times\exp(-1000/T)$	Atkinson et al. (2006)
Propane	$7.6\times10^{-12}\times\exp(-585/T)$	Atkinson et al. (2006)
n-Butane	$9.8\times10^{-12}\times\exp(-425/T)$	Atkinson et al. (2006)
i-Butane	$1.17\times10^{-17}\times T^2\times\exp(213/T)$	Atkinson (2003)
n-Pentane	$2.52\times10^{-17}\times T^2\times\exp(158/T)$	Atkinson (2003)
i-Pentane	3.6×10^{-12}	Atkinson (2003)
n-Hexane	$2.54\times10^{-14}\times T\times\exp(-112/T)$	Atkinson (2003)
Methyl-cyclopentane	7.65×10^{-12}	Sprengnether et al. (2009)
Cyclohexane	$3.26\times10^{-17}\times T^2\times\exp(262/T)$	Atkinson (2003)
Methyl-cyclohexane	9.43×10^{-12}	Sprengnether et al. (2009)
n-Heptane	$1.95\times10^{-17}\times T^2\times\exp(406/T)$	Atkinson (2003)
n-Octane	$2.72\times10^{-17}\times T^2\times\exp(361/T)$	Atkinson (2003)
n-Nonane	$2.53\times10^{-17}\times T^2\times\exp(436/T)$	Atkinson (2003)
n-Decane	$3.17\times10^{-17}\times T^2\times\exp(406/T)$	Atkinson (2003)
Alkenes		
Ethylene	$7.84\times10^{-12,a}$	Atkinson et al. (2006)
Propene	$2.86\times10^{-11,a}$	Atkinson et al. (2006)
1-butene	$6.6\times10^{-12}\times\exp(465/T)$	Atkinson et al. (2006)
i-butene	$9.4\times10^{-12}\times\exp(505/T)$	Atkinson et al. (2006)
cis-butene	$1.1\times10^{-11}\times\exp(485/T)$	Atkinson et al. (2006)
trans-butene	$1.0\times10^{-11}\times\exp(553/T)$	Atkinson et al. (2006)
1,3-butadiene	$1.48\times10^{-11}\times\exp(448/T)$	Atkinson and Arey (2003)
Aromatics		
Benzene	$2.3\times10^{-12}\times\exp(-190/T)$	Atkinson et al. (2006)
Toluene	$1.8\times10^{-12}\times\exp(340/T)$	Atkinson et al. (2006)
Ethylbenzene	7×10^{-12}	Atkinson and Arey (2003)
Isopropylbenzene	6.3×10^{-12}	Atkinson and Arey (2003)
n-propylbenzene	5.8×10^{-12}	Atkinson and Arey (2003)
Styrene	5.8×10^{-11}	Atkinson and Arey (2003)
m+p-xylene	$1.87\times10^{-11,b}$	Atkinson and Arey (2003)
o-xylene	1.36×10^{-11}	Atkinson and Arey (2003)
1,3,5-trimethylbenzene	$1.32\times10^{-11}\times\exp(450/T)$	Bohn and Zetzsch (2012)
1,2,3-trimethylbenzene	$3.61\times10^{-12}\times\exp(620/T)$	Bohn and Zetzsch (2012)
1,2,4-trimethylbenzene	$2.73\times10^{-12}\times\exp(730/T)$	Bohn and Zetzsch (2012)
3-Ethyltoluene	1.2×10^{-11}	Atkinson and Arey (2003)
4-Ethyltoluene	1.2×10^{-11}	Atkinson and Arey (2003)
S/IVOCs		

S/IVOC	2×10^{-11}	Ma et al. (2017)
Biogenics		
Isoprene	$2.7\times10^{-11}\times\exp(390/T)$	Atkinson et al. (2006)
α-pinene	$1.2\times10^{-11}\times\exp(440/T)$	Atkinson et al. (2006)
β-pinene	$1.55\times10^{-11}\times\exp(467/T)$	Atkinson and Arey (2003)
Radicals		
$NO + RO_2$	$2.8\times10^{-12}\times\exp(300/T)$	Sander et al. (2011)
$HO_2 + RO_2$	$4.1\times10^{-13}\times\exp(750/T)$	Sander et al. (2011)
$RO_2 + RO_2$	$9.5\times10^{-14}\times\exp(390/T)$	Sander et al. (2011)

[a]Showing the rate constant at 298 K, 1013 hPa. However, for this study, we used the temperature and pressure dependent formulation listed in each respective reference.
[b]This is the average of m-xylene and p-xylene rate constants.

SI 6. Potential SOA Calculations

To determine the amount of SOA produced from the observed precursors, Eq. S3 was used, where *Y* is the stoichiometric aerosol yield for each hydrocarbon (RH) species *i*, similar to other studies (e.g., Zhao et al., 2014). The updated yields from Ma et al. (2017) were used, which incorporate a correction for the gas-phase partitioning of semi-volatile compounds to chamber walls (Krechmer et al., 2016). Since there were no direct measurements of S/IVOC concentrations, an estimated (Robinson et al., 2007; Dzepina et al., 2009) relationship between the amount of gas-phase S/IVOC co-emitted with POA at the typical temperatures (~20°C) and OA mass concentrations (~10 μg sm^{-3}) observed over Seoul were used. The POA is taken from Figure 5b and is within the range of values observed in other urban environments (Zhang et al., 2005; Hayes et al., 2013; Ait-Helal et al., 2014; Kim et al., 2018) (13 μg sm^{-3} $ppmv^{-1}$ in Seoul versus 4.5 – 28.8 μg sm^{-3} $ppmv^{-1}$ in other studies).

$$P(OA) = \sum_i Y_i \times \Delta RH_i \quad \text{(S3)}$$

$$\Delta RH = \frac{RH(t)}{e^{(-k[OH]t)}} - RH(t) \quad \text{(S4)}$$

The hydrocarbons measured on the DC-8 were the concentrations at time, *t*; thus, Eq. SS4 was used, which takes into account the amount of OH that oxidized the hydrocarbon (OH_{exp} =

329 [OH]t) between emissions and measurement, and k is the OH rate constant for each specific
330 hydrocarbon (SI Table 3).

331 Finally, to determine the fate of the RO_2 radical in the reactions over Seoul (high/low NO_x
332 regime), and thus, what aerosol yields to use, the RO_2 lifetime with reaction of NO, HO_2, and RO_2
333 versus photochemical age was calculated (SI Figure 22). The measured NO and HO_2 was used in
334 the calculations, we assumed RO_2 was approximately the same concentration as HO_2 in this
335 calculation (Thornton et al., 2002), and the rate constants in SI Table 3 were used to calculated the
336 lifetime and fractional fate of RO_2. The fate of RO_2 with autoxidation is not included as the rate is
337 still uncertain (Crounse et al., 2013) and it should be less important in highly polluted
338 environments such as Seoul, especially at the lower photochemical ages (< 0.5 eq. days) where
339 most SOA is observed to be formed. The dominant sink of RO_2 over Seoul during KORUS-AQ is
340 the reaction with NO, suggesting that the SOA yields for “high NO” conditions should be used to
341 describe the production of SOA.

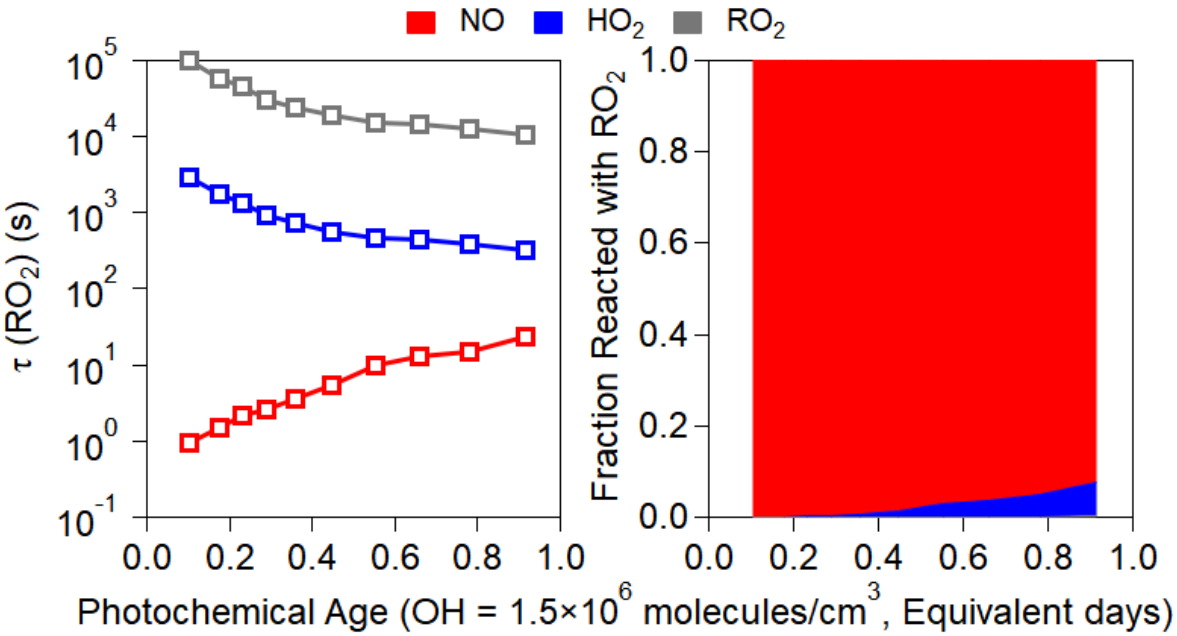

SI Figure 22. (left) Lifetime of RO_2 due to reactions with NO (red), HO_2 (blue), and RO_2 (grey) versus NO_x photochemical clock, normalized by OH = 1.5×10^6 molecules/cm^3. (right) Fraction of RO_2 reacting with NO (red), HO_2 (blue), or RO_2 (red) versus NO_x photochemical clock, normalized by OH = 1.5×10^6 molecules/cm^3. Values are calculated using observations over Seoul, South Korea, during KORUS-AQ, and RO_2 is assumed to be approximately equal to HO_2 (Thornton et al., 2002).

SI 7. FLEXPART Source Analysis

Source contributions have been estimated using Lagrangian backtrajectory calculations with the FLEXPART-WRF model (Brioude et al., 2013) in version 3.3.1, driven by meteorological output from NCEP GFS (NCEP) analyses downscaled to 5 km horizontal resolution using the Weather Research and Forecasting (WRF) model (Skamarock et al., 2008) in combination with the CREATE emission inventory (Woo et al., 2013). Approximately 20,000 parcels are released in 1 min intervals from the then-current location of the DC-8 during its research flights and parcel trajectories are followed back in time for 24 hours. The total time parcels spent in the lowermost 100 m—as surrogate for air having contact with an emission source at the ground—is recorded (residence time, [s kg^{-1} m^3]) and then folded with the emission fluxes ([kg m^{-2} s^{-1}]) given by the CREATE inventory for different compounds and source regions. This delivers an estimate of the source contribution (as increment in volume mixing ratio at the receptor, i.e., the DC-8 location) of the emissions of a given compound from a given region, assuming a perfect transport simulation and an inert compound.

SI 8. Intercomparisons of CU-AMS with Other Measurements on the NASA DC-8

We evaluate the measurement comparisons of the CU-AMS versus other aerosol measurements on-board the DC-8 during KORUS-AQ. We start with the mist chamber / ion chromatograph instrument (MC/IC), which has a comparable size cut as the AMS. The comparisons for SO_4 show good correlation ($R^2 = 0.76$) and slope close to 1 (0.95) (SI Figure 23). The higher scatter for the MC/IC is thought to arise from the lag and smearing in the measurements that has been observed in prior studies (TAbMET, 2009). For example, the correlation between instruments without lag and smearing have R^2 of 0.87 – 0.91 (CU-AMS versus extinction and CU-AMS vs K-AMS for certain RFs). If the MC/IC and CU-AMS SO_4 measurements are averaged to the sampling frequency of the University of New Hampshire filters (not shown), the R^2 improves (0.82) with no impact on the slope.

The comparison between the UNH filters and CU-AMS SO_4 shows higher R^2 (0.86) but lower slope (0.80), compared to MC/IC vs. CU-AMS. The higher R^2 is likely due to longer averaging time and lack of smearing that occurred with the MC/IC. As a comparison, the R^2 between MC/IC and filters are 0.84. The lower slope for the filters than the MC/IC is thought to be due to the different size cut-offs for the two measurements. For the filters, the upper size cut-off is ~4 μm (McNaughton et al., 2007); whereas, the upper size cut-off for the MC/IC is comparable to the AMS aerosol size cut-off (~ 1 μm aerodynamic). This means that the filter samples may include SO_4^{2-} from sea salt (sodium and calcium) and dust (calcium) (Heo et al., 2009; Kim et al., 2016; Heim et al., 2018). This is shown in SI Figure 24 and described in detail in Heim et al. (2018). Heim et al. (2018) found that dust dominated supermicron aerosol for approximately half of the campaign, and during these periods, supermicron SO_4^{2-} accounted for ~50% of the total SO_4^{2-} (sub plus supermicron). Taken together, the comparisons of SO_4 mass

concentrations from the CU-AMS from these two different methods (filter and MC/IC) indicate that the CU-AMS quantitatively captures the concentrations of SO_4.

Next, we compare the non-refractory species concentrations measured by the CU- and K-AMS. Intercomparisons between these two measurements for a few flights have been presented in prior publications (Hu et al., 2018a, 2018b). The K-AMS used a capture vaporizer, which leads to CE of ~1 for all ambient species (Hu et al., 2017a, 2017b; Xu et al., 2017). Here, we investigate the entire campaign. As shown in SI Figure 25, $R^2 > 0.80$ for all five species, and all slopes fall within ±20% of unity, which is within the combined uncertainty of both AMSs (~27%). However, at high concentrations (greater than ~5 – 10 μg sm^{-3}), the scatter between the two measurements increases, and for some species (e.g., SO_4), there is a slight curvature in the comparisons, where CU-AMS is greater than K-AMS. We believe this discrepancy originated from differences in transmission vs. particle size through the aerosol inlet and focusing lens (SI Figure 26). In-field calibrations showed that The K-AMS had 50% transmission at 615 nm (vacuum aerodynamic diameter; DeCarlo et al. (2004)), compared to the CU-AMS 50% transmission occurring at 900 nm. The reasons for the smaller transmission of the K-AMS are likely related to the PCI design (Bahreini et al., 2008, 2009) or possibly an underperforming aerodynamic lens in K-AMS (Liu et al., 2007). It was found that, in general, the RFs could be split between RFs generally below the K-AMS size cut-off (RFs 1 – 9, 11, 15, and 19) and above the size cut-off (RFs 10, 12 – 14, 16 – 18, 20) (SI Figure 27). The slopes and R^2 greatly improves for the observations below the K-AMS cut-off versus above (for slopes, 1.02 versus 0.84 and for R^2, 0.91 versus 0.82).

Finally, the ratios of the total AMS PM_1 masses measured by CU-AMS and K-AMS remain nearly constant about one (within ±11%) for the entire campaign and show no trend with estimated CE (for the standard vaporizer only) using the Middlebrook et al. (2012) algorithm (SI Figure 28).

Thus, when accounting for transmission effects, the two AMSs agree to within 10%, and the CU-AMS agrees to within 20% with the other co-located aerosol mass concentration measurements (filters and MC/IC) on the DC-8. This provides overall confidence in the calculated CE for the standard vaporizer (Middlebrook et al., 2012), RIE, and transmission of PM_1 for the CU-AMS measurements.

Besides directly comparing species mass, another well-established method to investigate aerosol instrument quantification is to compare the measured PM_1 mass (CU-AMS plus BC from SP2) versus the submicron extinction measured using methods described in Section 2.3.2 (nephlometer for scattering and absorption by PSAP) (e.g., DeCarlo et al., 2008). During KORUS-AQ, the slope between mass and extinction is 6.00 $m^2\ g^{-1}$ (SI Figure 29) with an R^2 of 0.87. The high correlation and similar slope compared to prior comparisons (Hand and Malm, 2007; DeCarlo et al., 2008; Dunlea et al., 2009; Shinozuka et al., 2009; Liu et al., 2017) indicates that the CU-AMS was not substantially impacted by the aerosol transmission effects discussed above. Also, the strong correlation ($R^2 = 0.87$) between the two instruments, which both have comparable, very high time resolution, indicate that the CU-AMS did not experience any plume recovery artifacts that were observed with the MC/IC or artifacts in measuring highly concentrated plumes.

Finally, we compare the PM_1 volume concentrations estimated from the LAS PM_1 versus the CU-AMS plus SP2. For this comparison, we use the calibrated AMS transmission curve during this campaign (SI Figure 30), which is consistent with those from recent studies (Knote et al., 2011; Hu et al., 2017b), to correct for particle transmission differences between the instruments. The LAS diameters were corrected by a factor of 1.115 from the PSL-calibrated values, to account for the lower refractive index of ambient particles, similar to Liu et al. (2017). To estimate the volume concentration from the combined AMS and BC measurements, we assume additive species

volumes (DeCarlo et al., 2004). Species densities of 1.78 g cm^{-3} for NH_4, pNO_3, and SO_4 (Lide, 1991; Salcedo et al., 2006), 1.52 g cm^{-3} for Chl (Lide, 1991; Salcedo et al., 2006), 1.77 g cm^{-3} for BC (Park et al., 2004), and the OA density is estimated from the CU-AMS O/C and H/C ratios of OA using the parameterization of Kuwata et al. (2012). The comparison between total PM_1 volume estimated from the CU-AMS plus BC vs. versus LAS shows a correlation (R^2) of 0.86. However, the volume from AMS plus SP2 is higher (slope of 1.56) when comparing all of KORUS-AQ. We hypothesize that this may be due to saturation of the LAS detector at high particle concentrations that were frequently observed in this campaign (greater than 1800 particles cm^{-3} or total CU-AMS plus SP2 mass greater than 40 μg sm^{-3}), as has been observed in prior comparisons (Liu et al., 2017), or a change in the refractive index when OA becomes dominant at these high concentrations (Moise et al., 2015). Different filters are tested and shown in SI Figure 30 and SI ***Figure 31***, using both values reported in literature and values that represent a stable ratio between LAS and calculated CU-AMS plus SP2 volume. If we filter for data when there is less than 20 μg sm^{-3}, the slope drops to 1.00, showing agreement between within the combined uncertainties (R^2 = 0.79), and providing strong evidence that LAS saturation at higher concentrations is the main reason for the apparent disagreement when analyzing the entire campaign.

We further investigate (SI Figure 31) whether the slope could be due to LAS saturation or a bias in RIE_{OA}, or in CE, vs. the values used in our analyses (Jimenez et al., 2016; Xu et al., 2018). There is a slight increase in the ratio of AMS plus SP2 to LAS volumes versus OA/total CU-AMS mass at high fractions of OA, although still within the combined measurement uncertainties. With filtered data (less than 1600 particles cm^{-3} or total CU-AMS mass less than 20 μg sm^{-3}), the volume ratios remain nearly flat, even at high *f*(OA). This confirms that LAS saturation is the most likely cause for the differences. Finally, a recent study (Xu et al., 2018) has reported new laboratory

measurements of RIE_{OA} = 1.6±0.5, although these authors indicated that it was unclear whether this value was applicable to ambient particles, and the value of RIE_{OA} = 1.4 used in this study is well within their reported uncertainty. When using RIE_{OA} = 1.6 in our analysis (not shown) the slope for the entire dataset decrease by only 6% (1.56 to 1.47), indicating that RIE uncertainties cannot explain the bulk of the observed difference.

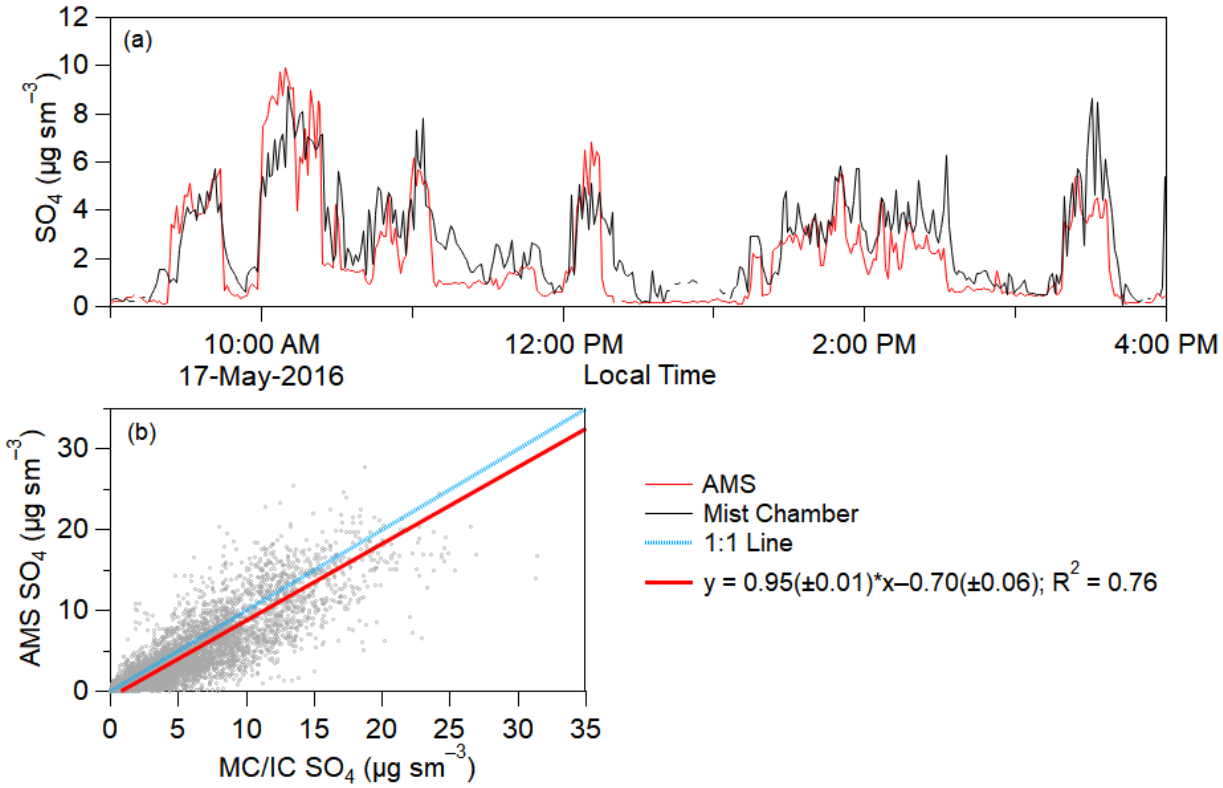

SI Figure 23. (top) Time series of mist-chamber (dark red line) and CU-AMS (red line) SO_4 for one flight (RF17). (bottom) Scatter plot of CU-AMS SO_4 versus mist-chamber ion-chromatograph (MC/IC) SO_4 for entire KORUS-AQ campaign.

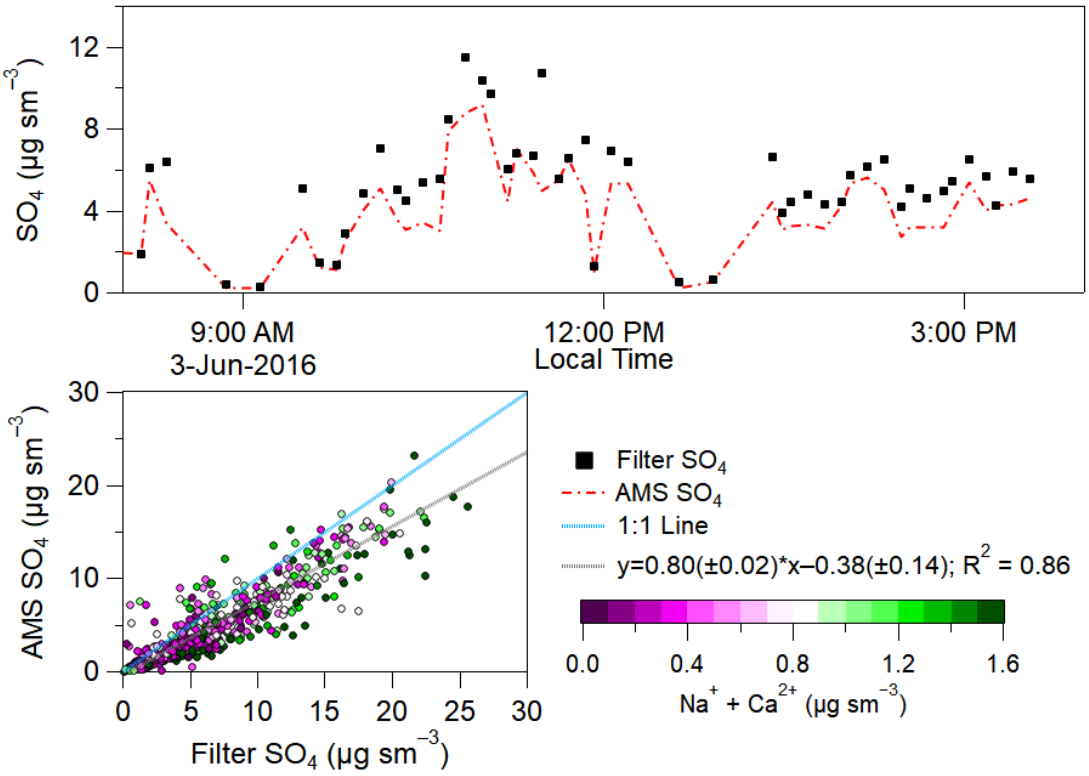

466

467 **SI Figure 24.** (top) Time series of filter (black squares) and CU-AMS (red line) SO_4 for one flight
468 (RF17). The CU-AMS data has been averaged to the filter sampling time. (bottom) Scatter plot of
469 CU-AMS SO_4 versus filter SO_4 for entire KORUS-AQ campaign. The points are colored by the
470 total sodium (Na^+) and calcium (Ca^{2+}) measured by the filters, as indicators of sea salt and dust,
471 respectively.

472

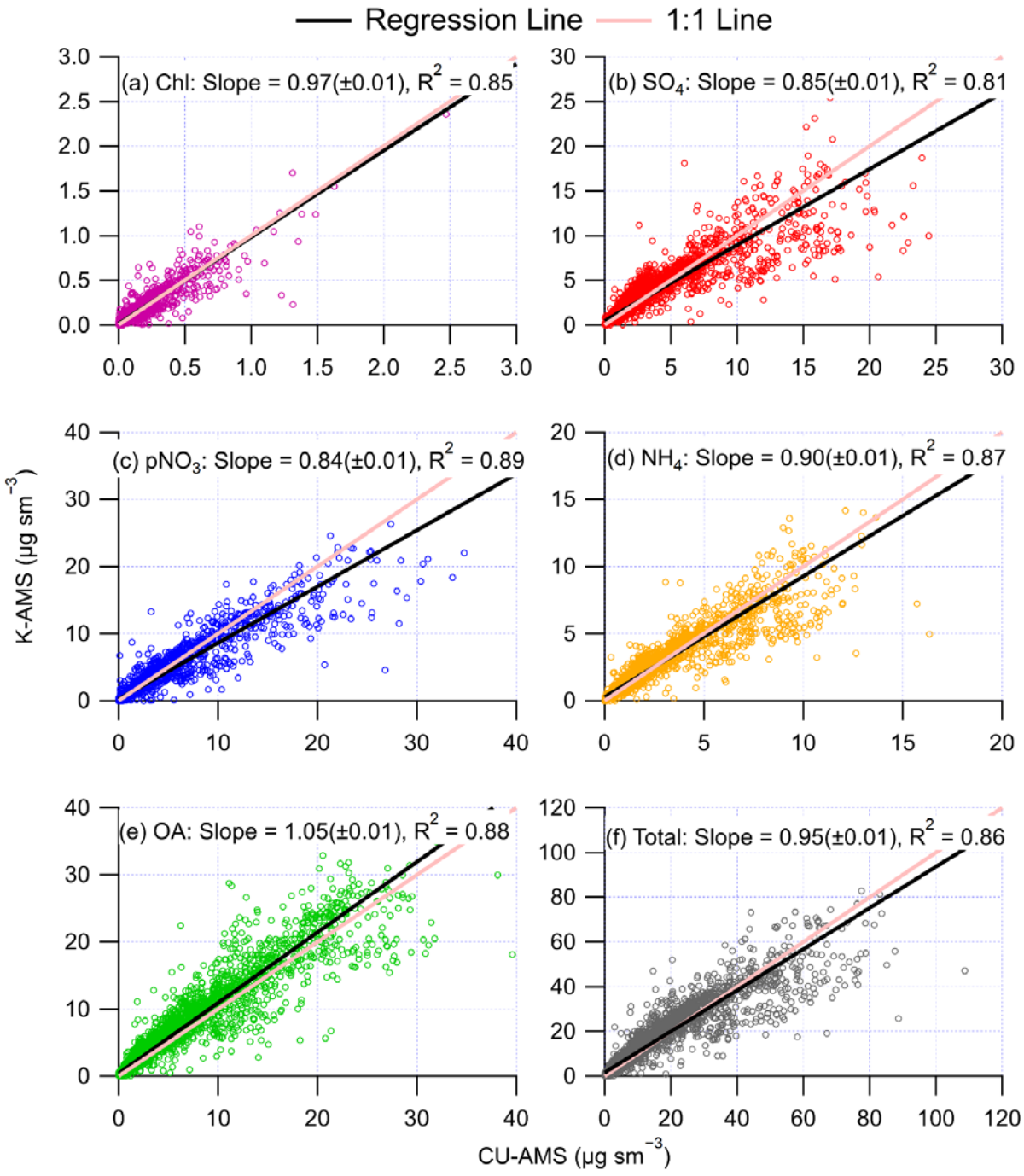

473

474 **SI Figure 25.** Scatter plot of not transmission corrected K-AMS versus CU-AMS mass
475 concentrations for all of KORUS-AQ for (a) Chl, (b) SO_4, (c) pNO_3, (d) NH_4, (e) OA, and (f) total
476 AMS mass. The slopes and R^2 for all comparisons are shown in each scatter plot.

477

478

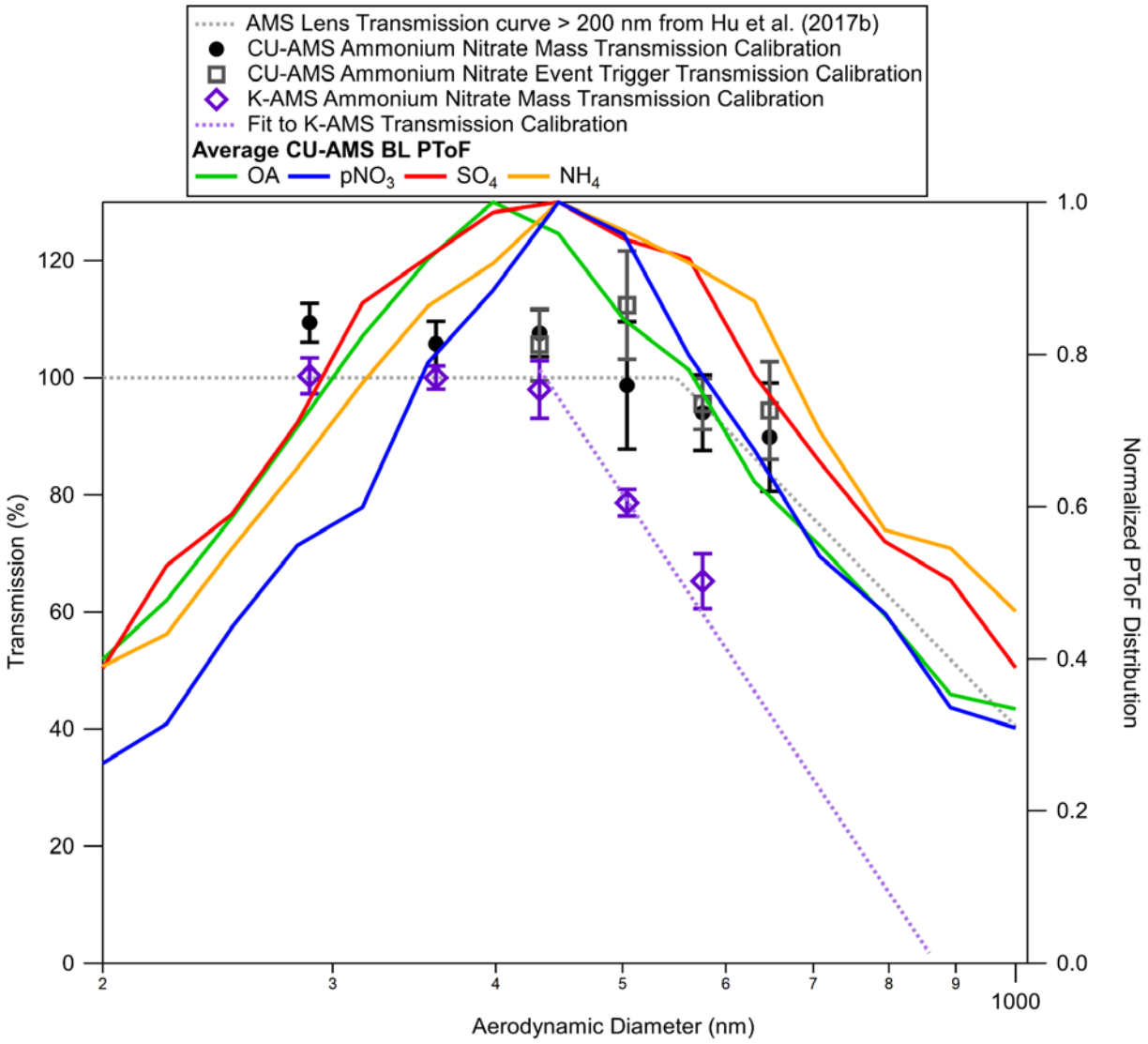

SI Figure 26. (left axis) Transmission curve for CU-AMS (black circle and dark grey square) and K-AMS (purple diamond). The curve from literature (Knote et al., 2011; Hu et al., 2017b), which describes the CU-AMS, is shown (grey dotted line). The fit for K-AMS transmission is shown with the purple dotted line. (right axis) Average mass distributions for OA (green), pNO_3 (blue), SO_4 (red), and NH_4 (orange) measured by CU-AMS in the boundary layer during KORUS-AQ. Note that some of the apparent signal at larger particle sizes is caused by the limited time response of the AMS detection system.

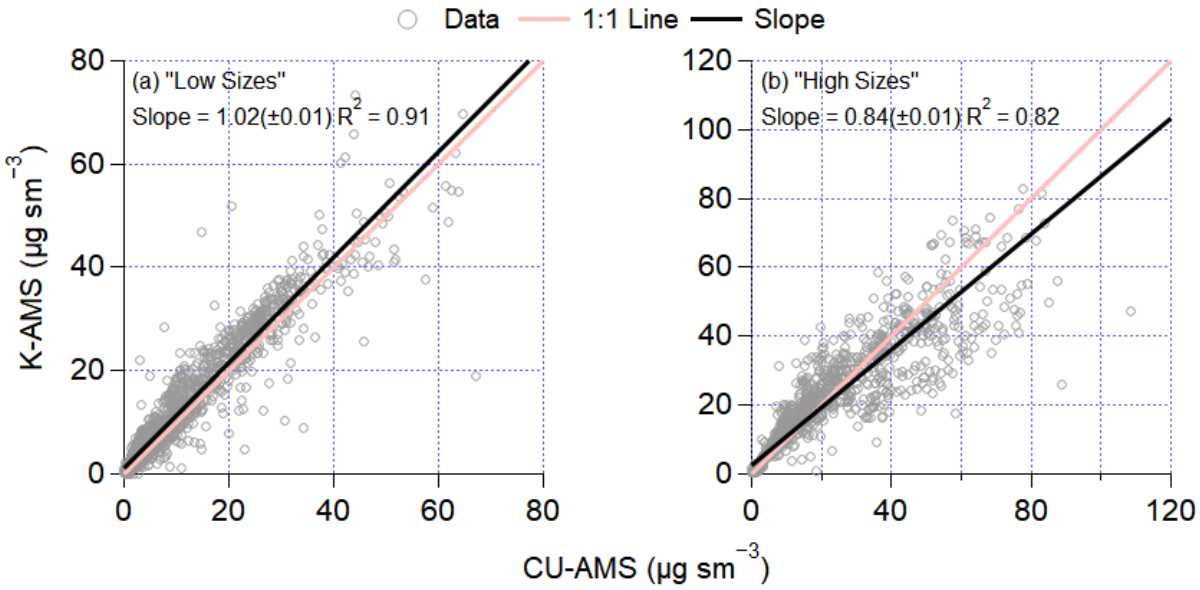

488

489 **SI Figure 27.** Scatter plot of K-AMS versus CU-AMS total mass concentrations (a) RFs 1 – 9, 11,
490 15, and 19 and (b) RFs 10, 12 – 14, 16 – 18, and 20. These are flights where the average sizes were
491 found below (a) and above (b) the K-AMS size cut-off (SI Figure 26). The slopes and R^2 for all
492 comparisons are shown in each scatter plot.

493

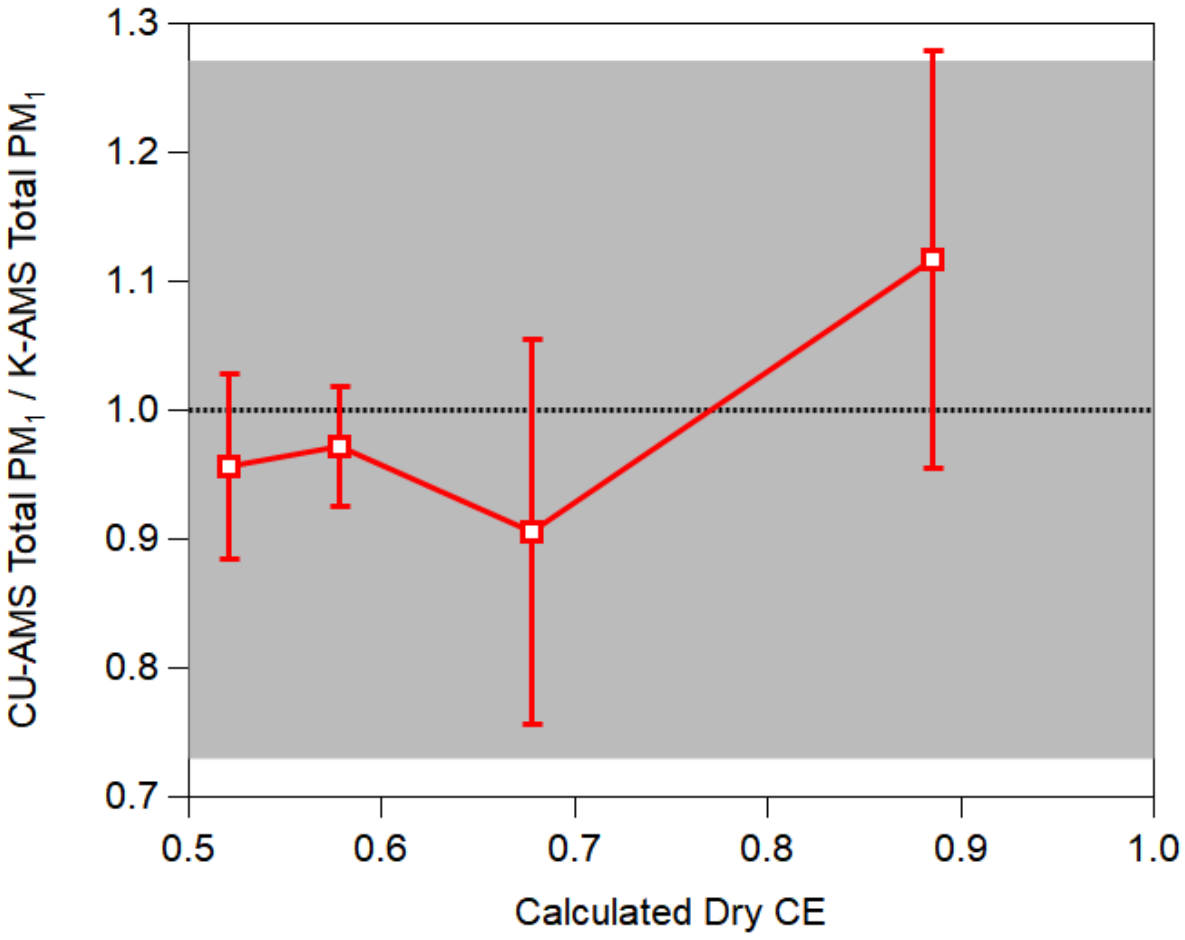

SI Figure 28. Binned total PM_1 AMS mass ratios, normalized by the average ratio, versus the calculated CE used for the CU-AMS measurements. The error bars are the standard error about the mean, and the shaded grey area is the combined uncertainty of the two AMS measurements (±27%). The data is only for flights where the PM_1 sizes were typically below the K-AMS size cut-off (RFs 1 – 9, 11, 15, and 19).

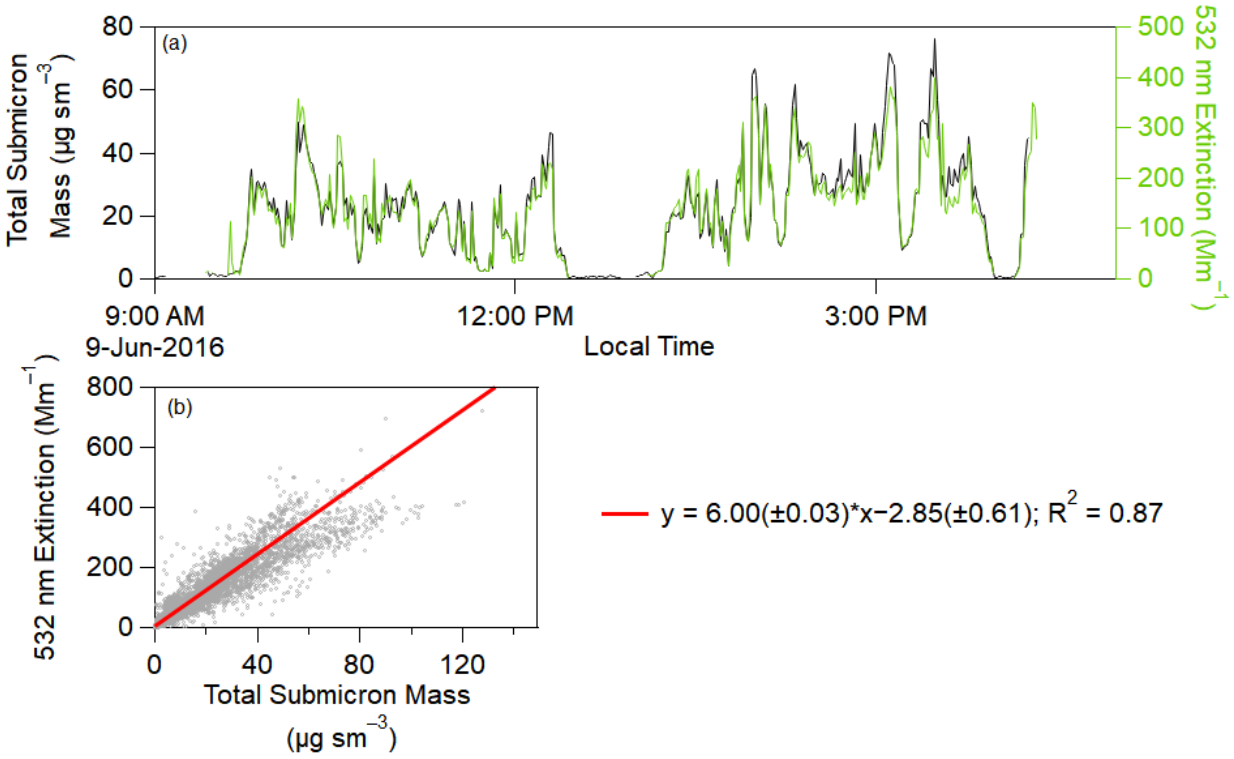

500

501 **SI Figure 29.** (top) Time series of total submicron mass (black, left axis) and 532 nm extinction
502 (green, right axis) for one flight (RF19). (bottom) Scatter plot of 532 nm extinction versus total
503 submicron mass (black carbon + CU-AMS species) for the entire KORUS-AQ campaign.

504

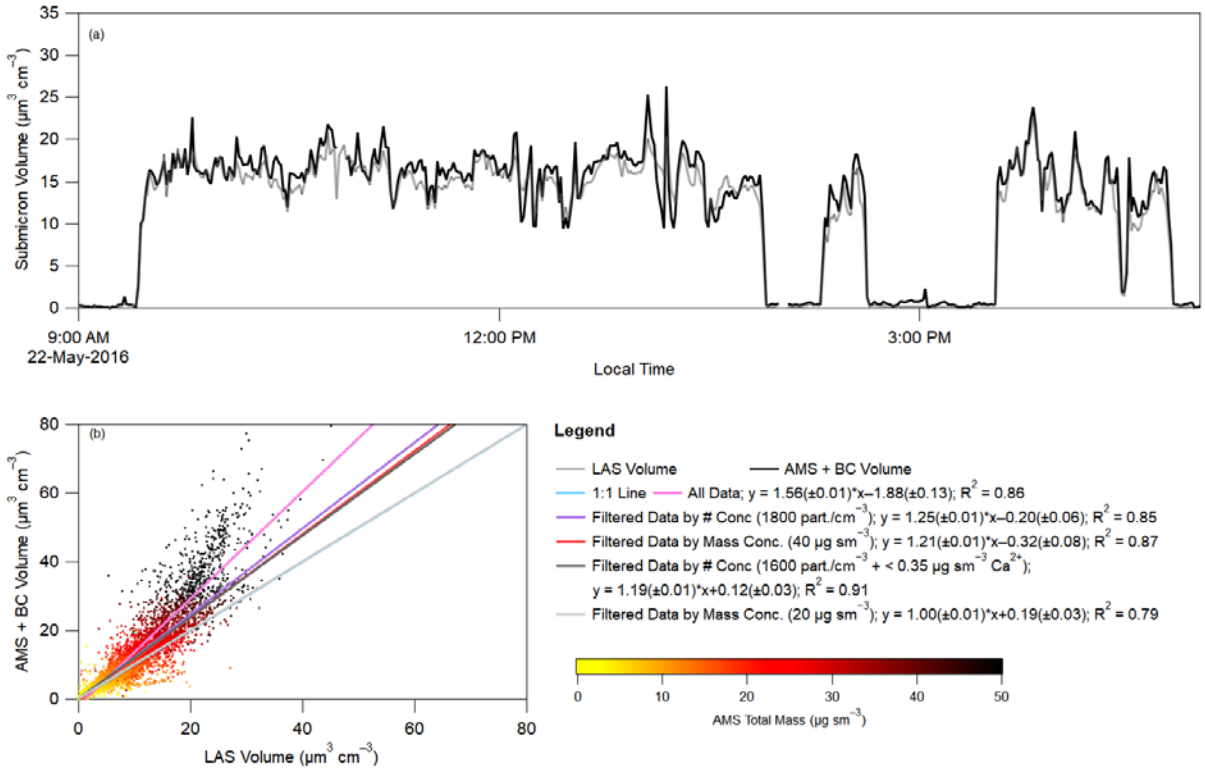

SI Figure 30. (top) Time series of total submicron volume from LAS (grey dashed line) and CU-AMS plus black carbon (black) for one flight (RF11). (bottom) Scatter plot of total submicron volume (black carbon + CU-AMS species) versus LAS volume for entire KORUS-AQ campaign. The data is colored by total CU-AMS mass. Pink line is a fit to all data, the purple line is a fit to data where the particle number concentration is less than 1800 particles scm^{-3}. The red line is a fit to the data where the CU-AMS plus SP2 total mass is less than 40 μg sm^{-3}. The black line is a fit to the data where the particle number concentration is less than 1600 particles scm^{-3} and Ca^{2+} concentration is less than 0.35 μg sm^{-3}. Finally, the grey line is a fit to the data where the CU-AMS plus BC total mass is less than 20 μg sm^{-3}.

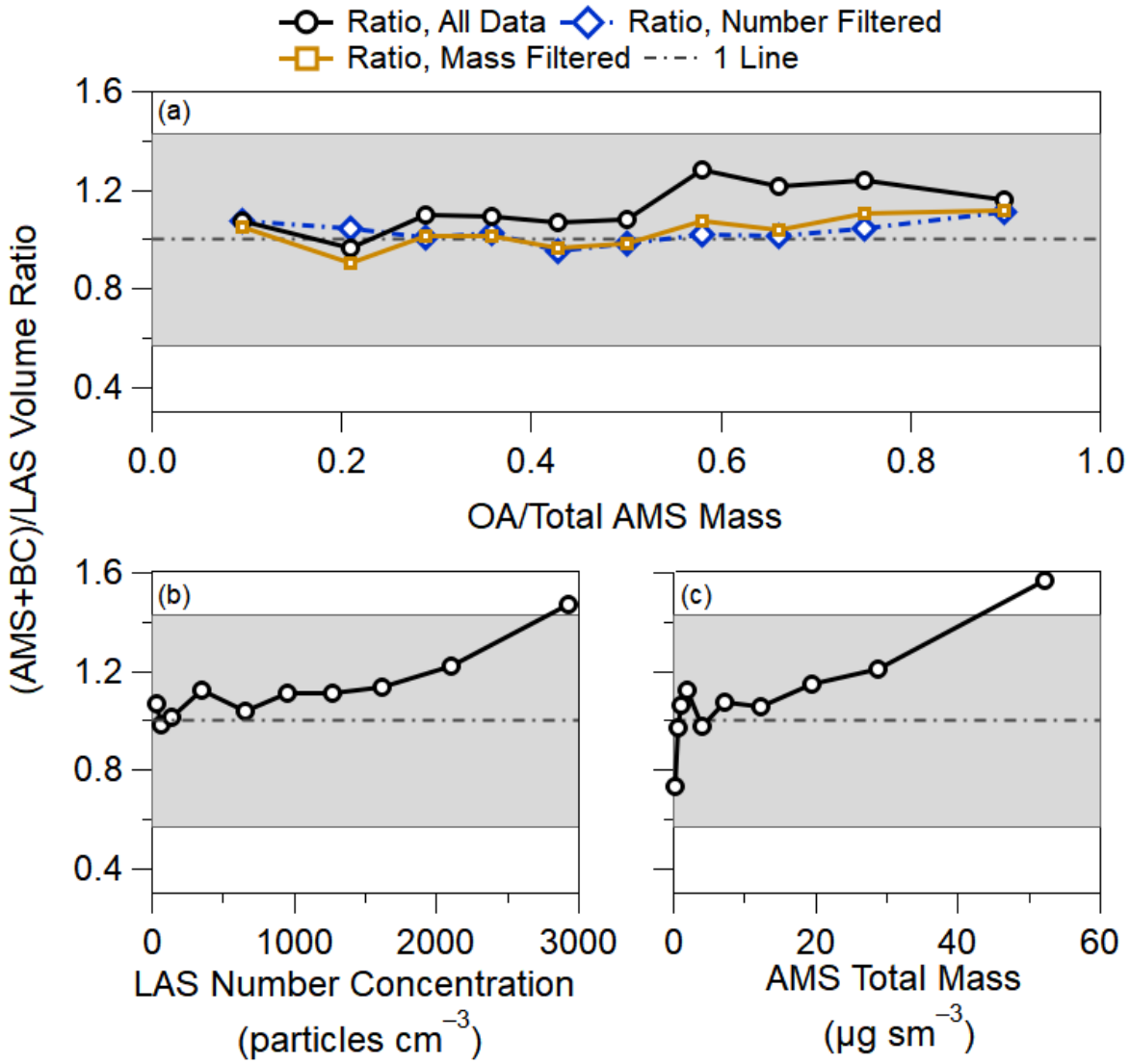

516

517 **SI Figure 31.** (a) Binned volume ratio (CU-AMS plus black carbon volume/LAS Volume) versus
518 fraction of organic aerosol (OA) to total CU-AMS mass. (b) Binned volume ratio versus LAS
519 particle number concentration. (c) Binned volume ratio versus CU-AMS total mass. In all figures,
520 the black data is for all data whereas the blue data is for the volume ratio where the particle number
521 concentration is less than 1600 particles cm^{-3} and the orange data is for the volume ratio where the
522 CU-AMS total mass concentration is less than 20 µg sm^{-3}. Also, the shaded area represents the
523 combined uncertainty in both measurements (Bahreini et al., 2009).

524

SI 9. Fractional PM_1 Contribution to Vertical Profile

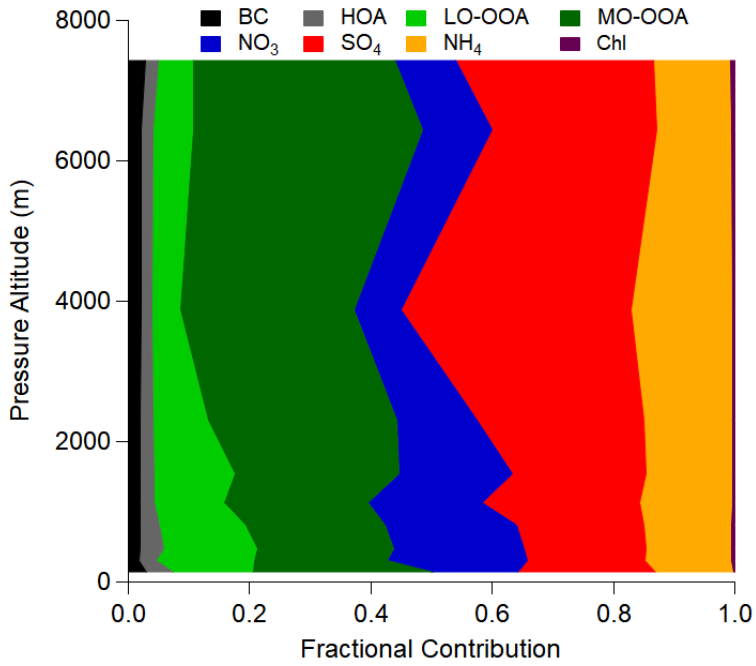

SI Figure 32. Fractional contribution of PM_1 contribution vertical profile for all of KORUS-AQ.

SI 10. Observed Aerosol Production over Seoul, South Korea

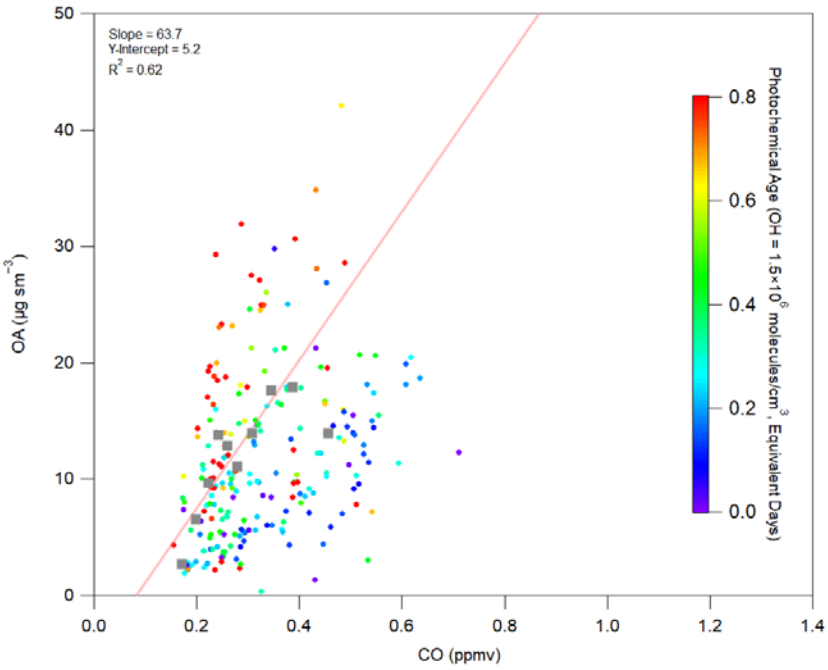

SI Figure 33. Scatter plot of OA versus CO, observed over Seoul, during KORUS-AQ. The points are colored by the NO_x photochemical clock. The fit is for the decile binned data.

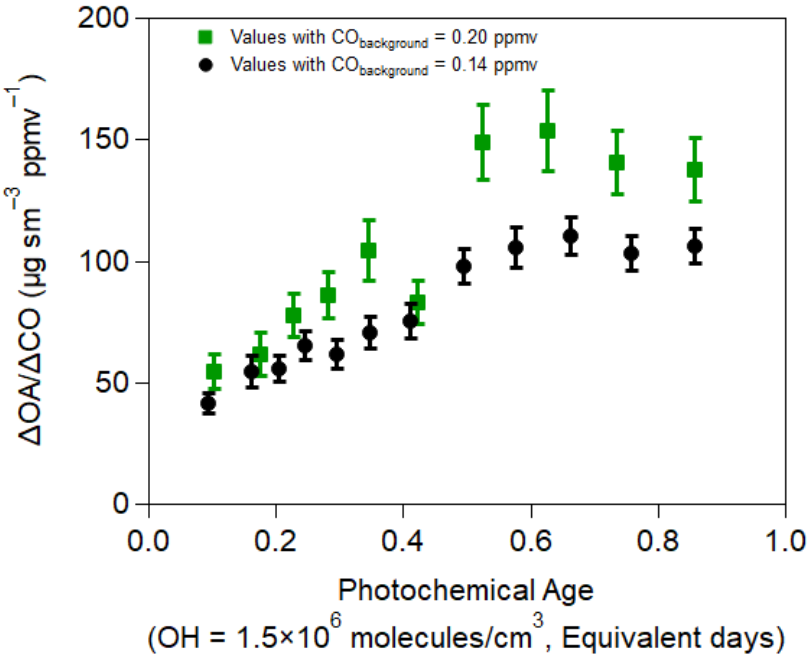

SI Figure 34. Comparison of ΔOA/ΔCO observed over Seoul with different CO backgrounds.

SI Table 4. Compilation of slopes used to convert from ΔOA/ΔCO to ΔOA/ΔCO$_2$ used in this study.

Location	*Slope (ppmv CO/ppmv CO$_2$)*	*Study*
Mexico City	0.045	Vay et al. (2009)
Los Angeles	0.009	Peischl et al., (2013)
Beijing	0.02	Wang et al. (2010)
		Silva et al. (2013)
		Tohjima et al. (2014)
Outflow China	0.02	Wang et al. (2010)
		Silva et al. (2013)
		Tohjima et al. (2014)
Seoul	0.01	Silva et al. (2013)
		Tang et al. (2018)

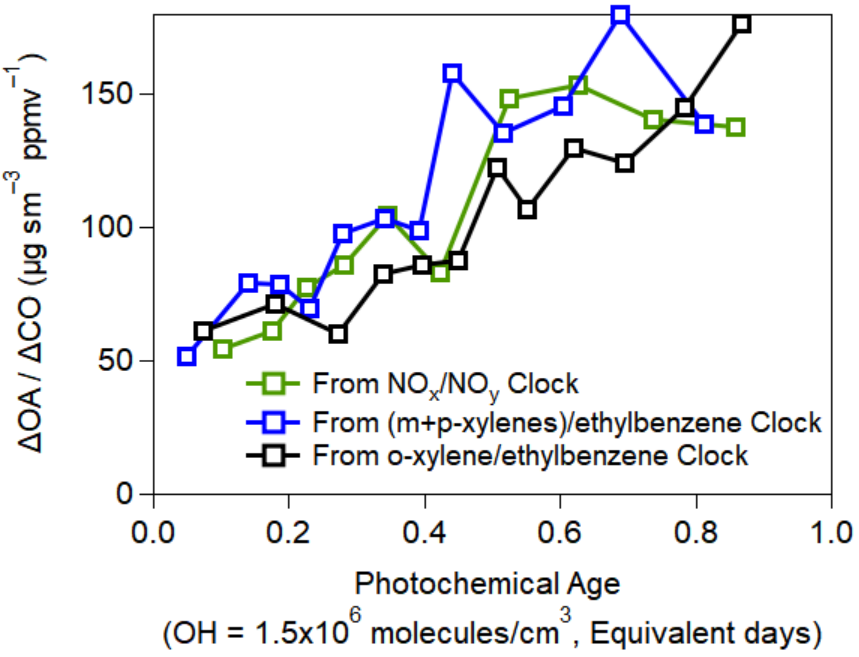

SI Figure 35. Same as **Figure 4**(a), but comparing results using three different photochemical clocks (SI Figure 21).

SI 11. Oxidation of OA

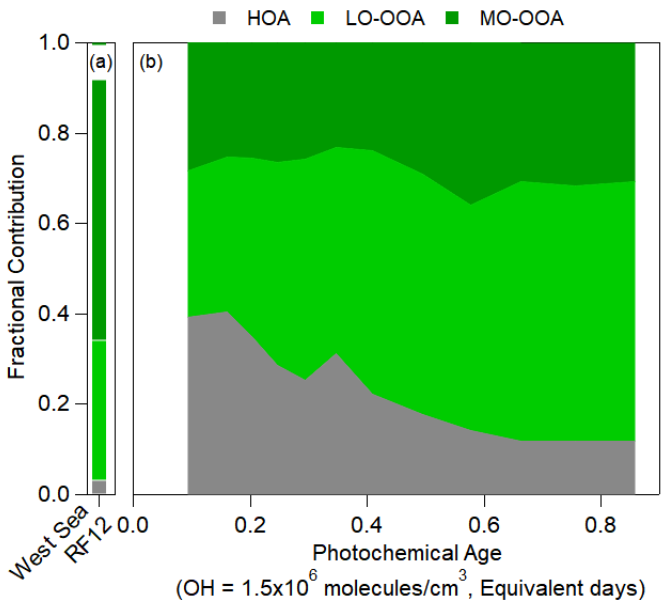

SI Figure 36. Same as **Figure 6**b, but speciated for MO-OOA, LO-OOA, and HOA. (a) is over the West Sea (RF12) and (b) is over Seoul.

First, we briefly discuss how the AMS OA source tracers typically used to investigate OA chemistry evolved over Seoul (SI Figure 37). During KORUS-AQ, there was no appreciable influence from isoprene production of IEPOX-SOA (Hu et al., 2015), as the ion indicative of isoprene IEPOX-SOA ($C_5H_6O^+$) remained at background values typical of air without isoprene SOA influence.

Similarly, biomass burning OA (BBOA) appeared to be present but dilute in its contribution to OA. Most of the OA had $f_{C_2H_4O_2}$, an ion indicative of biomass burning and levoglucosan (Schneider et al., 2006; Aiken et al., 2010), below 0.1 over Seoul, and the PMF factors fall near the limit of detection for BBOA (Cubison et al., 2011) and lower than the values that typically indicate ambient and laboratory BBOA emissions at various stages of chemical evolution (Cubison et al., 2011; Ortega et al., 2013). We speculate that the limited BBOA is highly

mixed into the OA from the numerous, small agricultural fires that were observed during the campaign and have been observed during this time period, during other years, in South Korea (Kang et al., 2006). However, the amount of fresher BBOA was not high enough, nor as strong of a feature as observed in prior studies (Aiken et al., 2010; DeCarlo et al., 2010; Cubison et al., 2011; Hu et al., 2016), to reliably resolve a separate BBOA PMF factor. As shown in SI Figure 11, typical gas-phase biomass burning tracers (CO, NO_x, acetonitrile, HCN, and black carbon) do not show a consistent strong correlation with any of the PMF factors, further suggesting that BBOA is not a major contributor, and any BBOA present is highly mixed with HOA and the oxidized OA. Consistent with our results, Kim et al. (2017) did not resolve a BBOA factor from a ground site in Seoul during the KORUS campaign.

Similar to other studies over urban areas or for chamber studies oxidizing urban VOCs (e.g., benzene, xylenes, etc.) (Ng et al., 2010; Freney et al., 2014a; Ortega et al., 2016), marked chemical evolution was observed as tracked by the $C_2H_3O^+$ and CO_2^+ ions. The evolution of these two ions, as a fraction of total OA, fall in the same space as has been observed in these prior studies, indicating consistent photochemical evolution of SOA over urban locations.

Finally, unlike Kim et al. (2017), we did not observe clear indication for cooking organic aerosol (COA) in our PMF results. The COA was at a minimum (less than 1 $\mu g\ m^{-3}$) at the surface in Seoul during the times the DC-8 overpassed (Kim et al., 2018); thus, we speculate the amount of COA sampled was a small fraction of OA and was mostly lumped into the HOA factor. This does not affect our characterization of HOA as POA, since COA is also a primary aerosol emission.

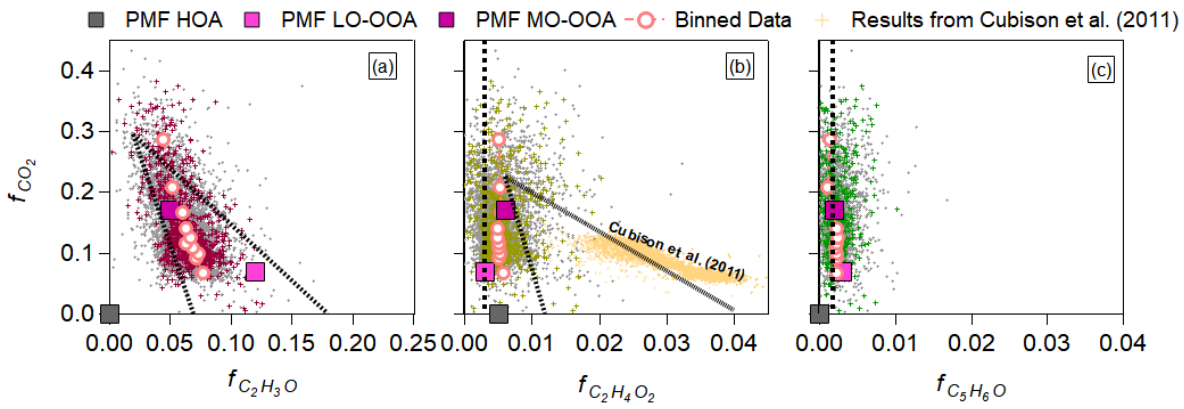

581

582 **SI Figure 37.** Plots of (a) f_{CO_2} versus $f_{C_2H_3O}$, (b) f_{CO_2} versus $f_{C_2H_4O_2}$, and (c) f_{CO_2} versus $f_{C_5H_6O}$.
583 Points highlighted in color refer to observations over Seoul, South Korea, during KORUS-AQ. In
584 (a), the triangle is from Ng et al. (2010); in (b), the triangle is from Cubison et al. (2011), and the
585 vertical line is the typical "background" values for $f_{C_2H_4O_2}$ from Cubison et al. (2011); and, in (c),
586 the vertical line is the typical "background" values for $f_{C_5H_6O}$ from Hu et al. (2015). The PMF
587 results for each triangle plot are shown in squares, where grey is HOA, light pink is LO-OOA, and
588 dark pink is MO-OOA. The light orange dots in (b) are the observations from ARCTAS forest
589 fires (Cubison et al., 2011), as an example for data strongly impacted by biomass burning. The
590 binned values for each comparison are shown in light red crosses.

591

592

References

Aiken, A. C., Salcedo, D., Cubison, M. J., Huffman, J. A., DeCarlo, P. F., Ulbrich, I. M., Docherty, K. S., Sueper, D., Kimmel, J. R., Worsnop, D. R., Trimborn, A., Northway, M., Stone, E. A., Schauer, J. J., Volkamer, R. M., Fortner, E., de Foy, B., Wang, J., Laskin, A., Shutthanandan, V., Zheng, J., Zhang, R., Gaffney, J., Marley, N. A., Paredes-Miranda, G., Arnott, W. P., Molina, L. T., Sosa, G. and Jimenez, J. L.: Mexico City aerosol analysis during MILAGRO using high resolution aerosol mass spectrometry at the urban supersite (T0) – Part 1: Fine particle composition and organic source apportionment, Atmos. Chem. Phys, 9(9), 6633–6653, doi:10.5194/acpd-9-8377-2009, 2009.

Aiken, A. C., de Foy, B., Wiedinmyer, C., DeCarlo, P. F., Ulbrich, I. M., Wehrli, M. N., Szidat, S., Prévôt, A. S. H., Noda, J., Wacker, L., Volkamer, R., Fortner, E., Wang, J., Laskin, A., Shutthanandan, V., Zheng, J., Zhang, R., Paredes-Miranda, G., Arnott, W. P., Molina, L. T., Sosa, G., Querol, X. and Jimenez, J. L.: Mexico City aerosol analysis during MILAGRO using high resolution aerosol mass spectrometry at the urban supersite (T0)-Part 2: Analysis of the biomass burning contribution and the non-fossil carbon fraction, Atmos. Chem. Phys., 10(12), 5315–5341, doi:10.5194/acp-10-5315-2010, 2010.

Ait-Helal, W., Borbon, A., Sauvage, S., De Gouw, J. A., Colomb, A., Gros, V., Freutel, F., Crippa, M., Afif, C., Baltensperger, U., Beekmann, M., Doussin, J.-F. F., Durand-Jolibois, R., Fronval, I., Grand, N., Leonardis, T., Lopez, M., Michoud, V., Miet, K., Perrier, S., Prévôt, A. S. H., Schneider, J., Siour, G., Zapf, P. and Locoge, N.: Volatile and intermediate volatility organic compounds in suburban Paris: Variability, origin and importance for SOA formation, Atmos. Chem. Phys., 14(19), 10439–10464, doi:10.5194/acp-14-10439-2014, 2014.

Akagi, S. K., Craven, J. S., Taylor, J. W., Mcmeeking, G. R., Yokelson, R. J., Burling, I. R., Urbanski, S. P., Wold, C. E., Seinfeld, J. H., Coe, H., Alvarado, M. J. and Weise, D. R.: Evolution of trace gases and particles emitted by a chaparral fire in California, Atmos. Chem. Phys., 12, 1397–1421, doi:10.5194/acp-12-1397-2012, 2012.

Aknan, A. and Chen, G.: KORUS-AQ DC-8 Aircraft Dataset, [online] Available from: https://www-air.larc.nasa.gov/cgi-bin/ArcView/korusaq (Accessed 6 December 2018), 2018.

Al-Saadi, J., Carmichael, G., Crawford, J., Emmons, L., Korean, S. K., Group, S., Song, C.-K., Chang, L.-S., Lee, G., Kim, J. and Park, R.: NASA Contributions to KORUS-AQ: An International Cooperative Air Quality Field Study in Korea, 2015.

Anderson, T. L. and Ogren, J. A.: Determining Aerosol Radiative Properties Using the TSI 3563 Integrating Nephelometer, Aerosol Sci. Technol., 29(1), 57–69, doi:10.1080/02786829808965551, 1998.

Arnold, S. R., Methven, J., Evans, M. J., Chipperfield, M. P., Lewis, A. C., Hopkins, J. R., Mcquaid, J. B., Watson, N., Purvis, R. M., Lee, J. D., Atlas, E. L., Blake, D. R. and Rappenglück, B.: Statistical inference of OH concentrations and air mass dilution rates from successive observations of nonmethane hydrocarbons in single air masses, J. Geophys. Res. Atmos., 112, D10S40, doi:10.1029/2006JD007594, 2007.

Atkinson, R.: Kinetics of the gas-phase reactions of OH radicals with alkanes and cycloalkanes, Atmos. Chem. Phys., 3(6), 2233–2307, doi:10.5194/acp-3-2233-2003, 2003.

Atkinson, R. and Arey, J.: Atmospheric Degradation of Volatile Organic Compounds, Chem. Rev.,

103, 4605–4638, doi:10.1021/CR0206420, 2003.

Atkinson, R., Baulch, D. L., Cox, R. A., Crowley, J. N., Hampson, R. F., Hynes, R. G., Jenkin, M. E., Rossi, M. J. and Troe, J.: Evaluated kinetic and photochemical data for atmospheric chemistry: Volume I - gas phase reactions of Ox, HO_x , NO_x and SO_x species, Atmos. Chem. Phys., 4(6), 1461–1738, doi:10.5194/acp-4-1461-2004, 2004.

Atkinson, R., Baulch, D. L., Cox, R. A., Crowley, J. N., Hampson, R. F., Hynes, R. G., Jenkin, M. E., Rossi, M. J., Troe, J. and IUPAC Subcommittee: Evaluated kinetic and photochemical data for atmospheric chemistry: Volume II - gas phase reactions of organic species, Atmos. Chem. Phys., 6(11), 3625–4055, doi:10.5194/acp-6-3625-2006, 2006.

Bahreini, R., Dunlea, E. J., Matthew, B. M., Simons, C., Docherty, K. S., DeCarlo, P. F., Jimenez, J. L., Brock, C. A. and Middlebrook, A. M.: Design and Operation of a Pressure-Controlled Inlet for Airborne Sampling with an Aerodynamic Aerosol Lens, Aerosol Sci. Technol., 42(6), 465–471, doi:10.1080/02786820802178514, 2008.

Bahreini, R., Ervens, B., Middlebrook, A. M., Warneke, C., de Gouw, J. A., DeCarlo, P. F., Jimenez, J. L., Brock, C. A., Neuman, J. A., Ryerson, T. B., Stark, H., Atlas, E., Brioude, J., Fried, A., Holloway, J. S., Peischl, J., Richter, D., Walega, J., Weibring, P., Wollny, A. G. and Fehsenfeid, F. C.: Organic aerosol formation in urban and industrial plumes near Houston and Dallas, Texas, J. Geophys. Res., 114(16), D00F16, doi:10.1029/2008JD011493, 2009.

Baklanov, A., Molina, L. T. and Gauss, M.: Megacities, Air Quality and Climate, Atmos. Environ., 126, 235–249, doi:10.1016/j.atmosenv.2015.11.059, 2016.

Blake, N. J., Blake, D. R., Sive, B. C., Katzenstein, A. S., Meinardi, S., Wingenter, O. W., Atlas, E. L., Flocke, F., Ridley, B. A. and Rowland, F. S.: The seasonal evolution of NMHC's and light alkyl nitrates at middle to northern latitudes during TOPSE, J. Geophys. Res., 108(D4), 8359, 2003.

Bohn, B. and Zetzsch, C.: Kinetics and mechanism of the reaction of OH with the trimethylbenzenes – experimental evidence for the formation of adduct isomers, Phys. Chem. Chem. Phys., 14(40), 13933, doi:10.1039/c2cp42434g, 2012.

Brioude, J., Arnold, D., Stohl, A., Cassiani, M., Morton, D., Seibert, P., Angevine, W., Evan, S., Dingwell, A., Fast, J. D., Easter, R. C., Pisso, I., Burkhart, J. and Wotawa, G.: The Lagrangian particle dispersion model FLEXPART-WRF version 3.1, Geosci. Model Dev., 6(6), 1889–1904, doi:10.5194/gmd-6-1889-2013, 2013.

Campuzano-Jost, P., Day, D. A., Nault, B. A., Schroder, J. C. and Jimenez, J. L.: Temporal Variability of the Pieber Effect and Some Notes on AMS Dection Limits, in 17th AMS Users' Meeting, Portland. [online] Available from: http://cires1.colorado.edu/jimenez-group/UsrMtgs/UsersMtg17/10-14-2016_PCJ_AMSUsersMtg_Prez.pdf (Accessed 5 April 2018), 2016.

Canagaratna, M. R., Jayne, J. T., Jimenez, J. L., Allan, J. D., Alfarra, M. R., Zhang, Q., Onasch, T. B., Drewnick, F., Coe, H., Middlebrook, A. M., Delia, A., Williams, L. R., Trimborn, A. M., Northway, M. J., DeCarlo, P. F., Kolb, C. E., Davidovits, P. and Worsnop, D. R.: Chemical and microphysical characterization of ambient aerosols with the Aerodyne Aerosol Mass Spectrometer, Mass Spectrom. Rev., 26(2), 185–222, doi:10.1002/mas, 2007.

Canagaratna, M. R., Jimenez, J. L., Kroll, J. H., Chen, Q., Kessler, S. H., Massoli, P., Hildebrandt

Ruiz, L., Fortner, E., Williams, L. R., Wilson, K. R., Surratt, J. D., Donahue, N. M., Jayne, J. T. and Worsnop, D. R.: Elemental ratio measurements of organic compounds using aerosol mass spectrometry: characterization, improved calibration, and implications, Atmos. Chem. Phys., 15(1), 253–272, doi:10.5194/acp-15-253-2015, 2015.

Cappa, C. D. and Jimenez, J. L.: Quantitative estimates of the volatility of ambient organic aerosol, Atmos. Chem. Phys., 10(12), 5409–5424, doi:10.5194/acp-10-5409-2010, 2010.

Cappa, C. D., Jathar, S. H., Kleeman, M. J., Docherty, K. S., Jimenez, J. L., Seinfeld, J. H. and Wexler, A. S.: Simulating secondary organic aerosol in a regional air quality model using the statistical oxidation model – Part 2: Assessing the influence of vapor wall losses, Atmos. Chem. Phys., 16(5), 3041–3059, doi:10.5194/acp-16-3041-2016, 2016.

Chen, Q., Heald, C. L., Jimenez, J. L., Canagaratna, M. R., He, L., Huang, X.-F., Campuzano-Jost, P., Palm, B. B., Poulain, L., Kuwata, M., Martin, S. T., Abbatt, J. P. D., Lee, A. K. Y., Liggio, J., Zhang, Q., He, L. and Huang, X.-F.: Elemental composition of organic aerosol: The gap between ambient and laboratory measurements, Geophys. Res. Lett., 42(10), 4182–4189, doi:10.1002/2015GL063693, 2015.

Choi, J. K., Heo, J. B., Ban, S. J., Yi, S. M. and Zoh, K. D.: Chemical characteristics of PM2.5 aerosol in Incheon, Korea, Atmos. Environ., 60, 583–592, doi:10.1016/j.atmosenv.2012.06.078, 2012.

Collier, S., Zhou, S., Onasch, T. B., Jaffe, D. A., Kleinman, L., Sedlacek, A. J., Briggs, N. L., Hee, J., Fortner, E., Shilling, J. E., Worsnop, D., Yokelson, R. J., Parworth, C., Ge, X., Xu, J., Butterfield, Z., Chand, D., Dubey, M. K., Pekour, M. S., Springston, S. and Zhang, Q.: Regional Influence of Aerosol Emissions from Wildfires Driven by Combustion Efficiency: Insights from the BBOP Campaign, Environ. Sci. Technol., 50(16), 8613–8622, doi:10.1021/acs.est.6b01617, 2016.

Craven, J. S., Metcalf, A. R., Bahreini, R., Middlebrook, A., Hayes, P. L., Duong, H. T., Sorooshian, A., Jimenez, J. L., Flagan, R. C. and Seinfeld, J. H.: Los Angeles Basin airborne organic aerosol characterization during CalNex, J. Geophys. Res. Atmos., 118(19), 11,453-11,467, doi:10.1002/jgrd.50853, 2013.

Crippa, M., Canonaco, F., Lanz, V. A., Äijälä, M., Allan, J. D., Carbone, S., Capes, G., Ceburnis, D., Dall'Osto, M., Day, D. A., DeCarlo, P. F., Ehn, M., Eriksson, A., Freney, E., Hildebrandt Ruiz, L. H., Hillamo, R., Jimenez, J. L., Junninen, H., Kiendler-Scharr, A., Kortelainen, A.-M., Kulmala, M., Laaksonen, A., Mensah, A. A., Mohr, C., Nemitz, E., O'Dowd, C., Ovadnevaite, J., Pandis, S. N., Petäjä, T., Poulain, L., Saarikoski, S., Sellegri, K., Swietlicki, E., Tiitta, P., Worsnop, D. R., Baltensperger, U. and Prévôt, A. S. H.: Organic aerosol components derived from 25 AMS data sets across Europe using a consistent ME-2 based source apportionment approach, Atmos. Chem. Phys., 14(12), 6159–6176, doi:10.5194/acp-14-6159-2014, 2014.

Crounse, J., McKinney, K. A., Kwan, A. J. and Wennberg, P. O.: Measurement of gas-phase hydroperoxides by chemical ionization mass spectrometry, Anal. Chem., 78(19), 6726–6732, doi:doi:10.1021/ac0604235, 2006.

Crounse, J. D., Nielsen, L. B., Jørgensen, S., Kjaergaard, H. G. and Wennberg, P. O.: Autoxidation of Organic Compounds in the Atmosphere, J. Phys. Chem. Lett., 4(20), 3513–3520, doi:10.1021/jz4019207, 2013.

Cubison, M. J., Ortega, A. M., Hayes, P. L., Farmer, D. K., Day, D. A., Lechner, M. J., Brune, W. H., Apel, E., Diskin, G. S., Fisher, J. A., Fuelberg, H. E., Hecobian, A., Knapp, D. J., Mikoviny, T., Riemer, D., Sachse, G. W., Sessions, W., Weber, R. J., Weinheimer, A. J., Wisthaler, A. and Jimenez, J. L.: Effects of aging on organic aerosol from open biomass burning smoke in aircraft and laboratory studies, Atmos. Chem. Phys., 11(23), 12049–12064, doi:10.5194/acp-11-12049-2011, 2011.

Day, D. A., Wooldridge, P. J., Dillon, M. B., Thornton, J. A. and Cohen, R. C.: A thermal dissociation laser-induced fluorescence instrument for in situ detection of NO_2, peroxy nitrates, alkyl nitrates, and HNO_3, J. Geophys. Res., 107(D5-6), 4046, doi:10.1029/2001JD000779, 2002.

DeCarlo, P. F., Slowik, J. G., Worsnop, D. R., Davidovits, P., Jimenez, J. L., Stainken, K., Williams, L., Jayne, J., Kolb, C. and Rudich, Y.: Particle Morphology and Density Characterization by Combined Mobility and Aerodynamic Diameter Measurements. Part 1: Theory, Aerosol Sci. Technol., 38(12), 1185–1205, doi:10.1080/027868290903907, 2004.

DeCarlo, P. F., Kimmel, J. R., Trimborn, A., Northway, M. J., Jayne, J. T., Aiken, A. C., Gonin, M., Fuhrer, K., Horvath, T., Docherty, K. S., Worsnop, D. R. and Jimenez, J. L.: Field-Deployable, High-Resolution, Time-of-Flight Aerosol Mass Spectrometer, Anal. Chem., 78(24), 8281–8289, doi:10.1021/ac061249n, 2006.

DeCarlo, P. F., Dunlea, E. J., Kimmel, J. R., Aiken, A. C., Sueper, D., Crounse, J., Wennberg, P. O., Emmons, L., Shinozuka, Y., Clarke, A., Zhou, J., Tomlinson, J., Collins, D. R., Knapp, D., Weinheimer, A. J., Montzka, D. D., Campos, T. and Jimenez, J. L.: Fast airborne aerosol size and chemistry measurements above Mexico City and Central Mexico during the MILAGRO campaign, Atmos. Chem. Phys., 8(14), 4027–4048, doi:10.5194/acp-8-4027-2008, 2008.

DeCarlo, P. F., Ulbrich, I. M., Crounse, J., de Foy, B., Dunlea, E. J., Aiken, A. C., Knapp, D., Weinheimer, A. J., Campos, T., Wennberg, P. O. and Jimenez, J. L.: Investigation of the sources and processing of organic aerosol over the Central Mexican Plateau from aircraft measurements during MILAGRO, Atmos. Chem. Phys., 10(12), 5257–5280, doi:10.5194/acp-10-5257-2010, 2010.

Deming, B., Pagonis, D., Liu, X., Talukdar, R. K., Roberts, J. M., Veres, P. R., Krechmer, J. E., de Gouw, J. A., Jimenez, J. L. and Zieman, P. J.: Measurements of Delays of Gas-Phase Compounds in a Wide Variety of Tubing Materials due to Gas-Wall Partitioning, Atmos. Meas. Tech., In Prep., 2018.

Dibb, J. E., Talbot, R. W., Scheuer, E. M., Seid, G., Avery, M. A. and Singh, H. B.: Aerosol chemical composition in Asian continental outflow during the TRACE-P campaign: Comparison with PEM-West B, J. Geophys. Res., 108(D21), 8815, doi:10.1029/2002JD003111, 2003.

Diskin, G. S., Podolske, J. R., Sachse, G. W. and Slate, T. A.: Open-path airborne tunable diode laser hygrometer, vol. 4817, edited by A. Fried, p. 196, International Society for Optics and Photonics., 2002.

Docherty, K. S., Aiken, A. C., Huffman, J. A., Ulbrich, I. M., DeCarlo, P. F., Sueper, D., Worsnop, D. R., Snyder, D. C., Peltier, R. E., Weber, R. J., Grover, B. D., Eatough, D. J., Williams, B. J., Goldstein, A. H., Ziemann, P. J. and Jimenez, J. L.: The 2005 Study of Organic Aerosols at Riverside (SOAR-1): instrumental intercomparisons and fine particle composition, Atmos. Chem. Phys., 11(23), 12387–12420, doi:DOI 10.5194/acp-11-12387-2011, 2011.

762 Drewnick, F., Hings, S. S., Alfarra, M. R., Prevot, A. S. H. and Borrmann, S.: Aerosol
763 quantification with the Aerodyne Aerosol Mass Spectrometer: detection limits and ionizer
764 background effects, Atmos. Meas. Tech., 2(1), 33–46, doi:10.5194/amt-2-33-2009, 2009.

765 Dunlea, E. J., DeCarlo, P. F., Aiken, A. C., Kimmel, J. R., Peltier, R. E., Weber, R. J., Tomlison,
766 J., Collins, D. R., Shinozuka, Y., McNaugthon, C. S., Howell, S. G., Clarke, A. D., Emmons, L.
767 K., Apel, E. C., Pfister, G. G., van Donkelaar, A., Martin, R. V., Millett, D. B., Heald, C. L. and
768 Jimenez, J. L.: Evolution of Asian aerosols during transpacific transport in INTEX-B, Atmos.
769 Chem. Phys., 9(19), 7257–7287, doi:10.5194/acp-9-7257-2009, 2009.

770 Dzepina, K., Volkamer, R. M. R., Madronich, S., Tulet, P., Ulbrich, I. M., Zhang, Q., Cappa, C.
771 D., Ziemann, P. J. and Jimenez, J. L.: Evaluation of recently-proposed secondary organic aerosol
772 models for a case study in Mexico City, Atmos. Chem. Phys., 9(15), 5681–5709, doi:10.5194/acp-
773 9-5681-2009, 2009.

774 Dzepina, K., Cappa, C. D., Volkamer, R. M., Madronich, S., DeCarlo, P. F., Zaveri, R. A. and
775 Jimenez, J. L.: Modeling the Multiday Evolution and Aging of Secondary Organic Aerosol During
776 MILAGRO 2006, Environ. Sci. Technol., 45(8), 3496–3503, doi:10.1021/es103186, 2011.

777 Faloona, I. C., Tan, D., Lesher, R. L., Hazen, N. L., Frame, C. L., Simpas, J. B., Harder, H.,
778 Martinez, M., Di Carlo, P., Ren, X. and Brune, W. H.: A Laser-induced Fluorescence Instrument
779 for Detecting Tropospheric OH and HO_2 : Characteristics and Calibration, J. Atmos. Chem., 47(2),
780 139–167, doi:10.1023/B:JOCH.0000021036.53185.0e, 2004.

781 Farmer, D. K., Matsunaga, A., Docherty, K. S., Surratt, J. D., Seinfeld, J. H., Ziemann, P. J. and
782 Jimenez, J. L.: Response of an aerosol mass spectrometer to organonitrates and organosulfates and
783 implications for atmospheric chemistry, Proc. Natl. Acad. Sci. U. S. A., 107(15), 6670–6675,
784 doi:10.1073/pnas.0912340107, 2010.

785 Freney, E. J., Sellegri, K., Canonaco, F., Colomb, A., Borbon, A., Michoud, V., Doussin, J.-F.,
786 Crumeyrolle, S., Amarouche, N., Pichon, J.-M., Bourianne, T., Gomes, L., Prevot, A. S. H.,
787 Beekmann, M. and Schwarzenböeck, A.: Characterizing the impact of urban emissions on regional
788 aerosol particles: airborne measurements during the MEGAPOLI experiment, Atmos. Chem.
789 Phys., 14(3), 1397–1412, doi:10.5194/acp-14-1397-2014, 2014a.

790 Freney, E. J., Sellegri, K., Canonaco, F., Colomb, A., Borbon, A., Michoud, V., Crumeyrolle, S.,
791 Amarouche, N., Bourianne, T., Gomes, L., Prevot, A. S. H., Beekmann, M. and Schwarzenböeck,
792 A.: Characterizing the impact of urban emissions on regional aerosol particles: Airborne
793 measurements during the MEGAPOLI experiment, Atmos. Chem. Phys., 14(3), 1397–1412,
794 doi:10.5194/acp-14-1397-2014, 2014b.

795 Fried, A., Cantrell, C., Olson, J., Crawford, J. H., Weibring, P., Walega, J., Richter, D.,
796 Junkermann, W., Volkamer, R., Sinreich, R., Heikes, B. G., O'Sullivan, D., Blake, D. R., Blake,
797 N., Meinardi, S., Apel, E., Weinheimer, A., Knapp, D., Perring, A., Cohen, R. C., Fuelberg, H.,
798 Shetter, R. E., Hall, S. R., Ullmann, K., Brune, W. H., Mao, J., Ren, X., Huey, L. G., Singh, H. B.,
799 Hair, J. W., Riemer, D., Diskin, G. and Sachse, G.: Detailed comparisons of airborne formaldehyde
800 measurements with box models during the 2006 INTEX-B and MILAGRO campaigns: Potential
801 evidence for significant impacts of unmeasured and multi-generation volatile organic carbon
802 compounds, Atmos. Chem. Phys., 11(22), 11867–11894, doi:10.5194/acp-11-11867-2011, 2011.

803 Fry, J. L., Draper, D. C., Zarzana, K. J., Campuzano-Jost, P., Day, D. A., Jimenez, J. L., Brown,
804 S. S., Cohen, R. C., Kaser, L., Hansel, A., Cappellin, L., Karl, T., Hodzic Roux, A., Turnipseed,

A., Cantrell, C., Lefer, B. L. and Grossberg, N.: Observations of gas- and aerosol-phase organic nitrates at BEACHON-RoMBAS 2011, Atmos. Chem. Phys., 13(17), 8585–8605, doi:10.5194/acp-13-8585-2013, 2013.

Ge, X., Setyan, A., Sun, Y. and Zhang, Q.: Primary and secondary organic aerosols in Fresno, California during wintertime: Results from high resolution aerosol mass spectrometry, J. Geophys. Res. Atmos., 117(D19), n/a-n/a, doi:10.1029/2012JD018026, 2012.

George, I. J., Slowik, J. and Abbatt, J. P. D.: Chemical aging of ambient organic aerosol from heterogeneous reaction with hydroxyl radicals, Geophys. Res. Lett., 35(13), L13811, doi:10.1029/2008GL033884, 2008.

Goldberg, D. L., Vinciguerra, T. P., Hosley, K. M., Loughner, C. P., Canty, T. C., Salawitch, R. . and Dickerson, R. R.: Evidence for an increase in the ozone photochemical lifetime in the eastern United States using a regional air quality model, J. Geophys. Res. Atmos., 120, 12,778-12,793, doi:10.1002/2015JD02390, 2015.

Gordon, T. D., Tkacik, D. S., Presto, A. A., Zhang, M., Jathar, S. H., Nguyen, N. T., Massetti, J., Truong, T., Cicero-Fernandez, P., Maddox, C., Rieger, P., Chattopadhyay, S., Maldonado, H., Maricq, M. M. and Robinson, A. L.: Primary Gas- and Particle-Phase Emissions and Secondary Organic Aerosol Production from Gasoline and Diesel Off-Road Engines, Environ. Sci. Technol., 47(24), 14137–14146, doi:10.1021/es403556e, 2013.

de Gouw, J. A., Middlebrook, A. M., Warneke, C., Goldan, P. D., Kuster, W. C., Roberts, J. M., Fehsenfeld, F. C., Worsnop, D. R., Canagaratna, M. R., Pszenny, A. A. P., Keene, W. C., Marchewka, M. L., Bertman, S. B. and Bates, T. S.: Budget of organic carbon in a polluted atmosphere: Results from the New England Air Quality Study in 2002, J. Geophys. Res., 110(16), D16305, doi:10.1029/2004JD005623, 2005.

de Gouw, J. A., Brock, C. A., Atlas, E. L., Bates, T. S., Fehsenfeld, F. C., Goldan, P. D., Holloway, J. S., Kuster, W. C., Lerner, B. M., Matthew, B. M., Middlebrook, A. M., Onasch, T. B., Peltier, R. E., Quinn, P. K., Senff, C. J., Stohl, A., Sullivan, A. P., Trainer, M., Warneke, C., Weber, R. J. and Williams, E. J.: Sources of particulate matter in the northeastern United States in summer: 1. Direct emissions and secondary formation of organic matter in urban plumes, J. Geophys. Res., 113(8), D08301, doi:10.1029/2007JD009243, 2008.

de Gouw, J. A., Welsh-Bon, D., Warneke, C., Kuster, W. C., Alexander, L., Baker, A. K., Beyersdorf, A. J., Blake, D. R., Canagaratna, M., Celada, a. T., Huey, L. G., Junkermann, W., Onasch, T. B., Salcido, A., Sjostedt, S. J., Sullivan, A. P., Tanner, D. J., Vargas, O., Weber, R. J., Worsnop, D. R., Yu, X. Y. and Zaveri, R.: Emission and chemistry of organic carbon in the gas and aerosol phase at a sub-urban site near Mexico City in March 2006 during the MILAGRO study, Atmos. Chem. Phys., 9(10), 3425–3442, doi:10.5194/acp-9-3425-2009, 2009.

de Gouw, J. A., Gilman, J. B., Kim, S.-W., Lerner, B. M., Isaacman-VanWertz, G., McDonald, B. C., Warneke, C., Kuster, W. C., Lefer, B. L., Griffith, S. M., Dusanter, S., Stevens, P. S. and Stutz, J.: Chemistry of Volatile Organic Compounds in the Los Angeles basin: Nighttime Removal of Alkenes and Determination of Emission Ratios, J. Geophys. Res., 122(21), 11,843-11,861, doi:10.1002/2017JD027459, 2017.

Grieshop, A. P., Miracolo, M. A., Donahue, N. M. and Robinson, A. L.: Constraining the Volatility Distribution and Gas-Particle Partitioning of Combustion Aerosols Using Isothermal Dilution and Thermodenuder Measurements, Environ. Sci. Technol., 43(13), 4750–4756,

doi:10.1021/Es8032378, 2009.

Griffin, R. J., Chen, J., Carmody, K., Vutukuru, S. and Dabdub, D.: Contribution of gas phase oxidation of volatile organic compounds to atmospheric carbon monoxide levels in two areas of the United States, J. Geophys. Res. Atmos., 112(D10), doi:10.1029/2006JD007602, 2007.

Hallquist, M., Wenger, J. C., Baltensperger, U., Rudich, Y., Simpson, D., Claeys, M., Dommen, J., Donahue, N. M., George, C., Goldstein, A. H., Hamilton, J. F., Herrmann, H., Hoffmann, T., Iinuma, Y., Jang, M., Jenkin, M. E., Jimenez, J. L., Kiendler-Scharr, A., Maenhaut, W., McFiggans, G., Mentel, T. F., Monod, A., Prévôt, A. S. H., Seinfeld, J. H., Surratt, J. D., Szmigielski, R. and Wildt, J.: The formation, properties and impact of secondary organic aerosol: current and emerging issues, Atmos. Chem. Phys., 9(14), 5155–5236, doi:10.5194/acp-9-5155-2009, 2009.

Hand, J. L. and Malm, W. C.: Review of aerosol mass scattering efficiencies from ground-based measurements since 1990, J. Geophys. Res., 112(D16), D16203, doi:10.1029/2007JD008484, 2007.

Hayes, P. L., Ortega, A. M., Cubison, M. J., Froyd, K. D., Zhao, Y., Cliff, S. S., Hu, W. W., Toohey, D. W., Flynn, J. H., Lefer, B. L., Grossberg, N., Alvarez, S., Rappenglück, B., Taylor, J. W., Allan, J. D., Holloway, J. S., Gilman, J. B., Kuster, W. C., de Gouw, J. A., Massoli, P., Zhang, X., Liu, J., Weber, R. J., Corrigan, A. L., Russell, L. M., Isaacman, G., Worton, D. R., Kreisberg, N. M., Goldstein, A. H., Thalman, R., Waxman, E. M., Volkamer, R., Lin, Y. H., Surratt, J. D., Kleindienst, T. E., Offenberg, J. H., Dusanter, S., Griffith, S., Stevens, P. S., Brioude, J., Angevine, W. M. and Jimenez, J. L.: Organic aerosol composition and sources in Pasadena, California, during the 2010 CalNex campaign, J. Geophys. Res., 118(16), 9233–9257, doi:10.1002/jgrd.50530, 2013.

Hayes, P. L., Carlton, A. G., Baker, K. R., Ahmadov, R., Washenfelder, R. A., Alvarez, S., Rappenglück, B., Gilman, J. B., Kuster, W. C., de Gouw, J. A., Zotter, P., Prévôt, A. S. H., Szidat, S., Kleindienst, T. E., Ma, P. K. and Jimenez, J. L.: Modeling the formation and aging of secondary organic aerosols in Los Angeles during CalNex 2010, Atmos. Chem. Phys., 15(10), 5773–5801, doi:10.5194/acp-15-5773-2015, 2015.

Heald, C. L., Kroll, J. H., Jimenez, J. L., Docherty, K. S., Decarlo, P. F., Aiken, A. C., Chen, Q., Martin, S. T., Farmer, D. K. and Artaxo, P.: A simplified description of the evolution of organic aerosol composition in the atmosphere, Geophys. Res. Lett., 37(8), L08803, doi:10.1029/2010GL042737, 2010.

Heim, E., Dibb, J., Scheuer, E., Campuzano-Jost, P., Nault, B. A., Jimenez, J. L., Peterson, D., Knote, C., Fenn, M., Hair, J., Beyersdorf, A. J. and Anderson, B. E.: Asian Dust Observed during KORUS-AQ Facilitates the Uptake and Incorporation of Soluble Pollutants during Transport to South Korea: The Hwangsa Anthropogenic Model, J. Geophys. Res. Atmos., submitted, 2018.

Hennigan, C. J., Sullivan, A. P., Fountoukis, C. I., Nenes, A., Hecobian, A., Vargas, O., Peltier, R. E., Hanks, A. T. C., Huey, L. G., Lefer, B. L., Russell, A. G. and Weber, R. J.: On the volatility and production mechanisms of newly formed nitrate and water soluble organic aerosol in Mexico City, Atmos. Chem. Phys., 8(14), 3761–3768, doi:10.5194/acp-8-3761-2008, 2008.

Heo, J.-B., Hopke, P. K. and Yi, S.-M.: Source apportionment of PM2.5 in Seoul, Korea, Atmos. Chem. Phys., 9(14), 4957–4971, doi:10.5194/acp-9-4957-2009, 2009.

Herndon, S. C., Onasch, T. B., Wood, E. C., Kroll, J. H., Canagaratna, M. R., Jayne, J. T., Zavala,

M. A., Knighton, W. B., Mazzoleni, C., Dubey, M. K., Ulbrich, I. M., Jimenez, J. L., Seila, R., de Gouw, J. A., de Foy, B., Fast, J., Molina, L. T., Kolb, C. E. and Worsnop, D. R.: Correlation of secondary organic aerosol with odd oxygen in Mexico City, Geophys. Res. Lett., 35(15), doi:10.1029/2008GL034058, 2008.

Hersey, S. P., Craven, J. S., Metcalf, A. R., Lin, J., Lathem, T., Suski, K. J., Cahill, J. F., Duong, H. T., Sorooshian, A., Jonsson, H. H., Shiraiwa, M., Zuend, A., Nenes, A., Prather, K. A., Flagan, R. C. and Seinfeld, J. H.: Composition and hygroscopicity of the Los Angeles Aerosol: CalNex, J. Geophys. Res. Atmos., 118(7), 3016–3036, doi:10.1002/jgrd.50307, 2013.

Hildebrandt Ruiz, L., Paciga, A. L., Cerully, K. M., Nenes, A., Donahue, N. M. and Pandis, S. N.: Formation and aging of secondary organic aerosol from toluene: changes in chemical composition, volatility, and hygroscopicity, Atmos. Chem. Phys., 15(14), 8301–8313, doi:10.5194/acp-15-8301-2015, 2015.

Hodzic, A. and Jimenez, J. L.: Modeling anthropogenically controlled secondary organic aerosols in a megacity: A simplified framework for global and climate models, Geosci. Model Dev., 4(4), 901–917, doi:10.5194/gmd-4-901-2011, 2011.

Hodzic, A., Jimenez, J. L., Madronich, S., Canagaratna, M. R., DeCarlo, P. F., Kleinman, L. and Fast, J.: Modeling organic aerosols in a megacity: Potential contribution of semi-volatile and intermediate volatility primary organic compounds to secondary organic aerosol formation, Atmos. Chem. Phys., 10(12), 5491–5514, doi:10.5194/acp-10-5491-2010, 2010.

Hodzic, A., Madronich, S., Kasibhatla, P. S., Tyndall, G., Aumont, B., Jimenez, J. L., Lee-Taylor, J. and Orlando, J.: Organic photolysis reactions in tropospheric aerosols: effect on secondary organic aerosol formation and lifetime, Atmos. Chem. Phys., 15(16), 9253–9269, doi:10.5194/acp-15-9253-2015, 2015.

Hong, J.-W. and Hong, J.: Changes in the Seoul Metropolitan Area Urban Heat Environment with Residential Redevelopment, J. Appl. Meteorol. Climatol., 55, 1091–1106, doi:10.1175/JAMC-D-15-0321.1, 2016.

Hu, W., Hu, M., Hu, W., Jimenez, J. L., Yuan, B., Chen, W., Wang, M., Wu, Y., Chen, C., Wang, Z., Peng, J., Zeng, L. and Shao, M.: Chemical composition, sources and aging process of sub-micron aerosols in Beijing: contrast between summer and winter, J. Geophys. Res. Atmos., doi:10.1002/2015JD024020, 2016.

Hu, W., Campuzano-Jost, P., Day, D. A., Croteau, P., Canagaratna, M. R., Jayne, J. T., Worsnop, D. R. and Jimenez, J. L.: Evaluation of the new capture vaporizer for aerosol mass spectrometers (AMS) through field studies of inorganic species, , doi:10.1080/02786826.2017.1296104, 2017a.

Hu, W., Campuzano-Jost, P., Day, D. A., Croteau, P., Canagaratna, M. R., Jayne, J. T., Worsnop, D. R. and Jimenez, J. L.: Evaluation of the new capture vapourizer for aerosol mass spectrometers (AMS) through laboratory studies of inorganic species, Atmos. Meas. Tech., 10(6), 2897–2921, doi:10.5194/amt-10-2897-2017, 2017b.

Hu, W., Day, D. A., Campuzano-Jost, P., Nault, B. A., Park, T., Lee, T., Croteau, P., Canagaratna, M. R., Jayne, J. T., Worsnop, D. R. and Jimenez, J. L.: Evaluation of the new capture vaporizer for Aerosol Mass Spectrometers: Characterization of organic aerosol mass spectra, Aerosol Sci. Technol., 52(7), 752–739, doi:10.1080/02786826.2018.1454584, 2018a.

Hu, W., Day, D. A., Campuzano-Jost, P., Nault, B. A., Park, T., Lee, T., Croteau, P., Canagaratna,

M. R., Jayne, J. T., Worsnop, D. R. and Jimenez, J. L.: Evaluation of the New Capture Vaporizer for Aerosol Mass Spectrometers (AMS): Elemental Composition and Source Apportionment of Organic Aerosols (OA), ACS Earth Sp. Chem., 2(4), 410–421, doi:10.1021/acsearthspacechem.8b00002, 2018b.

Hu, W. W., Hu, M., Yuan, B., Jimenez, J. L., Tang, Q., Peng, J. F., Hu, W., Shao, M., Wang, M., Zeng, L. M., Wu, Y. S., Gong, Z. H., Huang, X. F. and He, L. Y.: Insights on organic aerosol aging and the influence of coal combustion at a regional receptor site of central eastern China, Atmos. Chem. Phys., 13(19), 10095–10112, doi:10.5194/acp-13-10095-2013, 2013.

Hu, W. W., Campuzano-Jost, P., Palm, B. B., Day, D. A., Ortega, A. M., Hayes, P. L., Krechmer, J. E., Chen, Q., Kuwata, M., Liu, Y. J., de Sá, S. S., McKinney, K., Martin, S. T., Hu, M., Budisulistiorini, S. H., Riva, M., Surratt, J. D., St. Clair, J. M., Isaacman-Van Wertz, G., Yee, L. D., Goldstein, A. H., Carbone, S., Brito, J., Artaxo, P., de Gouw, J. A., Koss, A., Wisthaler, A., Mikoviny, T., Karl, T., Kaser, L., Jud, W., Hansel, A., Docherty, K. S., Alexander, M. L., Robinson, N. H., Coe, H., Allan, J. D., Canagaratna, M. R., Paulot, F. and Jimenez, J. L.: Characterization of a real-time tracer for Isoprene Epoxydiols-derived Secondary Organic Aerosol (IEPOX-SOA) from aerosol mass spectrometer measurements, Atmos. Chem. Phys., 15(8), 11807–11833, doi:10.5194/acp-15-11807-2015, 2015.

Huang, C., Wang, H. L., Li, L., Wang, Q., Lu, Q., de Gouw, J. A., Zhou, M., Jing, S. A., Lu, J. and Chen, C. H.: VOC species and emission inventory from vehicles and their SOA formation potentials estimation in Shanghai, China, Atmos. Chem. Phys., 15(19), 11081–11096, doi:10.5194/acp-15-11081-2015, 2015.

Huey, L. G., Tanner, D. J., Slusher, D. L., Dibb, J. E., Arimoto, R., Chen, G., Davis, D., Buhr, M. P., Nowak, J. B., Mauldin III, R. L., Eisele, F. L. and Kosciuch, E.: CIMS measurements of HNO_3 and SO_2 at the South Pole during ISCAT 2000, Atmos. Environ., 38(32), 5411–5421, doi:10.1016/J.ATMOSENV.2004.04.037, 2004.

Huffman, J. A., Docherty, K. S., Aiken, A. C., Cubison, M. J., Ulbrich, I. M., DeCarlo, P. F., Sueper, D., Jayne, J. T., Worsnop, D. R., Ziemann, P. J. and Jimenez, J. L.: Chemically-resolved aerosol volatility measurements from two megacity field studies, Atmos. Chem. Phys., 9(1), 7161–7182, doi:doi:10.5194/acp-9-7161-2009, 2009.

Hunter, J. F., Day, D. A., Palm, B. B., Yatavelli, R. L. N., Chan, A. W. H., Kaser, L., Cappellin, L., Hayes, P. L., Cross, E. S., Carrasquillo, A. J., Campuzano-Jost, P., Stark, H., Zhao, Y., Hohaus, T., Smith, J. N., Hansel, A., Karl, T., Goldstein, A. H., Guenther, A., Worsnop, D. R., Thornton, J. A., Heald, C. L., Jimenez, J. L. and Kroll, J. H.: Comprehensive characterization of atmospheric organic carbon at a forested site, Nat. Geosci., 10(10), 748–753, doi:10.1038/ngeo3018, 2017.

Jacob, D. J.: Heterogeneous chemistry and tropospheric ozone, Atmos. Environ., 34, 2131–2159, doi:10.1016/S1352-2310(99)00462-8, 2000.

Janssen, R. H. H., Tsimpidi, A. P., Karydis, V. A., Pozzer, A., Lelieveld, J., Crippa, M., Prévôt, A. S. H., Ait-Helal, W., Borbon, A., Sauvage, S. and Locoge, N.: Influence of local production and vertical transport on the organic aerosol budget over Paris, J. Geophys. Res. Atmos., 1–21, doi:10.1002/2016JD026402, 2017.

Jathar, S. H., Miracolo, M. A., Tkacik, D. S., Donahue, N. M., Adams, P. J. and Robinson, A. L.: Secondary Organic Aerosol Formation from Photo-Oxidation of Unburned Fuel: Experimental Results and Implications for Aerosol Formation from Combustion Emissions, Environ. Sci.

Technol., 47(22), 12886–12893, doi:10.1021/es403445q, 2013.

Jathar, S. H., Gordon, T. D., Hennigan, C. J., Pye, H. O. T., Pouliot, G., Adams, P. J., Donahue, N. M. and Robinson, A. L.: Unspeciated organic emissions from combustion sources and their influence on the secondary organic aerosol budget in the United States., Proc. Natl. Acad. Sci. U. S. A., 111(29), 10473–10478, doi:10.1073/pnas.1323740111, 2014.

Jayne, J. T. and Worsnop, D. R.: Particle Capture Device Aerodyne Research, 2015.

Jeong, U., Kim, J., Lee, H. and Lee, Y. G.: Assessing the effect of long-range pollutant transportation on air quality in Seoul using the conditional potential source contribution function method, Atmos. Environ., 150, 33–44, doi:10.1016/j.atmosenv.2016.11.017, 2017.

Jimenez, J. L., Canagaratna, M. R., Donahue, N. M., Prevot, A. S. H., Zhang, Q., Kroll, J. H., DeCarlo, P. F., Allan, J. D., Coe, H., Ng, N. L., Aiken, A. C., Docherty, K. S., Ulbrich, I. M., Grieshop, A. P., Robinson, A. L., Duplissy, J., Smith, J. D., Wilson, K. R., Lanz, V. A., Hueglin, C., Sun, Y. L., Tian, J., Laaksonen, A., Raatikainen, T., Rautiainen, J., Vaattovaara, P., Ehn, M., Kulmala, M., Tomlinson, J. M., Collins, D. R., Cubison, M. J., Dunlea, E. J., Huffman, J. A., Onasch, T. B., Alfarra, M. R., Williams, P. I., Bower, K., Kondo, Y., Schneider, J., Drewnick, F., Borrmann, S., Weimer, S., Demerjian, K., Salcedo, D., Cottrell, L., Griffin, R., Takami, A., Miyoshi, T., Hatakeyama, S., Shimono, A., Sun, J. Y., Zhang, Y. M., Dzepina, K., Kimmel, J. R., Sueper, D., Jayne, J. T., Herndon, S. C., Trimborn, A. M., Williams, L. R., Wood, E. C., Middlebrook, A. M., Kolb, C. E., Baltensperger, U., Worsnop, D. R. and Worsnop, D. R.: Evolution of organic aerosols in the atmosphere., Science, 326(5959), 1525–1529, doi:10.1126/science.1180353, 2009.

Jimenez, J. L., Canagaratna, M. R., Donahue, N. M., Prévôt, A. S. H., Zhang, Q., Kroll, J. H., DeCarlo, P. F., Allan, J. D., Coe, H., Ng, N. L., Aiken, A. C., Docherty, K. S., Ulbrich, I. M., Grieshop, A. P., Robinson, A. L., Duplissy, J., Smith, J. D., Wilson, K. R., Lanz, V. A., Hueglin, C., Sun, Y. L., Tian, J., Laaksonen, A., Raatikainen, T., Rautiainen, J., Vaattovaara, P., Ehn, M., Kulmala, M., Tomlinson, J. M., Collins, D. R., Cubison, M. J., Dunlea, E. J., Huffman, J. A., Onasch, T. B., Alfarra, M. R., Williams, P. I., Bower, K., Kondo, Y., Schneider, J., Drewnick, F., Borrmann, S., Weimer, S., Demerjian, K., Salcedo, D., Cottrell, L., Griffin, R., Takami, A., Miyoshi, T., Hatakeyama, S., Shimono, A., Sun, J. Y., Zhang, Y. M., Dzepina, K., Kimmel, J. R., Sueper, D., Jayne, J. T., Herndon, S. C., Trimborn, A. M., Williams, L. R., Wood, E. C., Middlebrook, A. M., Kolb, C. E., Baltensperger, U. and Worsnop, D. R.: Evolution of Organic Aerosols in the Atmosphere, Science (80-.)., 326(5959), 1525–1529, doi:10.1126/science.1180353, 2009.

Jimenez, J. L., Canagaratna, M. R., Drewnick, F., Allan, J. D., Alfarra, M. R., Middlebrook, A. M., Slowik, J. G., Zhang, Q., Coe, H., Jayne, J. T. and Worsnop, D. R.: Comment on "The effects of molecular weight and thermal decomposition on the sensitivity of a thermal desorption aerosol mass spectrometer," Aerosol Sci. Technol., 50(9), i–xv, doi:10.1080/02786826.2016.1205728, 2016.

Jimenez, J. L., Campuzano-Jost, P., Day, D. A., Nault, B. A., Schroder, J. C. and Cubison, M. J.: Frequently AMS Questions for AMS Data Users, [online] Available from: http://cires.colorado.edu/jimenez-group/wiki/index.php?title=FAQ_for_AMS_Data_Users, accessed month-year (Accessed 6 December 2018), 2018.

Kang, C. M., Kang, B. W. and Lee, H. S.: Source identification and trends in concentrations of

gaseous and fine particulate principal species in Seoul, South Korea, J. Air Waste Manag. Assoc., 56(7), 911–921, doi:10.1080/10473289.2006.10464506, 2006.

Kang, E., Root, M. J., Toohey, D. W. and Brune, W. H.: Introducing the concept of Potential Aerosol Mass (PAM), Atmos. Chem. Phys., 7(22), 5727–5744, doi:10.5194/acp-7-5727-2007, 2007.

Kang, E., Lee, M., Brune, W. H., Lee, T., Park, T., Ahn, J. and Shang, X.: Photochemical aging of aerosol particles in different air masses arriving at Baengnyeong Island, Korea, Atmos. Chem. Phys., 18(9), 6661–6677, doi:10.5194/acp-18-6661-2018, 2018.

Khare, P. and Gentner, D. R.: Considering the future of anthropogenic gas-phase organic compound emissions and the increasing influence of non-combustion sources on urban air quality, Atmos. Chem. Phys., 18(8), 5391–5413, doi:10.5194/acp-18-5391-2018, 2018.

Kim, B. M., Seo, J., Kim, J. Y., Lee, J. Y. and Kim, Y.: Transported vs. local contributions from secondary and biomass burning sources to PM2.5, Atmos. Environ., 144, 24–36, doi:10.1016/j.atmosenv.2016.08.072, 2016.

Kim, H., Zhang, Q., Bae, G.-N., Kim, J. Y. and Lee, S. B.: Sources and atmospheric processing of wintertime aerosols in Seoul, Korea: Insights from real-time measurements using a high-resolution aerosol mass spectrometer, Atmos. Chem. Phys. Discuss., 17(3), 2009–2003, doi:10.5194/acp-17-2009-2017, 2017.

Kim, H., Zhang, Q. and Heo, J.: Influence of Intense secondary aerosol formation and long-range transport on aerosol chemistry and properties in the Seoul Metropolitan Area during spring time : Results from KORUS-AQ, Atmos. Chem. Phys., 18, 7149–7168, doi:10.51944/acp-2017-947, 2018.

Kim, H. C., Kim, E. H., Kim, B. U. and Kim, S.: Regional Contributions to the Particulate Matter Concentration in the Seoul Metropolitan Area, Korea: Seasonal Variation and Sensitivity to Meteorology, Atmos. Chem. Phys, 17(17), 10315–10332, doi:10.5194/acp-17-10315-2017, 2017.

Kim, H. S., Huh, J. B., Hopke, P. K., Holsen, T. M. and Yi, S. M.: Characteristics of the major chemical constituents of PM2.5 and smog events in Seoul, Korea in 2003 and 2004, Atmos. Environ., 41(32), 6762–6770, doi:10.1016/j.atmosenv.2007.04.060, 2007.

Kim, S., Huey, L. G., Stickel, R. E., Tanner, D. J., Crawford, J. H., Olson, J. R., Chen, G., Brune, W. H., Ren, X., Lesher, R., Wooldridge, P. J., Bertram, T. H., Perring, A., Cohen, R. C., Lefer, B. L., Shetter, R. E., Avery, M., Diskin, G. and Sokolik, I.: Measurement of HO_2NO_2 in the free troposphere during the Intercontinental Chemical Transport Experiment–North America 2004, J. Geophys. Res., 112, D12S01, doi:10.1029/2006JD007676, 2007.

Kim, Y. J., Woo, J. H., Ma, Y. Il, Kim, S., Nam, J. S., Sung, H., Choi, K. C., Seo, J., Kim, J. S., Kang, C. H., Lee, G., Ro, C. U., Chang, D. and Sunwoo, Y.: Chemical characteristics of long-range transport aerosol at background sites in Korea, Atmos. Environ., 43(34), 5556–5566, doi:10.1016/j.atmosenv.2009.03.062, 2009.

Kimmel, J. R., Farmer, D. K., Cubison, M. J., Sueper, D., Tanner, C., Nemitz, E., Worsnop, D. R., Gonin, M. and Jimenez, J. L.: Real-time aerosol mass spectrometry with millisecond resolution, Int. J. Mass Spectrom., 303(1), 15–26, doi:10.1016/j.ijms.2010.12.004, 2011.

Kleinman, L., Kuang, C., Sedlacek, A., Senum, G., Springston, S., Wang, J., Zhang, Q., Jayne, J.,

Fast, J., Hubbe, J., Shilling, J. and Zaveri, R.: What do correlations tell us about anthropogenic-biogenic interactions and SOA formation in the Sacramento plume during CARES?, Atmos. Chem. Phys., 16(3), 1729–1746, doi:10.5194/acp-16-1729-2016, 2016.

Kleinman, L. I., Daum, P. H., Lee, Y.-N., Senum, G. I., Springston, S. R., Wang, J., Berkowitz, C., Hubbe, J., Zaveri, R. A., Brechtel, F. J., Jayne, J., Onasch, T. B. and Worsnop, D.: Aircraft observations of aerosol composition and ageing in New England and Mid-Atlantic States during the summer 2002 New England Air Quality Study field campaign, J. Geophys. Res., 112(D9), D09310, doi:10.1029/2006JD007786, 2007.

Kleinman, L. I., Springston, S. R., Daum, P. H., Lee, Y.-N., Nunnermacker, L. J., Senum, G. I., Wang, J., Weinstein-Lloyd, J., Alexander, M. L., Hubbe, J., Ortega, J., Canagaratna, M. R. and Jayne, J.: The time evolution of aerosol composition over the Mexico City plateau, Atmos. Chem. Phys., 8(6), 1559–1575, doi:10.5194/acp-8-1559-2008, 2008.

Kleinman, L. I., Springston, S. R., Wang, J., Daum, P. H., Lee, Y.-N. N., Nunnermacker, L. J., Senum, G. I., Weinstein-Lloyd, J., Alexander, M. L., Hubbe, J., Ortega, J., Zaveri, R. A., Canagaratna, M. R. and Jayne, J.: The time evolution of aerosol size distribution over the Mexico City plateau, Atmos. Chem. Phys., 9(13), 4261–4278, doi:10.5194/acpd-9-1621-2009, 2009.

Knote, C., Brunner, D., Vogel, H., Allan, J., Asmi, A., Äijälä, M., Carbone, S., van der Gon, H. D., Jimenez, J. L., Kiendler-Scharr, A., Mohr, C., Poulain, L., Prévôt, A. S. H., Swietlicki, E. and Vogel, B.: Towards an online-coupled chemistry-climate model: evaluation of trace gases and aerosols in COSMO-ART, Geosci. Model Dev., 4(4), 1077–1102, doi:10.5194/gmd-4-1077-2011, 2011.

Knote, C., Hodzic, A., Jimenez, J. L., Volkamer, R., Orlando, J. J., Baidar, S., Brioude, J., Fast, J., Gentner, D. R., Goldstein, A. H., Hayes, P. L., Knighton, W. B., Oetjen, H., Setyan, A., Stark, H., Thalman, R., Tyndall, G., Washenfelder, R., Waxman, E. and Zhang, Q.: Simulation of semi-explicit mechanisms of SOA formation from glyoxal in aerosol in a 3-D model, Atmos. Chem. Phys., 14(12), 6213–6239, doi:10.5194/acp-14-6213-2014, 2014.

Krechmer, J. E., Pagonis, D., Ziemann, P. J. and Jimenez, J. L.: Quantification of Gas-Wall Partitioning in Teflon Environmental Chambers Using Rapid Bursts of Low-Volatility Oxidized Species Generated in Situ, Environ. Sci. Technol., 50(11), 5757–5765, doi:10.1021/acs.est.6b00606, 2016.

Krechmer, J. E., Day, D. A., Ziemann, P. J. and Jimenez, J. L.: Direct Measurements of Gas/Particle Partitioning and Mass Accommodation Coefficients in Environmental Chambers, Environ. Sci. Technol., 51(20), 11867–11875, doi:10.1021/acs.est.7b02144, 2017.

Kroll, J. H. and Seinfeld, J. H.: Chemistry of secondary organic aerosol: Formation and evolution of low-volatility organics in the atmosphere, Atmos. Environ., 42(16), 3593–3624, doi:10.1016/J.ATMOSENV.2008.01.003, 2008.

Kroll, J. H., Donahue, N. M., Jimenez, J. L., Kessler, S. H., Canagaratna, M. R., Wilson, K. R., Altieri, K. E., Mazzoleni, L. R., Wozniak, A. S., Bluhm, H., Mysak, E. R., Smith, J. D., Kolb, C. E. and Worsnop, D. R.: Carbon oxidation state as a metric for describing the chemistry of atmospheric organic aerosol., Nat. Chem., 3(2), 133–139, doi:10.1038/nchem.948, 2011.

Kuwata, M., Zorn, S. R. and Martin, S. T.: Using Elemental Ratios to Predict the Density of Organic Material Composed of Carbon, Hydrogen, and Oxygen, Environ. Sci. Technol., 46(2),

787–794, doi:10.1021/es202525q, 2012.

Lambe, A. T., Ahern, A. T., Williams, L. R., Slowik, J. G., Wong, J. P. S., Abbatt, J. P. D., Brune, W. H., Ng, N. L., Wright, J. P., Croasdale, D. R., Worsnop, D. R., Davidovits, P. and Onasch, T. B.: Characterization of aerosol photooxidation flow reactors: heterogeneous oxidation, secondary organic aerosol formation and cloud condensation nuclei activity measurements, Atmos. Meas. Tech., 4(3), 445–461, doi:10.5194/amt-4-445-2011, 2011.

Lambe, A. T., Onasch, T. B., Croasdale, D. R., Wright, J. P., Martin, A. T., Franklin, J. P., Massoli, P., Kroll, J. H., Canagaratna, M. R., Brune, W. H., Worsnop, D. R. and Davidovits, P.: Transitions from Functionalization to Fragmentation Reactions of Laboratory Secondary Organic Aerosol (SOA) Generated from the OH Oxidation of Alkane Precursors, Environ. Sci. Technol., 46(10), 5430–5437, doi:10.1021/Es300274t, 2012.

Landrigan, P. J., Fuller, R., Acosta, N. J. R., Adeyi, O., Arnold, R., Basu, N., Baldé, A. B., Bertollini, R., Bose-O'Reilly, S., Boufford, J. I., Breysse, P. N., Chiles, T., Mahidol, C., Coll-Seck, A. M., Cropper, M. L., Fobil, J., Fuster, V., Greenstone, M., Haines, A., Hanrahan, D., Hunter, D., Khare, M., Krupnick, A., Lanphear, B., Lohani, B., Martin, K., Mathiasen, K. V, McTeer, M. A., Murray, C. J. L., Ndahimananjara, J. D., Perera, F., Potočnik, J., Preker, A. S., Ramesh, J., Rockström, J., Salinas, C., Samson, L. D., Sandilya, K., Sly, P. D., Smith, K. R., Steiner, A., Stewart, R. B., Suk, W. A., van Schayck, O. C. P., Yadama, G. N., Yumkella, K. and Zhong, M.: The Lancet Commission on pollution and health, Lancet, 391(10119), 462–512, doi:10.1016/S0140-6736(17)32345-0, 2018.

Lee, G., Choi, H. S., Lee, T., Choi, J., Park, J. S. and Ahn, J. Y.: Variations of regional background peroxyacetyl nitrate in marine boundary layer over Baengyeong Island, South Korea, Atmos. Environ., 61, 533–541, doi:10.1016/j.atmosenv.2012.07.075, 2012.

Lee, H. M., Park, R. J., Henze, D. K., Lee, S., Shim, C., Shin, H. J., Moon, K. J. and Woo, J. H.: PM2.5 source attribution for Seoul in May from 2009 to 2013 using GEOS-Chem and its adjoint model, Environ. Pollut., 221, 377–384, doi:10.1016/j.envpol.2016.11.088, 2017.

Lee, S., Ho, C.-H., Lee, Y. G., Choi, H.-J. and Song, C.-K.: Influence of transboundary air pollutants from China on the high-PM10 episode in Seoul, Korea for the period October 16–20, 2008, Atmos. Environ., 77, 430–439, doi:10.1016/J.ATMOSENV.2013.05.006, 2013.

Lee, T., Choi, J., Lee, G., Ahn, J., Park, J. S., Atwood, S. A., Schurman, M., Choi, Y., Chung, Y. and Collett, J. L.: Characterization of aerosol composition, concentrations, and sources at Baengnyeong Island, Korea using an aerosol mass spectrometer, Atmos. Environ., 120, 297–306, doi:10.1016/j.atmosenv.2015.08.038, 2015.

Lelieveld, J., Evans, J. S., Fnais, M., Giannadaki, D. and Pozzer, A.: The contribution of outdoor air pollution sources to premature mortality on a global scale, Nature, 525(7569), 367–371, doi:10.1038/nature15371, 2015.

Li, R., Palm, B. B., Ortega, A. M., Hlywiak, J., Hu, W., Peng, Z., Day, D. A., Knote, C., Brune, W. H., de Gouw, J. A. and Jimenez, J. L.: Modeling the radical chemistry in an oxidation flow reactor: radical formation and recycling, sensitivities, and the OH exposure estimation equation., J. Phys. Chem. A, 119(19), 4418–4432, doi:10.1021/jp509534k, 2015.

Lide, D. R.: CRC Handbook of Chemistry and Physics, CRC Press Inc., USA., 1991.

Liu, P. S. K., Deng, R., Smith, K. A., Williams, L. R., Jayne, J. T., Canagaratna, M. R., Moore,

K., Onasch, T. B., Worsnop, D. R. and Deshler, T.: Transmission Efficiency of an Aerodynamic Focusing Lens System: Comparison of Model Calculations and Laboratory Measurements for the Aerodyne Aerosol Mass Spectrometer, Aerosol Sci. Technol., 41(8), 721–733, doi:10.1080/02786820701422278, 2007.

Liu, T., Wang, X., Deng, W., Hu, Q., Ding, X., Zhang, Y., He, Q., Zhang, Z., Lü, S., Bi, X., Chen, J. and Yu, J.: Secondary organic aerosol formation from photochemical aging of light-duty gasoline vehicle exhausts in a smog chamber, Atmos. Chem. Phys., 15(15), 9049–9062, doi:10.5194/acp-15-9049-2015, 2015.

Liu, X., Huey, L. G., Yokelson, R. J., Selimovic, V., Simpson, I. J., Müller, M., Jimenez, J. L., Campuzano-Jost, P., Beyersdorf, A. J., Blake, D. R., Butterfield, Z., Choi, Y., Crounse, J. D., Day, D. A., Diskin, G. S., Dubey, M. K., Fortner, E., Hanisco, T. F., Hu, W., King, L. E., Kleinman, L., Meinardi, S., Mikoviny, T., Onasch, T. B., Palm, B. B., Peischl, J., Pollack, I. B., Ryerson, T. B., Sachse, G. W., Sedlacek, A. J., Shilling, J. E., Springston, S., St. Clair, J. M., Tanner, D. J., Teng, A. P., Wennberg, P. O., Wisthaler, A. and Wolfe, G. M.: Airborne measurements of western U.S. wildfire emissions: Comparison with prescribed burning and air quality implications, J. Geophys. Res., 122(11), 6108–6129, doi:10.1002/2016JD026315, 2017.

Ma, P. K., Zhao, Y., Robinson, A. L., Worton, D. R., Goldstein, A. H., Ortega, A. M., Jimenez, J.-L., Zotter, P., Prévôt, A. S. H., Szidat, S. and Hayes, P. L.: Evaluating the impact of new observational constraints on P-S/IVOC emissions, multi-generation oxidation, and chamber wall losses on SOA modeling for Los Angeles, CA, Atmos. Chem. Phys., 17(15), 9237–9259, doi:10.5194/acp-17-9237-2017, 2017.

Mao, J., Ren, X., Brune, W. H., Olson, J. R., Crawford, J. H., Fried, a., Huey, L. G., Cohen, R. C., Heikes, B., Singh, H. B., Blake, D. R., Sachse, G. W., Diskin, G. S., Hall, S. R. and Shetter, R. E.: Airborne measurement of OH reactivity during INTEX-B, Atmos. Chem. Phys., 9(1), 163–173, doi:10.5194/acp-9-163-2009, 2009.

Matsunaga, A. and Ziemann, P. J.: Gas-Wall Partitioning of Organic Compounds in a Teflon Film Chamber and Potential Effects on Reaction Product and Aerosol Yield Measurements, Aerosol Sci. Technol., 44(10), 881–892, doi:10.1080/02786826.2010.501044, 2010.

McDonald, B. C., de Gouw, J. A., Gilman, J. B., Jathar, S. H., Akherati, A., Cappa, C. D., Jimenez, J. L., Lee-Taylor, J., Hayes, P. L., McKeen, S. A., Cui, Y. Y., Kim, S.-W., Gentner, D. R., Isaacman-VanWertz, G., Goldstein, A. H., Harley, R. A., Frost, G. J., Roberts, J. M., Ryerson, T. B. and Trainer, M.: Volatile chemical products emerging as largest petrochemical source of urban organic emissions., Science, 359(6377), 760–764, doi:10.1126/science.aaq0524, 2018.

McKeen, S. A., Liu, S. C., Hsie, E.-Y., Lin, X., Bradshaw, J. D., Smyth, S., Gregory, G. L. and Blake, D. R.: Hydrocarbon ratios during PEM-WEST A: A model perspective, J. Geophys. Res. Atmos., 101(D1), 2087–2109, doi:10.1029/95JD02733, 1996.

McMeeking, G. R., Bart, M., Chazette, P., Haywood, J. M., Hopkins, J. R., McQuaid, J. B., Morgan, W. T., Raut, J.-C., Ryder, C. L., Savage, N., Turnbull, K. and Coe, H.: Airborne measurements of trace gases and aerosols over the London metropolitan region, Atmos. Chem. Phys., 12(11), 5163–5187, doi:10.5194/acp-12-5163-2012, 2012.

McNaughton, C. S., Clarke, A. D., Howell, S. G., Pinkerton, M., Anderson, B., Thornhill, L., Hudgins, C., Winstead, E., Dibb, J. E., Scheuer, E. and Maring, H.: Results from the DC-8 Inlet Characterization Experiment (DICE): Airborne versus surface sampling of mineral dust and sea

salt aerosols, Aerosol Sci. Technol., 41(2), 136–159, doi:10.1080/02786820601118406, 2007.

Middlebrook, A. M., Bahreini, R., Jimenez, J. L. and Canagaratna, M. R.: Evaluation of Composition-Dependent Collection Efficiencies for the Aerodyne Aerosol Mass Spectrometer using Field Data, Aerosol Sci. Technol., 46(3), 258–271, doi:10.1080/02786826.2011.620041, 2012.

Miracolo, M. A., Presto, A. A., Lambe, A. T., Hennigan, C. J., Donahue, N. M., Kroll, J. H., Worsnop, D. R. and Robinson, A. L.: Photo-Oxidation of Low-Volatility Organics Found in Motor Vehicle Emissions: Production and Chemical Evolution of Organic Aerosol Mass, Environ. Sci. Technol., 44(5), 1638–1643, doi:10.1021/es902635c, 2010.

Mitroo, D., Sun, Y., Combest, D. P., Kumar, P. and Williams, B. J.: Assessing the degree of plug flow in oxidation flow reactors (OFRs): a study on a potential aerosol mass (PAM) reactor, Atmos. Meas. Tech, 11, 1741–1756, doi:10.5194/amt-11-1741-2018, 2018.

Moise, T., Flores, J. M. and Rudich, Y.: Optical Properties of Secondary Organic Aerosols and Their Changes by Chemical Processes, Chem. Rev., 115(10), 4400–4439, doi:10.1021/cr5005259, 2015.

Mollner, A. K., Valluvadasan, S., Feng, L., Sprague, M. K., Okumura, M., Milligan, D. B., Bloss, W. J., Sander, S. P., Martien, P. T., Harley, R. a, McCoy, A. B. and Carter, W. P. L.: Rate of Gas Phase Association of Hydroxyl Radical and Nitrogen Dioxide, Science (80-.)., 330(6004), 646–9, doi:10.1126/science.1193030, 2010.

Monks, P. S., Granier, C., Fuzzi, S., Stohl, A., Williams, M. L., Akimoto, H., Amann, M., Baklanov, A., Baltensperger, U., Bey, I., Blake, N., Blake, R. S., Carslaw, K., Cooper, O. R., Dentener, F., Fowler, D., Fragkou, E., Frost, G. J., Generoso, S., Ginoux, P., Grewe, V., Guenther, A., Hansson, H. C., Henne, S., Hjorth, J., Hofzumahaus, A., Huntrieser, H., Isaksen, I. S. A., Jenkin, M. E., Kaiser, J., Kanakidou, M., Klimont, Z., Kulmala, M., Laj, P., Lawrence, M. G., Lee, J. D., Liousse, C., Maione, M., McFiggans, G., Metzger, A., Mieville, A., Moussiopoulos, N., Orlando, J. J., O'Dowd, C. D., Palmer, P. I. I., Parrish, D. D., Petzold, A., Platt, U., Pöschl, U., Prévôt, A. S. H., Reeves, C. E., Reimann, S., Rudich, Y., Sellegri, K., Steinbrecher, R., Simpson, D., ten Brink, H., Theloke, J., van der Werf, G. R., Vautard, R., Vestreng, V., Vlachokostas, C. and von Glasow, R.: Atmospheric composition change - global and regional air quality, Atmos. Environ., 43(33), 5268–5350, doi:10.1016/j.atmosenv.2009.08.021, 2009.

Morino, Y., Tanabe, K., Sato, K. and Ohara, T.: Secondary organic aerosol model intercomparison based on secondary organic aerosol to odd oxygen ratio in Tokyo, J. Geophys. Res. Atmos., 119(23), 13,489-13,505, doi:10.1002/2014JD021937, 2014.

Müller, M., Mikoviny, T., Feil, S., Haidacher, S., Hanel, G., Hartungen, E., Jordan, A., Märk, L., Mutschlechner, P., Schottkowsky, R., Sulzer, P., Crawford, J. H. and Wisthaler, A.: A compact PTR-ToF-MS instrument for airborne measurements of volatile organic compounds at high spatiotemporal resolution, Atmos. Meas. Tech., 7(11), 3763–3772, doi:10.5194/amt-7-3763-2014, 2014.

Murphy, B. N., Donahue, N. M., Fountoukis, C. and Pandis, S. N.: Simulating the oxygen content of ambient organic aerosol with the 2D volatility basis set, Atmos. Chem. Phys., 11(15), 7859–7873, doi:10.5194/acp-11-7859-2011, 2011.

Murphy, B. N., Woody, M. C., Jimenez, J. L., Carlton, A. M. G., Hayes, P. L., Liu, S., Ng, N. L.,

Russell, L. M., Setyan, A., Xu, L., Young, J., Zaveri, R. A., Zhang, Q. and Pye, H. O. T.: Semivolatile POA and parameterized total combustion SOA in CMAQv5.2: impacts on source strength and partitioning, Atmos. Chem. Phys., 17(18), 11107–11133, doi:10.5194/acp-17-11107-2017, 2017.

Murphy, D. M.: The effects of molecular weight and thermal decomposition on the sensitivity of a thermal desorption aerosol mass spectrometer, Aerosol Sci. Technol., 50(2), 118–125, doi:10.1080/02786826.2015.1136403, 2016.

Myhre, G., Shindell, D., Bréon, F.-M., Collins, W., Fuglestvedt, J., Huang, J., Koch, D., Lamarque, J.-F., Lee, D., Mendoza, B., Nakajima, T., Robock, A., Stephens, G., Takemura, T. and Zhang, H.: Anthropogenic and Natural Radiative Forcing, in Climate Change 2013: The Physical Science Basis. Contribution of Working Group I to the Fifth Assessment Report of the Intergovernmental Panel on Climate Change, edited by T. F. Stocker, D. Qin, G.-K. Plattner, M. Tignor, S. K. Allen, J. Boschung, A. Nauels, Y. Xia, V. Bex, and P. M. Midgley, p. 659, Cambridge University Press, Cambridge, United Kingdom and New York, NY, USA, United Kingdom and New York, NY, USA. [online] Available from: https://www.ipcc.ch/report/ar5/wg1/, 2013.

Nault, B. A., Campuzano-Jost, P., Schroder, J. C., Sueper, D. and Jimenez, J. L.: Using Event Trigger Panel for IE/AB and Transmission Curve Calibrations, in 17th AMS Users' Meeting, Portland. [online] Available from: http://cires1.colorado.edu/jimenez-group/wiki/index.php/AMSUsrMtgs#17th_AMS_Users_Meeting.2C_Portland.2C_Oregon, 2016.

NCEP: National Centers for Environmental Prediction, [online] Available from: http://www.emc.ncep.noaa.gov/GFS/doc.php (Accessed 16 November 2017), n.d.

Neuman, J. A., Parrish, D. D., Ryerson, T. B., Brock, C. A., Wiedinmyer, C., Frost, G. J., Holloway, J. S. and Fehsenfeld, F. C.: Nitric acid loss rates measured in power plant plumes, J. Geophys. Res., 109(23), 1–13, doi:10.1029/2004JD005092, 2004.

Ng, N. L., Canagaratna, M. R., Zhang, Q., Jimenez, J. L., Tian, J., Ulbrich, I. M., Kroll, J. H., Docherty, K. S., Chhabra, P. S., Bahreini, R., Murphy, S. M., Seinfeld, J. H., Hildebrandt, L., Donahue, N. M., Decarlo, P. F., Lanz, V. A., Prévôt, A. S. H., Dinar, E., Rudich, Y. and Worsnop, D. R.: Organic aerosol components observed in Northern Hemispheric datasets from Aerosol Mass Spectrometry, Atmos. Chem. Phys., 10(10), 4625–4641, doi:10.5194/acp-10-4625-2010, 2010.

Nguyen, T. B., Crounse, J. D., Teng, A. P., St. Clair, J. M., Paulot, F., Wolfe, G. M. and Wennberg, P. O.: Rapid deposition of oxidized biogenic compounds to a temperate forest, Proc. Natl. Acad. Sci., 112(5), E392–E401, doi:10.1073/pnas.1418702112, 2015.

Novelli, P. C., Crotwell, A., Lang, P. M. and Mund, J.: Atmospheric Carbon Monoxide Dry Air Mole Fractions from the NOAA ESRL Carbon Cycle Cooperative Global Air Sampling Network, 1988-2016, Version: 2017-07-28, [online] Available from: ftp://aftp.cmdl.noaa.gov/data/trace_gases/co/flask/surface/, 2017.

OECD: Exposure to PM2.5 in countries and regions : Exposure to PM2.5 in macroregions, [online] Available from: https://stats.oecd.org/index.aspx?queryid=72722 (Accessed 1 August 2018), 2018.

Ortega, A. M., Day, D. A., Cubison, M. J., Brune, W. H., Bon, D., de Gouw, J. A. and Jimenez, J. L.: Secondary organic aerosol formation and primary organic aerosol oxidation from biomass-

1270 burning smoke in a flow reactor during FLAME-3, Atmos. Chem. Phys., 13(22), 11551–11571,
1271 doi:10.5194/acp-13-11551-2013, 2013.

1272 Ortega, A. M., Hayes, P. L., Peng, Z., Palm, B. B., Hu, W., Day, D. A., Li, R., Cubison, M. J.,
1273 Brune, W. H., Graus, M., Warneke, C., Gilman, J. B., Kuster, W. C., de Gouw, J. A., Gutiérrez-
1274 Montes, C. and Jimenez, J. L.: Real-time measurements of secondary organic aerosol formation
1275 and aging from ambient air in an oxidation flow reactor in the Los Angeles area, Atmos. Chem.
1276 Phys., 16(11), 7411–7433, doi:10.5194/acp-16-7411-2016, 2016.

1277 Ots, R., Vieno, M., Allan, J. D., Reis, S., Nemitz, E., Young, D. E., Coe, H., Di Marco, C.,
1278 Detournay, A., Mackenzie, I. A., Green, D. C. and Heal, M. R.: Model simulations of cooking
1279 organic aerosol (COA) over the UK using estimates of emissions based on measurements at two
1280 sites in London, Atmos. Chem. Phys., 16(21), 13773–13789, doi:10.5194/acp-16-13773-2016,
1281 2016.

1282 Pagonis, D., Krechmer, J. E., de Gouw, J., Jimenez, J. L. and Ziemann, P. J.: Effects of gas–wall
1283 partitioning in Teflon tubing and instrumentation on time-resolved measurements of gas-phase
1284 organic compounds, Atmos. Meas. Tech., 10(12), 4687–4696, doi:10.5194/amt-10-4687-2017,
1285 2017.

1286 Palm, B. B., Campuzano-Jost, P., Ortega, A. M., Day, D. A., Kaser, L., Jud, W., Karl, T., Hansel,
1287 A., Hunter, J. F., Cross, E. S., Kroll, J. H., Peng, Z., Brune, W. H. and Jimenez, J. L.: In situ
1288 secondary organic aerosol formation from ambient pine forest air using an oxidation flow reactor,
1289 Atmos. Chem. Phys., 16(5), 2943–2970, doi:10.5194/acp-16-2943-2016, 2016.

1290 Palm, B. B., Campuzano-Jost, P., Day, D. A., Ortega, A. M., Fry, J. L., Brown, S. S., Zarzana, K.
1291 J., Dube, W., Wagner, N. L., Draper, D. C., Kaser, L., Jud, W., Karl, T., Hansel, A., Gutiérrez-
1292 Montes, C. and Jimenez, J. L.: Secondary organic aerosol formation from in situ OH, O3, and NO3
1293 oxidation of ambient forest air in an oxidation flow reactor, Atmos. Chem. Phys., 17(8), 5331–
1294 5354, doi:10.5194/acp-17-5331-2017, 2017.

1295 Palm, B. B., de Sá, S. S., Day, D. A., Campuzano-Jost, P., Hu, W., Seco, R., Sjostedt, S. J., Park,
1296 J.-H., Guenther, A. B., Kim, S., Brito, J., Wurm, F., Artaxo, P., Thalman, R., Wang, J., Yee, L. D.,
1297 Wernis, R., Isaacman-VanWertz, G., Goldstein, A. H., Liu, Y., Springston, S. R., Souza, R.,
1298 Newburn, M. K., Alexander, M. L., Martin, S. T. and Jimenez, J. L.: Secondary organic aerosol
1299 formation from ambient air in an oxidation flow reactor in central Amazonia, Atmos. Chem. Phys.,
1300 18(1), 467–493, doi:10.5194/acp-18-467-2018, 2018.

1301 Park, K., Kittelson, D. B., Zachariah, M. R. and McMurry, P. H.: Measurement of Inherent
1302 Material Density of Nanoparticle Agglomerates, J. Nanoparticle Res., 6(2/3), 267–272,
1303 doi:10.1023/B:NANO.0000034657.71309.e6, 2004.

1304 Park, M.-S., Park, S.-H., Chae, J.-H., Choi, M.-H., Song, Y., Kang, M. and Roh, J.-W.: High-
1305 resolution urban observation network for user-specific meteorological information service in the
1306 Seoul Metropolitan Area, South Korea, Atmos. Meas. Tech, 10, 1575–1594, doi:10.5194/amt-10-
1307 1575-2017, 2017.

1308 Park, M. E., Song, C. H., Park, R. S., Lee, J., Kim, J., Lee, S., Woo, J.-H., Carmichael, G. R., Eck,
1309 T. F., Holben, B. N., Lee, S.-S., Song, C. K. and Hong, Y. D.: New approach to monitor
1310 transboundary particulate pollution over Northeast Asia, Atmos. Chem. Phys, 14, 659–674,
1311 doi:10.5194/acp-14-659-2014, 2014.

Park, S. S., Kim, J.-H. and Jeong, J.-U.: Abundance and sources of hydrophilic and hydrophobic water-soluble organic carbon at an urban site in Korea in summer., J. Environ. Monit., 14(1), 224–32, doi:10.1039/c1em10617a, 2012.

Parrish, D. D., Stohl, A., Forster, C., Atlas, E. L., Blake, D. R., Goldan, P. D., Kuster, W. C. and de Gouw, J. A.: Effects of mixing on evolution of hydrocarbon ratios in the troposphere, J. Geophys. Res., 112(D10), D10S34, doi:10.1029/2006JD007583, 2007.

Parrish, D. D., Ryerson, T. B., Mellqvist, J., Johansson, J., Fried, A., Richter, D., Walega, J. G., Washenfelder, R. A., de Gouw, J. A., Peischl, J., Aikin, K. C., McKeen, S. A., Frost, G. J., Fehsenfeld, F. C. and Herndon, S. C.: Primary and secondary sources of formaldehyde in urban atmospheres: Houston Texas region, Atmos. Chem. Phys., 12(7), 3273–3288, doi:10.5194/acp-12-3273-2012, 2012.

Peischl, J., Ryerson, T. B., Brioude, J., Aikin, K. C., Andrews, A. E., Atlas, E., Blake, D., Daube, B. C., de Gouw, J. A., Dlugokencky, E., Frost, G. J., Gentner, D. R., Gilman, J. B., Goldstein, A. H., Harley, R. A., Holloway, J. S., Kofler, J., Kuster, W. C., Lang, P. M., Novelli, P. C., Santoni, G. W., Trainer, M., Wofsy, S. C. and Parrish, D. D.: Quantifying sources of methane using light alkanes in the Los Angeles basin, California, J. Geophys. Res. Atmos., 118(10), 4974–4990, doi:10.1002/jgrd.50413, 2013.

Peng, J. F., Hu, M., Wang, Z. B., Huang, X. F., Kumar, P., Wu, Z. J., Guo, S., Yue, D. L., Shang, D. J., Zheng, Z. and He, L. Y.: Submicron aerosols at thirteen diversified sites in China: size distribution, new particle formation and corresponding contribution to cloud condensation nuclei production, Atmos. Chem. Phys., 14(18), 10249–10265, doi:10.5194/acp-14-10249-2014, 2014.

Peng, Z., Day, D. A., Stark, H., Li, R., Lee-Taylor, J., Palm, B. B., Brune, W. H. and Jimenez, J. L.: HO_x radical chemistry in oxidation flow reactors with low-pressure mercury lamps systematically examined by modeling, Atmos. Meas. Tech., 8(11), 4863–4890, doi:10.5194/amt-8-4863-2015, 2015.

Peng, Z., Day, D. A., Ortega, A. M., Palm, B. B., Hu, W., Stark, H., Li, R., Tsigaridis, K., Brune, W. H. and Jimenez, J. L.: Non-OH chemistry in oxidation flow reactors for the study of atmospheric chemistry systematically examined by modeling, Atmos. Chem. Phys., 16(7), 4283–4305, doi:10.5194/acp-16-4283-2016, 2016.

Perring, A. E., Bertram, T. H., Farmer, D. K., Wooldridge, P. J., Dibb, J., Blake, N. J., Blake, D. R., Singh, H. B., Fuelberg, H., Diskin, G., Sachse, G. and Cohen, R. C.: The production and persistence of $\Sigma RONO_2$ in the Mexico City plume, Atmos. Chem. Phys., 10(15), 7215–7229, doi:10.5194/acp-10-7215-2010, 2010.

Pieber, S. M., El Haddad, I., Slowik, J. G., Canagaratna, M. R., Jayne, J. T., Platt, S. M., Bozzetti, C., Daellenbach, K. R., Fröhlich, R., Vlachou, A., Klein, F., Dommen, J., Miljevic, B., Jiménez, J. L., Worsnop, D. R., Baltensperger, U. and Prévôt, A. S. H.: Inorganic Salt Interference on CO2+ in Aerodyne AMS and ACSM Organic Aerosol Composition Studies, Environ. Sci. Technol., 50(19), 10494–10503, doi:10.1021/acs.est.6b01035, 2016.

Platt, S. M., El Haddad, I., Zardini, A. A., Clairotte, M., Astorga, C., Wolf, R., Slowik, J. G., Temime-Roussel, B., Marchand, N., Ježek, I., Drinovec, L., Močnik, G., Möhler, O., Richter, R., Barmet, P., Bianchi, F., Baltensperger, U. and Prévôt, A. S. H.: Secondary organic aerosol formation from gasoline vehicle emissions in a new mobile environmental reaction chamber, Atmos. Chem. Phys., 13(18), 9141–9158, doi:10.5194/acp-13-9141-2013, 2013.

Platt, S. M., El Haddad, I., Pieber, S. M., Zardini, A. A., Suarez-Bertoa, R., Clairotte, M., Daellenbach, K. R., Huang, R.-J., Slowik, J. G., Hellebust, S., Temime-Roussel, B., Marchand, N., de Gouw, J., Jimenez, J. L., Hayes, P. L., Robinson, A. L., Baltensperger, U., Astorga, C. and Prévôt, A. S. H.: Gasoline cars produce more carbonaceous particulate matter than modern filter-equipped diesel cars, Sci. Rep., 7(1), 4926, doi:10.1038/s41598-017-03714-9, 2017.

Presto, A. A., Gordon, T. D. and Robinson, A. L.: Primary to secondary organic aerosol: Evolution of organic emissions from mobile combustion sources, Atmos. Chem. Phys., 14(10), 5015–5036, doi:10.5194/acp-14-5015-2014, 2014.

Price, H. U., Jaffe, D. A., Cooper, O. R. and Doskey, P. V: Photochemistry, ozone production, and dilution during long-range transport episodes from Eurasia to the northwest United States, J. Geophys. Res. Atmos., 109, D23S13, doi:10.1029/2003JD004400, 2004.

Pye, H. O. T. and Seinfeld, J. H.: A global perspective on aerosol from low-volatility organic compounds, Atmos. Chem. Phys. Atmos. Chem. Phys., 10(9), 4377–4401, doi:10.5194/acp-10-4377-2010, 2010.

Richter, D., Weibring, P., Walega, J. G., Fried, A., Spuler, S. M. and Taubman, M. S.: Compact highly sensitive multi-species airborne mid-IR spectrometer, Appl. Phys. B, 119(1), 119–131, doi:10.1007/s00340-015-6038-8, 2015.

Robinson, A. L., Donahue, N. M., Shrivastava, M. K., Weitkamp, E. A., Sage, A. M., Grieshop, A. P., Lane, T. E., Pierce, J. R. and Pandis, S. N.: Rethinking Organic Aerosols: Semivolatile Emissions and Photochemical Aging, Science (80-.)., 315(5816), 1259–1262, doi:10.1126/science.1133061, 2007.

Romer, P. S., Duffey, K. C., Wooldridge, P. J., Allen, H. M., Ayres, B. R., Brown, S. S., Brune, W. H., Crounse, J. D., de Gouw, J., Draper, D. C., Feiner, P. A., Fry, J. L., Goldstein, A. H., Koss, A., Misztal, P. K., Nguyen, T. B., Olson, K., Teng, A. P., Wennberg, P. O., Wild, R. J., Zhang, L. and Cohen, R. C.: The lifetime of nitrogen oxides in an isoprene-dominated forest, Atmos. Chem. Phys., 16(12), 7623–7637, doi:10.5194/acp-16-7623-2016, 2016.

Sachse, G. W., Hill, G. F., Wade, L. O. and Perry, M. G.: Fast-Response, High-Precision Carbon Monoxide Sensor using a Tunable Diode Laser Absorption Technique, J. Geophys. Res., 92(D2), 2071–2081, doi:doi:10.1029/JD092iD02p02071, 1987.

Salcedo, D., Onasch, T. B., Dzepina, K., Canagaratna, M. R., Zhang, Q., Huffman, J. A., Decarlo, P. F., Jayne, J. T., Mortimer, P., Worsnop, D. R., Kolb, C. E., Johnson, K. S., Zuberi, B., Marr, L. C., Volkamer, R., Molina, L. T., Molina, M. J., Cardenas, B., Bernabe, R. M., Marquez, C., Gaffney, J. S., Marley, N. A., Laskin, A., Shutthanandan, V., Xie, Y., Brune, W., Lesher, R., Shirley, T. and Jimenez, J. L.: Characterization of ambient aerosols in Mexico City during the MCMA-2003 campaign with Aerosol Mass Spectrometry: results from the CENICA Supersite, Atmos. Chem. Phys., 6(4), 925–946, doi:10.5194/acp-6-925-2006, 2006.

Sander, S. P., Abbatt, J. P. D., Barker, J. R., Burkholder, J. B., Friedl, R. R., Golden, D. M., Huie, R. E., Kolb, C. E., Kurylo, M. J., Moortgat, G. K., Orkin, V. L. and Wine, P. H.: Chemical Kinetics and Photochemical Data for Use in Atmospheric Studies, Evaluation No. 17, JPL Publ. 10-6, Jet Propuls. Lab. Pasadena, 2011.

Sato, K., Nakashima, Y., Morino, Y., Imamura, T., Kurokawa, J. and Kajii, Y.: Total OH reactivity measurements for the OH-initiated oxidation of aromatic hydrocarbons in the presence of NO_x,

Atmos. Environ., 171, 272–278, doi:10.1016/j.atmosenv.2017.10.036, 2017.

Schneider, J., Hings, S. S., Nele Hock, B., Weimer, S., Borrmann, S., Fiebig, M., Petzold, A., Busen, R. and Kärcher, B.: Aircraft-based operation of an aerosol mass spectrometer: Measurements of tropospheric aerosol composition, J. Aerosol Sci., 37(7), 839–857, doi:10.1016/j.jaerosci.2005.07.002, 2006.

Schroder, J. C., Campuzano-Jost, P., Day, D. A., Shah, V., Larson, K., Sommers, J. M., Sullivan, A. P., Campos, T., Reeves, J. M., Hills, A., Hornbrook, R. S., Blake, N. J., Scheuer, E., Guo, H., Fibiger, D. L., McDuffie, E. E., Hayes, P. L., Weber, R. J., Dibb, J. E., Apel, E. C., Jaeglé, L., Brown, S. S., Thronton, J. A. and Jimenez, J. L.: Sources and Secondary Production of Organic Aerosols in the Northeastern US during WINTER, J. Geophys. Res. Atmos., doi:10.1029/2018JD028475, 2018.

Schwantes, R. H., Schilling, K. A., McVay, R. C., Lignell, H., Coggon, M. M., Zhang, X., Wennberg, P. O. and Seinfeld, J. H.: Formation of Highly Oxygenated Low-Volatility Products from Cresol Oxidation, Atmos. Chem. Phys., 7(5), 3453–3474, doi:10.5194/acp-17-3453-2017, 2017.

Schwarz, J. P., Samset, B. H., Perring, A. E., Spackman, J. R., Gao, R. S., Stier, P., Schulz, M., Moore, F. L., Ray, E. A. and Fahey, D. W.: Global-scale seasonally resolved black carbon vertical profiles over the Pacific, Geophys. Res. Lett., 40(20), 5542–5547, doi:10.1002/2013GL057775, 2013.

Seo, J., Kim, J. Y., Youn, D., Lee, J. Y., Kim, H., Lim, Y. Bin, Kim, Y. and Jin, H. C.: On the multi-day haze in the Asian continental outflow: An important role of synoptic condition combined with regional and local sources, Atmos. Chem. Phys., 17(15), 9311–9332, doi:10.5194/acp-17-9311-2017, 2017.

Shinozuka, Y., Clarke, A. D., DeCarlo, P. F., Jimenez, J. L., Dunlea, E. J., Roberts, G. C., Tomlinson, J. M., Collins, D. R., Howell, S. G., Kapustin, V. N., McNaughton, C. S. and Zhou, J.: Aerosol optical properties relevant to regional remote sensing of CCN activity and links to their organic mass fraction: airborne observations over Central Mexico and the US West Coast during MILAGRO/INTEX-B, Atmos. Chem. Phys., 9(18), 6727–6742, 2009.

Shrivastava, M., Cappa, C. D., Fan, J., Goldstein, A. H., Guenther, A. B., Jimenez, J. L., Kuang, C., Laskin, A., Martin, S. T., Ng, N. L., Petaja, T., Pierce, J. R., Rasch, P. J., Roldin, P., Seinfeld, J. H., Shilling, J., Smith, J. N., Thornton, J. A., Volkamer, R., Wang, J., Worsnop, D. R., Zaveri, R. A., Zelenyuk, A. and Zhang, Q.: Recent advances in understanding secondary organic aerosol: Implications for global climate forcing, Rev. Geophys., 55(2), 509–559, doi:10.1002/2016RG000540, 2017.

Shrivastava, M. K., Lane, T. E., Donahue, N. M., Pandis, S. N. and Robinson, A. L.: Effects of gas particle partitioning and aging of primary emissions on urban and regional organic aerosol concentrations, J. Geophys. Res., 113(D18), D18301, doi:10.1029/2007JD009735, 2008.

Silva, S. J., Arellano, A. F. and Worden, H. M.: Toward anthropogenic combustion emission constraints from space-based analysis of urban CO_2/CO sensitivity, Geophys. Res. Lett., 40(18), 4971–4976, doi:10.1002/grl.50954, 2013.

Skamarock, C., Klemp, B., Dudhia, J., Gill, O., Barker, D., Duda, G., Huang, X., Wang, W. and Powers, G.: A Description of the Advanced Research WRF Version 3, , doi:10.5065/D68S4MVH,

2008.

Slusher, D. L., Huey, L. G., Tanner, D. J., Flocke, F. M. and Roberts, J. M.: A thermal dissociation–chemical ionization mass spectrometry (TD-CIMS) technique for the simultaneous measurement of peroxyacyl nitrates and dinitrogen pentoxide, J. Geophys. Res., 109(D19), D19315, doi:10.1029/2004JD004670, 2004.

Sprengnether, M. M., Demerjian, K. L., Dransfield, T. J., Clarke, J. S., Anderson, J. G. and Donahue, N. M.: Rate Constants of Nine C6-C9 Alkanes with OH from 230 to 379 K: Chemical Tracers for [OH], J. Phys. Chem. A2, 113, 5030–5038, doi:10.1021/jp810412m, 2009.

Stith, J. L., Ramanathan, V., Cooper, W. A., Roberts, G. C., DeMott, P. J., Carmichael, G., Hatch, C. D., Adhikary, B., Twohy, C. H., Rogers, D. C., Baumgardner, D., Prenni, A. J., Campos, T., Gao, R., Anderson, J. and Feng, Y.: An overview of aircraft observations from the Pacific Dust Experiment campaign, J. Geophys. Res., 114(D5), D05207, doi:10.1029/2008JD010924, 2009.

Sueper, D.: ToF-AMS Data Analysis Software Webpage, [online] Available from: http://cires1.colorado.edu/jimenez-group/wiki/index.php/ToF-AMS_Analysis_Software (Accessed 4 January 2017), 2018.

TAbMET: TAbMEP Assessment: POLARCAT HNO3 Summary, in TAbMEP POLARCAT/ICARTT Analysis, edited by G. Chen, https://www-air.larc.nasa.gov/TAbMEP2_polarcat.html, Boulder., 2009.

Talbot, R. W., Dibb, J. E., Lefer, B. L., Scheuer, E. M., Bradshaw, J. D., Sandholm, S. T., Smyth, S., Blake, D. R., Blake, N. J., Sachse, G. W., Collins, J. E. and Gregory, G. L.: Large-scale distributions of tropospheric nitric, formic, and acetic acids over the western Pacific basin during wintertime, J. Geophys. Res., 102(D23), 28303–28313, 1997.

Tang, W., Arellano, A. F., DiGangi, J. P., Choi, Y., Diskin, G. S., Agustí-Panareda, A., Parrington, M., Massart, S., Gaubert, B., Lee, Y., Kim, D., Jung, J., Hong, J., Hong, J.-W., Kanaya, Y., Lee, M., Stauffer, R. M., Thompson, A. M., Flynn, J. H. and Woo, J.-H.: Evaluating High-Resolution Forecasts of Atmospheric CO and CO_2 from a Global Prediction System during KORUS-AQ Field Campaign, Atmos. Chem. Phys. Discuss., 1–41, doi:10.5194/acp-2018-71, 2018.

Thornton, J. A., Wooldridge, P. J., Cohen, R. C., Martinez, M., Harder, H., Brune, W. H., Williams, E. J. J., Roberts, J. M. M., Fehsenfeld, F. C., Hall, S. R., Shetter, R. E. E., Wert, B. P. and Fried, A.: Ozone production rates as a function of NO_x abundances and HO_x production rates in the Nashville urban plume, J. Geophys. Res., 107(D12), 1–17, doi:10.1029/2001JD000932, 2002.

Tkacik, D. S., Lambe, A. T., Jathar, S., Li, X., Presto, A. A., Zhao, Y., Blake, D., Meinardi, S., Jayne, J. T., Croteau, P. L. and Robinson, A. L.: Secondary Organic Aerosol Formation from in-Use Motor Vehicle Emissions Using a Potential Aerosol Mass Reactor., Environ. Sci. Technol., 48(19), 11235–42, doi:10.1021/es502239v, 2014.

Tohjima, Y., Kubo, M., Minejima, C., Mukai, H., Tanimoto, H., Ganshin, A., Maksyutov, S., Katsumata, K., Machida, T. and Kita, K.: Temporal changes in the emissions of CH4 and CO from China estimated from CH4 / CO2 and CO / CO2 correlations observed at Hateruma Island, Atmos. Chem. Phys., 14(3), 1663–1677, doi:10.5194/acp-14-1663-2014, 2014.

Tritscher, T., Dommen, J., DeCarlo, P. F., Gysel, M., Barmet, P. B., Praplan, A. P., Weingartner, E., Prévôt, A. S. H., Riipinen, I., Donahue, N. M. and Baltensperger, U.: Volatility and

hygroscopicity of aging secondary organic aerosol in a smog chamber, Atmos. Chem. Phys., 11(22), 11477–11496, doi:10.5194/acp-11-11477-2011, 2011.

Tsimpidi, A. P., Karydis, V. A., Zavala, M., Lei, W., Molina, L., Ulbrich, I. M., Jimenez, J. L. and Pandis, S. N.: Evaluation of the volatility basis-set approach for the simulation of organic aerosol formation in the Mexico City metropolitan area, Atmos. Chem. Phys., 10(2), 525–546, doi:10.5194/acp-10-525-2010, 2010.

Tsimpidi, A. P., Karydis, V. A., Pandis, S. N. and Lelieveld, J.: Global-scale combustion sources of organic aerosols: sensitivity to formation and removal mechanisms, Atmos. Chem. Phys., 17(12), 7345–7364, doi:10.5194/acp-17-7345-2017, 2017.

Ulbrich, I. M., Canagaratna, M. R., Zhang, Q., Worsnop, D. R. and Jimenez, J. L.: Interpretation of organic components from Positive Matrix Factorization of aerosol mass spectrometric data, Atmos. Chem. Phys., 9(9), 2891–2918, doi:10.5194/acp-9-2891-2009, 2009.

UNDESA, P. D.: World Urbanization Prospects: The 2014 Revision., 2015.

Vay, S. A., Tyler, S. C., Choi, Y., Blake, D. R., Blake, N. J., Sachse, G. W., Diskin, G. S. and Singh, H. B.: Sources and transport of Δ14C in CO 2 within the Mexico City Basin and vicinity, Atmos. Chem. Phys., 9, 4973–4985, doi:10.159/acp-9-4973-2009, 2009.

Virkkula, A.: Correction of the Calibration of the 3-wavelength Particle Soot Absorption Photometer (3λ PSAP), Aerosol Sci. Technol., 44, 706–712, doi:10.1080/02786826.2010.482110, 2010.

Volkamer, R., Jimenez, J. L., San Martini, F., Dzepina, K., Zhang, Q., Salcedo, D., Molina, L. T., Worsnop, D. R. and Molina, M. J.: Secondary organic aerosol formation from anthropogenic air pollution: Rapid and higher than expected, Geophys. Res. Lett., 33(17), L17811, doi:10.1029/2006GL026899, 2006.

Wang, Y., Munger, J. W., Xu, S., McElroy, M. B., Hao, J., Nielsen, C. P. and Ma, H.: CO_2 and its correlation with CO at a rural site near Beijing: implications for combustion efficiency in China, Atmos. Chem. Phys., 10(18), 8881–8897, doi:10.5194/acp-10-8881-2010, 2010.

Weibring, P., Richter, D., Walega, J. G., Rippe, L. and Fried, A.: Difference frequency generation spectrometer for simultaneous multispecies detection, Opt. Express, 18(26), 27670, doi:10.1364/OE.18.027670, 2010.

Weinheimer, A. J., Walega, J. G., Ridley, B. A., Gary, B. L., Blake, D. R., Blake, N. J., Rowland, F. S., Sachse, G. W., Anderson, B. E. and Collins, J. E.: Meridional distributions of NOx , NOy , and other species in the lower stratosphere and upper troposphere during AASE II, Geophys. Res. Lett., 21(23), 2583–2586, doi:10.1029/94GL01897, 1994.

WHO: Ambient air pollution: A global assessment of exposure and burden of disease, World Health Organization., 2016.

Williams, L.: What is My Vaporizer Temperature? Vaporizer Temperature Power Curve for Several Systems, [online] Available from: http://cires1.colorado.edu/jimenez-group/UsrMtgs/UsersMtg11/WilliamsAMSUsersMtg_2010_VapT.pdf (Accessed 12 March 2018), 2010.

Wisthaler, A., Hansel, A., Dickerson, R. R. and Crutzen, P. J.: Organic trace gas measurements by PTR-MS during INDOEX 1999, J. Geophys. Res., 107(D19), 8024, doi:10.1029/2001JD000576,

2002.

Woo, J.-H., An, S.-M., Kim, D.-Y., Kim, H.-K., Choi, K.-C. and Kim, Y.-H.: Development of the Asia Emission Inventory in Support of Integrated Modeling of Climate and Air Quality (III), Incheon, Korea., 2013.

Wood, E. C., Canagaratna, M. R., Herndon, S. C., Onasch, T. B., Kolb, C. E., Worsnop, D. R., Kroll, J. H., Knighton, W. B., Seila, R., Zavala, M., Molina, L. T., DeCarlo, P. F., Jimenez, J. L., Weinheimer, A. J., Knapp, D. J., Jobson, B. T., Stutz, J., Kuster, W. C. and Williams, E. J.: Investigation of the correlation between odd oxygen and secondary organic aerosol in Mexico City and Houston, Atmos. Chem. Phys., 10(18), 8947–8968, doi:DOI 10.5194/acp-10-8947-2010, 2010.

Woody, M. C., Baker, K. R., Hayes, P. L., Jimenez, J. L., Koo, B. and Pye, H. O. T.: Understanding sources of organic aerosol during CalNex-2010 using the CMAQ-VBS, Atmos. Chem. Phys., 16(6), 4081–4100, doi:10.5194/acp-16-4081-2016, 2016.

Wooldridge, P. J., Perring, A. E., Bertram, T. H., Flocke, F. M., Roberts, J. M., Singh, H. B., Huey, L. G., Thornton, J. A., Wolfe, G. M., Murphy, J. G., Fry, J. L., Rollins, A. W., LaFranchi, B. W. and Cohen, R. C.: Total Peroxy Nitrates (ΣPNs) in the atmosphere: the Thermal Dissociation-Laser Induced Fluorescence (TD-LIF) technique and comparisons to speciated PAN measurements, Atmos. Meas. Tech., 3(3), 593–607, doi:DOI 10.5194/amt-3-593-2010, 2010.

Wu, W., Zhao, B., Wang, S. and Hao, J.: Ozone and secondary organic aerosol formation potential from anthropogenic volatile organic compounds emissions in China, J. Environ. Sci., 53, doi:10.1016/j.jes.2016.03.025, 2016.

Xu, W., Croteau, P., Williams, L., Canagaratna, M., Onasch, T., Cross, E., Zhang, X., Robinson, W., Worsnop, D. and Jayne, J.: Laboratory characterization of an aerosol chemical speciation monitor with $PM_{2.5}$ measurement capability, Aerosol Sci. Technol., 51(1), 69–83, doi:10.1080/02786826.2016.1241859, 2017.

Xu, W., Lambe, A., Silva, P., Hu, W., Onasch, T., Williams, L., Croteau, P., Zhang, X., Renbaum-Wolff, L., Fortner, E., Jimenez, J. L., Jayne, J., Worsnop, D. and Canagaratna, M.: Laboratory evaluation of species-dependent relative ionization efficiencies in the Aerodyne Aerosol Mass Spectrometer, Aerosol Sci. Technol., 1–16, doi:10.1080/02786826.2018.1439570, 2018.

Yuan, B., Hu, W. W., Shao, M., Wang, M., Chen, W. T., Lu, S. H., Zeng, L. M. and Hu, M.: VOC emissions, evolutions and contributions to SOA formation at a receptor site in eastern China, Atmos. Chem. Phys., 13(17), 8815–8832, doi:10.5194/acp-13-8815-2013, 2013.

Zhang, Q., Stanier, C. O., Canagaratna, M. R., Jayne, J. T., Worsnop, D. R., Pandis, S. N. and Jimenez, J. L.: Insights into the chemistry of new particle formation and growth events in Pittsburgh based on aerosol mass spectrometry, Environ. Sci. Technol., 38(18), 4797–4809, doi:Doi 10.1021/Es035417u, 2004.

Zhang, Q., Alfarra, M. R., Worsnop, D. R., James, D., Coe, H., Canagaratna, M. R. and Jimenez, J. L.: Deconvolution and Quantification of Hydrocarbon-like and Oxygenated Organic Aerosols Based on Aerosol Mass Spectrometry Deconvolution and Quantification of Hydrocarbon-like and Oxygenated Organic Aerosols Based on Aerosol Mass Spectrometry, Environ. Sci. Technol., 39(13), 4938–4952, doi:10.1021/es048568l, 2005.

Zhang, Q., Jimenez, J. L., Canagaratna, M. R., Allan, J. D., Coe, H., Ulbrich, I., Alfarra, M. R.,

Takami, A., Middlebrook, A. M., Sun, Y. L., Dzepina, K., Dunlea, E., Docherty, K., DeCarlo, P. F., Salcedo, D., Onasch, T., Jayne, J. T., Miyoshi, T., Shimono, A., Hatakeyama, S., Takegawa, N., Kondo, Y., Schneider, J., Drewnick, F., Borrmann, S., Weimer, S., Demerjian, K., Williams, P., Bower, K., Bahreini, R., Cottrell, L., Griffin, R. J., Rautiainen, J., Sun, J. Y., Zhang, Y. M. and Worsnop, D. R.: Ubiquity and dominance of oxygenated species in organic aerosols in anthropogenically-influenced Northern Hemisphere midlatitudes, Geophys. Res. Lett., 34(13), L13801, doi:10.1029/2007gl029979, 2007.

Zhang, Q. J., Beekmann, M., Freney, E., Sellegri, K., Pichon, J. M., Schwarzenboeck, A., Colomb, A., Bourrianne, T., Michoud, V. and Borbon, A.: Formation of secondary organic aerosol in the Paris pollution plume and its impact on surrounding regions, Atmos. Chem. Phys., 15(24), 13973–13992, doi:10.5194/acp-15-13973-2015, 2015.

Zhang, X., Smith, K. A., Worsnop, D. R., Jimenez, J., Jayne, J. T. and Kolb, C. E.: A Numerical Characterization of Particle Beam Collimation by an Aerodynamic Lens-Nozzle System: Part I. An Individual Lens or Nozzle, Aerosol Sci. Technol., 36, 617–631, doi:10.1080/02786820252883856, 2002.

Zhang, X., Smith, K. A., Worsnop, D. R., Jimenez, J. L., Jayne, J. T., Kolb, C. E., Morris, J. and Davidovits, P.: Numerical Characterization of Particle Beam Collimation: Part II Integrated Aerodynamic-Lens–Nozzle System, Aerosol Sci. Technol., 38, 619–638, doi:10.1080/02786820490479833, 2004.

Zhang, X., Cappa, C. D., Jathar, S. H., McVay, R. C., Ensberg, J. J., Kleeman, M. J., Seinfeld, J. H. and Christopher D. Cappa: Influence of vapor wall loss in laboratory chambers on yields of secondary organic aerosol., Proc. Natl. Acad. Sci. U. S. A., 111(16), 1–6, doi:10.1073/pnas.1404727111, 2014.

Zhao, Y., Hennigan, C. J., May, A. A., Tkacik, D. S., de Gouw, J. A., Gilman, J. B., Kuster, W. C., Borbon, A. and Robinson, A. L.: Intermediate-volatility organic compounds: a large source of secondary organic aerosol, Environ. Sci. Technol., 48(23), 13743–50, doi:10.1021/es5035188, 2014.

Zhao, Y., Nguyen, N. T., Presto, A. A., Hennigan, C. J., May, A. A. and Robinson, A. L.: Intermediate Volatility Organic Compound Emissions from On-Road Gasoline Vehicles and Small Off-Road Gasoline Engines, Environ. Sci. Technol., 50(8), 4554–4563, doi:10.1021/acs.est.5b06247, 2016.

Ziemba, L. D., Lee Thornhill, K., Ferrare, R., Barrick, J., Beyersdorf, A. J., Chen, G., Crumeyrolle, S. N., Hair, J., Hostetler, C., Hudgins, C., Obland, M., Rogers, R., Scarino, A. J., Winstead, E. L. and Anderson, B. E.: Airborne observations of aerosol extinction by in situ and remote-sensing techniques: Evaluation of particle hygroscopicity, Geophys. Res. Lett., 40(2), 417–422, doi:10.1029/2012GL054428, 2013.